工 學 博 士 學 位 論 文

# Rational design for enzyme engineering of CYP153 family and its application to production of ω-hydroxy palmitic acid

# CYP153 효소의 합리적 설계 및 오메가 수산화 팔미트산 생산에 관한 연구

2016 년 8 월


서울大學校 大學院

化學生物工學部

鄭 恩 玉

# Rational design for enzyme engineering of CYP153 family and its application to production of ω-hydroxy palmitic acid

A Thesis

Submitted to the Faculty of Seoul National University

by

**Eunok Jung**

In Partial Fulfillment of the Requirements

For the Degree of Doctor of Philosophy

Advisor: Professor Byung-Gee Kim, Ph. D.

August, 2016

# Abstract

## Rational design for enzyme engineering of CYP153 family and its application to production of ω-hydroxy palmitic acid

**Eunok Jung**

**School of Chemical and Biological Engineering**

**The Graduated School**

**Seoul National University**

In this study, the ω–specific hydroxylation of fatty acids using cytochrome P450 monooxygenase (CYPs) was investigated. Among bacterial CYPs in CYP153 family which reported as fatty acid ω-hydroxylase, CYP153As from *Marinobacter aquaeolei* VT8 (CYP153A33), *Alcanivorax borkumensis* SK2 (CYP153A13) and *Gordonia alkanivorans* (CYP153A35) were selected, and compared their specific activities and product yields of ω-hydroxy palmitic acid based on whole-cell reactions toward palmitic acid. Using CamAB as redox partner, CYP153A35 and CYP153A13 showed the highest product yields of ω-hydroxy palmitic acid by whole-cell and *in vitro* reactions, respectively.

To investigate electron transfer system for CYP153A35, artificial self-sufficient

CYP153A35-BMR was constructed by fusing it to the reductase domain of CYP102A1 (i.e. BM3) from *Bacillus megaterium,* and its catalytic activity was compared with CYP153A35 and CamAB system. Unlike the expectations, the system with CamAB resulted 1.5 fold higher yield of ω-hydroxy palmitic acid than that using A35-BMR in whole-cell reaction, whereas the electron coupling efficiency of CYP153A35-BM3 reductase was 4 times higher than that of CYP153A35 and CamAB system.

Furthermore, various CamAB expression systems according to gene arrangements of the three proteins and promoter strength in their gene expression were compared in terms of product yields and productivities. Tricistronic expression of the three proteins in the order of camB, cyp153A35 and camA, i.e. A35-AB2 construct, showed the highest product yield from 5 mM of palmitic acid within 9 h in batch reaction system owing to the concentration of CamB, which is the rate limiting factor for the activity of CYP153A35. However, in fed-batch reaction system, A35-AB1 construct, which expressed the three proteins individually using three T7 promoters, resulted the highest product yield of 17.0 mM (4.6 g/L) of ω-hydroxy palmitic acid from 20 mM (5.1 g/L) of palmitic acid in 30 h.

For the improvement of hydroxylation activity of CYP153A35, the structures of CYP153A35 were predicted by homology modelling, and the major cavities and the amino acid interacting with the fatty acid were revealed by CAVER 3.0. In order to screen mutants, a powerful high-throughput screening assay was developed, which used Purpald to sense formaldehyde produced as a by-product during O-dealkylation reaction. Saturation mutagenesis on 19 amino acids was

performed and D131S mutant showing 281.4 $min^{-1}mM^{-1}$ of catalytic constant which was more than 17 times higher value than that of wild-type (16.5 $min^{-1}mM^{-1}$).

To optimize the linker sequence between fatty acid ω-hydroxylase (CYP153A33) and reductase domain of CYP102A1, repeated flexible or rigid sequence are designed randomly and screened. The best mutant, EAAAK-$(GGGGS)_3$-EAAAK, showed the 50% higher specific activity than native BM3 linker, although poor expression level *in E.coli*.

**Student number:** 2009-21025

**Keywords**: ω-Hydroxy fatty acid, Cytochrome P450 monooxygenase, CYP153, Electron transfer system, Semi-rational engineering, Linker design, Protein expression optimization

# Contents

## List of Tables

## List of Figures

# Chapter 1.

# Introduction

## 1.1 ω-Hydroxy fatty acid for ceramide synthesis

### 1.1.1 Ceramides for cosmetic ingredient

Stratum corneum (SC), the outermost layer of the epidermis, is the most important organ for skin barrier function and composed with corneocytes and intercellular lipids (Figure 1.1a) (Haftek, Callejon et al. 2011). Various lipids exist in intracellular lipids such as ceramides, cholesterol, free fatty acids, triglycerides, squalene, etc. (Schürer and Elias 1991) Especially, ceramides are an important determinant of the water retention properties and play crucial roles in lamellar structure of stratum corneum. Therefore, ceramide deficiency may provide an etiologic basis for dry and barrier-disturbed skin (Yamamoto, Serizawa et al. 1991, Choi and Maibach 2005). However, natural ceramides have two drawbacks for cosmetic ingredient. Natural ceramide are broken down in the skin by the action of ceramidases to liberate sphingosine, and free sphingosine inhibits the activity of protein kinase C, which may be affect cell division (Downing 1992). In addition, isolation from natural sources is expensive, thus it is difficult to obtain in the quantities needed for application in cosmetic ingredient (Weber, Lambers et al. 2000).

Among the various human ceramides, ceramide I is the most significant for the formation of the lateral lipid packing as well as the long range lamellar ordering in SC (Bouwstra, Gooris et al. 1998). Ceramide I contained mainly 30 and 32-carbon saturated, straight-chained ω-hydroxy fatty acids (Wertz, Miethke et al. 1985). We designed new psuedoceramide similar to ceramide I, thus cost-effective supply of ω-hydroxy palmitic acid is key for synthesis of psuedoceramide (Figure 1.1b).

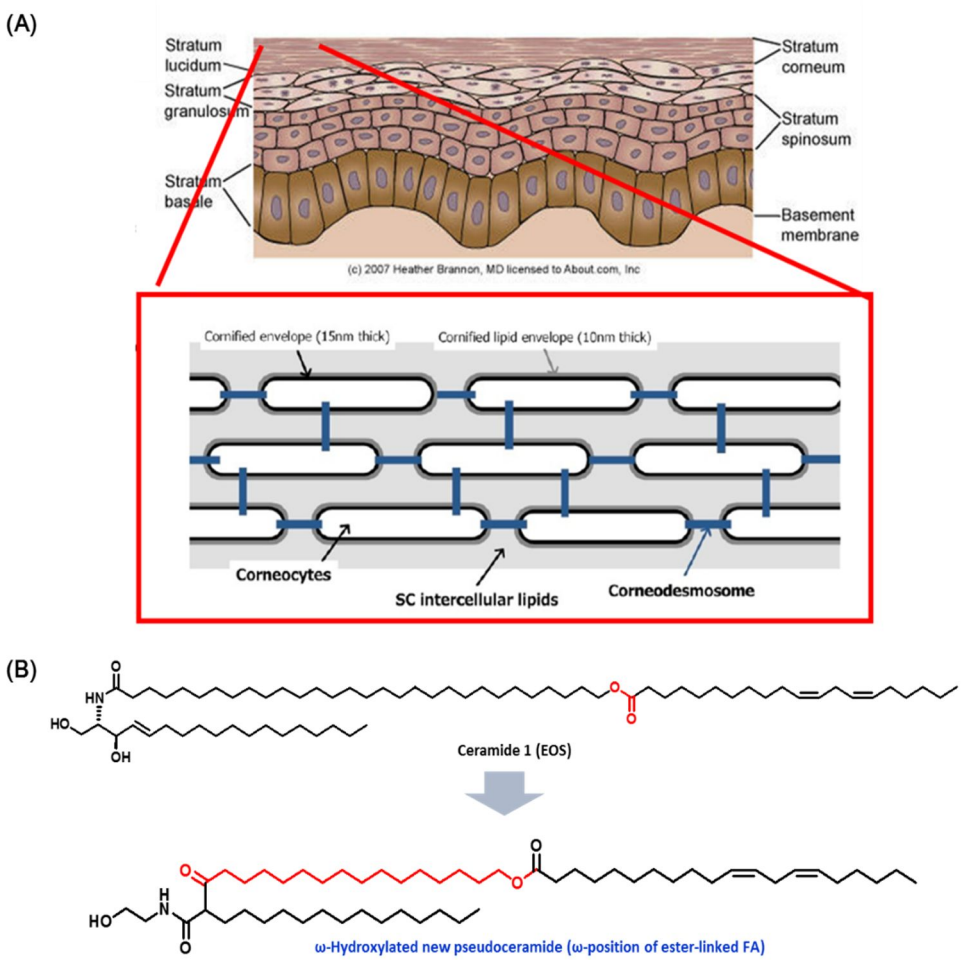


**Figure 1.1 Structure of stratum corneum and proposed psuedoceramide (A) Structure of the epidermis and stratum corneum (B) Structure of ceramide I and designed psuedoceramide**

### 1.1.2 Chemical and biological synthesis of ω-hydroxy fatty acids

ω-hydroxy fatty acids (ω-HFAs) are valuable chemicals for various synthesis of ceramide and additives such as lubricants, adhesives (Vandamme and Soetaert 2002, Metzger and Bornscheuer 2006). ω-HFAs can be chemically synthesized by oxidation of alkanediols (Scott, Crawford et al. 1993), reduction of dicarboxylic acids (Yokota and Watanabe 1993), or ring opening of lactones/enamines (Cho and DeFlorio 1996, Stephan and Mohar 2006), all these methods require multi-step reactions for controlled selectivity with high temperature, and also used expensive starting materials, which are major hurdles for their economic chemical syntheses (Labinger and Bercaw 2002, Labinger 2004). As alternatives, biological synthesises of ω-HFAs have been developed, for example, using alkane monooxygenase (AlkB) (Kusunose, Coon et al. 1964, McKenna and Coon 1970, Clomburg, Blankschien et al. 2015), or using multistep reactions supported by hydratase, alcohol dehydrogenase, Baeyer–Villiger monooxygenase and esterase (Song, Jeon et al. 2013). In addition, a chemo-enzymatic synthetic method using Baeyer–Villiger monooxygenase and RANEY® Ni catalyst was recently reported (Jang, Singha et al. 2016). Despite good attempts, these methods are limited only for medium-chain fatty acids ($C_{6:0}$–$C_{12:0}$).

## 1.2 Cytochrome P450s (CYPs)

Cytochrome P450s (CYPs) belong to monooxygenase and are widely distributed in nature (Hrycay and Bandiera 2015). CYPs were discovered in rat liver microsomes at first and a Soret peak at 450 nm was identified in reduced form of CYPs with CO, hence, it was named cytochrome P450 (Brodie, Axelrod et al. 1955,

Omura and Sato 1964). CYPs contain a heme which binds to a conserved cysteine covalently, which provide a reason for its spectroscopic properties and the Soret peak at 450 nm. CYPs play important roles in living organism such as the metabolism of xenobiotics, antibiotics and steroids (Anzenbacher and Anzenbacherova 2001). Because of those significance, CYPs are interesting powerful biocatalysts in chemical industry (Urlacher and Girhard 2012).

### 1.2.1 Reaction mechanism of CYPs

The catalytic mechanism of CYP was initially introduced in 1968 (Figure 1.1). The catalytic cycle of CYPs can be described in seven consecutive steps. First, the substrate binds $Fe^{III}$, displacing a molecule of water. Then, $Fe^{III}$ was reduced into $Fe^{II}$ by transferred an electron. An oxy-ferrous intermediate is generated by the binding of $Fe^{II}$ to dioxygen, and a second electron reduces the iron-peroxo complex, causing an iron-hydroperoxo intermediate. The intermediate is immediately cleaved, and one molecule of water was released, generating highly reactive iron-oxo ferryl specie, referred to as compound I. The activated oxygen atom of the compound I oxidized the substrate, and the product is released, displaying a water molecule.

### 1.2.2 Classification of CYP electrons transfer system

According to a general CYP reaction mechanism, two electrons are required sequentially to form compound I, and the electrons from NAD(P)H are transferred to P450 via various typed auxiliary redox proteins containing prosthetic groups such as FAD, FMN and Fe-S cluster depending upon the types of CYPs (Figure 1.2)

(Hannemann, Bichet et al. 2007). Therefore, optimization of electron flow between

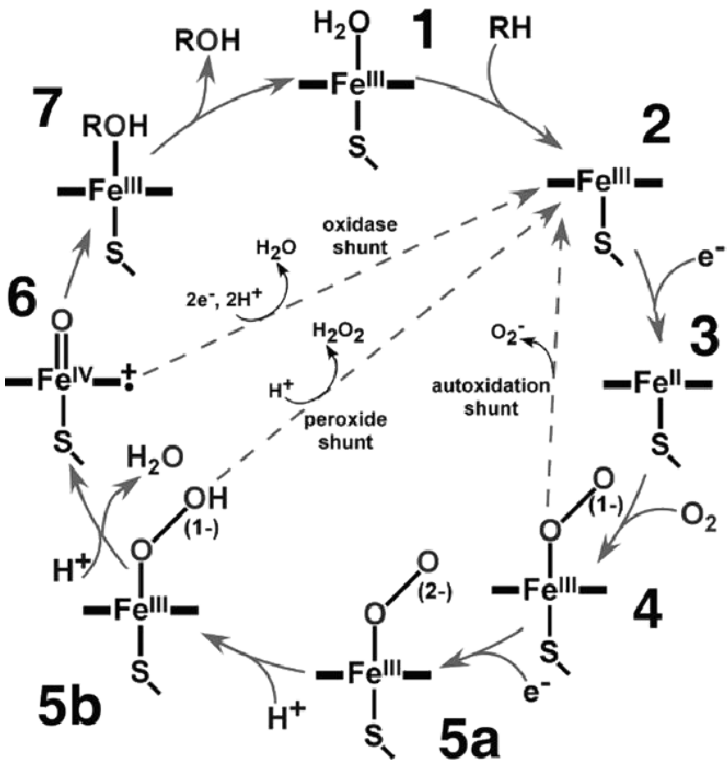


**Figure 1.1 Catalytic cycle of CYPs.**

The reaction requires the sequential input of two electrons and one dioxygen to catalyze hydroxylation reaction. (Adapted from Denisov et al. Chem. Rev. 2005, 105, 2253-2277) (Denisov, Makris et al. 2005)

the redox partner proteins can result enhanced active oxygen compound level leading to enhanced substrate conversion to product (Bernhardt and Urlacher 2014). To find out an optimum or efficient electron transfer system for a specified CYP among a large number of ferredoxins and ferredoxin reductases, screening approaches are generally used as a first trial such as comparison of various redox proteins from different origins (Choi, Kim et al. 2009, Bell, Dale et al. 2010, Bell, Xu et al. 2010). Another approach is designing a class VIII self-sufficient CYP, which is a fusion protein of CYP and CYP reductase domain with additional flexible linker peptide sequences to achieve high electron transfer efficiency (Fairhead, Giannini et al. 2005, Dodhia, Fantuzzi et al. 2006, Choi, Jung et al. 2012, Scheps, Honda Malca et al. 2013).

### 1.2.3 Structural features of CYP

Even though CYP sequences are various with only three conserved amino acids, Cys for heme binding and the EXXR-motif, the CYP-fold consists of thirteen conserved α–helices and five β–sheets, the α–helices are alphabetically named A-L and the β–sheets are numbered 1-5 (Figure 1.3) (Sevrioukova, Li et al. 1999). In this conserved fold six substrate recognition sites (SRSs) covering most of the substrate binding pocket and substrate entrance were identified (Figure 1.4) (Gotoh 1992). SRS1 is located on the BC-loop region, SRS2 is located on α-helix F, SRS3 on α-helix G, SRS4 on α-helix I, SRS5 covers β-strand 1-4 and the neighboring loops, and SRS6 spans over β-strands 4-1 and 4-2. SRS2 and 3 constitute most of the substrate access channel, whereas SRS1, 4, 5, and 6 form the walls of the binding pocket. Because the SRS positions not only directly interact with the

substrate but also

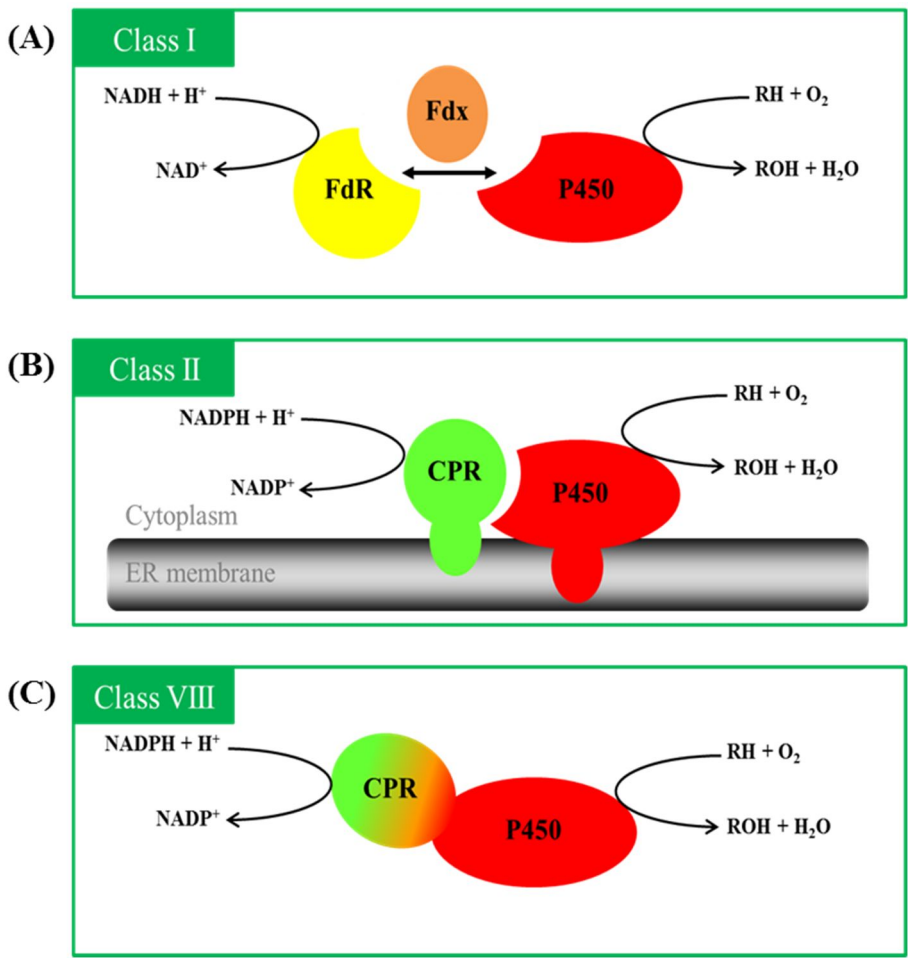


**Figure 1.2 Representatives among various CYP electron transfer systems**

(A) Class I; Three-protein systems, P450, ferredoxin and ferredoxin reductase are soluble in bacterial cytoplasm (B) Class II; Two-protein systems, cytochrome P450 reductase and P450 are membraned bound in eukaryote ER (C) Class VIII; One-protein systems, fusion protein of P450 and P450 reductase domain are soluble

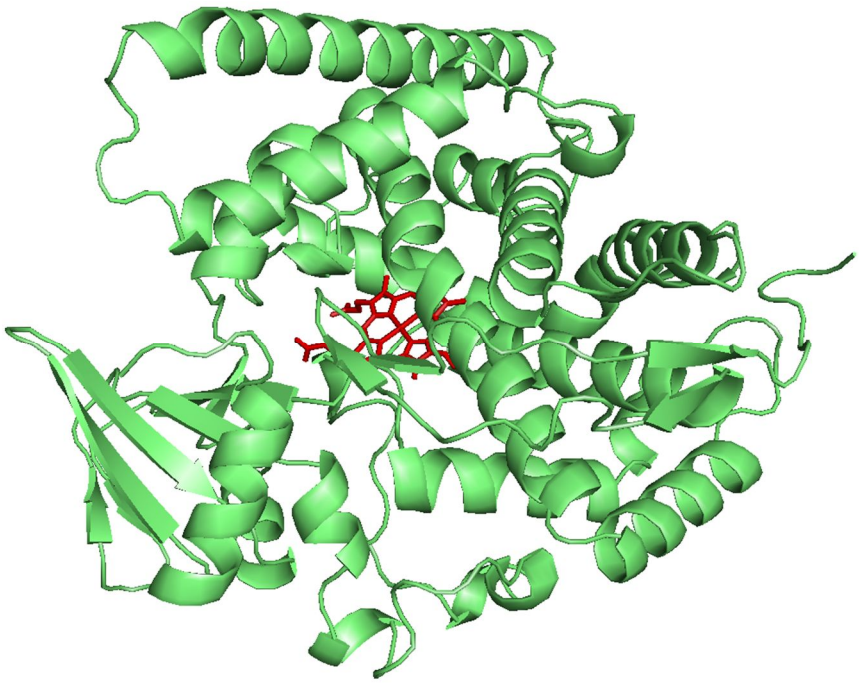

**Figure 1.3 Crystal structure of CYP102A1 BM3 from *Bacillus megaterium* [PDB:1BVY]**

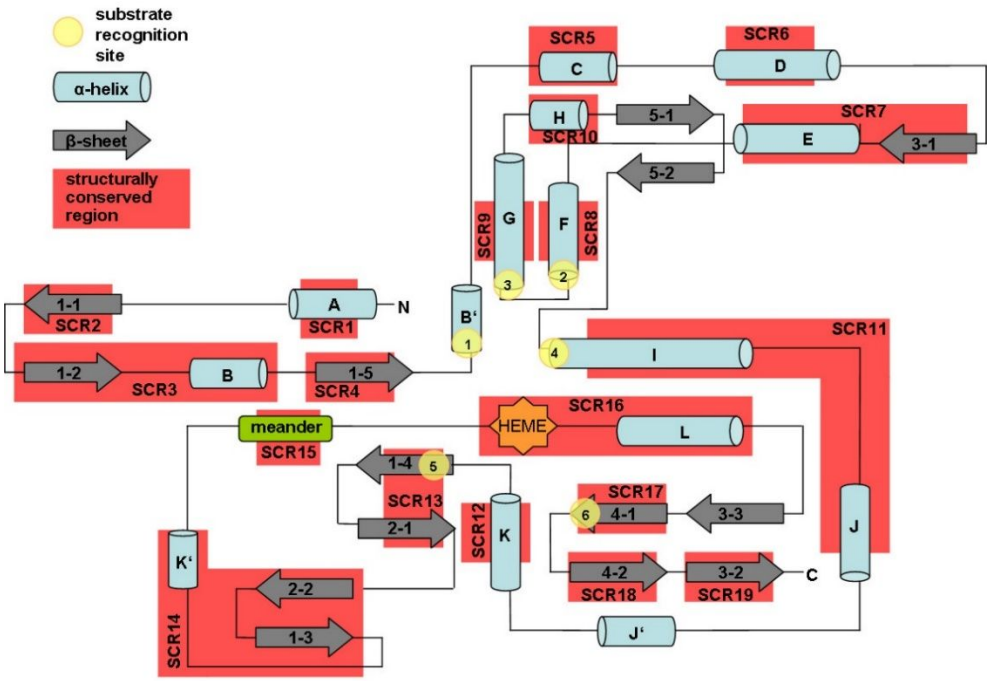


**Figure 1.4 Schematic representation of the CYP-fold.**

All α-helices are visualized as blue tubes, β-sheets as grey arrows and the SRS regions of CYPs are marked as yellow circles. (Adapted from Sirim et al. BMC Structural Biology 2010, 10:34) (Sirim, Widmann et al. 2010)

contribute to the general architecture and flexibility of the binding pocket, it is clear that some SRS positions will be more significant for the determination of selectivity and specificity than other (Li and Poulos 1997, Li and Poulos 1999).

### 1.2.4 Artificial self-sufficient CYP

CYP102A1 BM3 is a natural self-sufficient CYP in a single 119 kDa polypeptide chain containing CYP and reductase domain. BM3 catalyzes oxidation of arachidonic acid with $k_{cat}$ of >280 $s^{-1}$, which is dramatically faster than any CYP enzyme (Noble, Miles et al. 1999), therefore, numerous attempts have been designed to construct an artificial self-sufficient CYP (Dodhia, Fantuzzi et al. 2006, Choi, Jung et al. 2012). In addition, a flexible linker $(Gly\text{-}Gly\text{-}Ser)_n$ has been used to enhance the stability between the two fused domains (Scheps, Honda Malca et al. 2013).

Another natural self-sufficient CYPs, CYP116B family containing FAD and 2Fe-2S cluster, were recently discovered, which correspond with Class I bacterial CYP electron transfer system (De Mot and Parret 2002). Reductase domain of CYP116B2 RhF from *Rhodococcus* sp.was also suitable for the generation of efficient artificial self-sufficient CYP (Nodate, Kubota et al. 2006, Robin, Kohler et al. 2011). The artificial construct CYP153A13-RhF reductase successfully produced 1-octanol from octanol (Bordeaux, de Girval et al. 2014). Variation in linker length improved electron transfer efficiency between CYP153A33 and reductase domain of CYP116B3 PFOR from *Rhodococcus ruber*, although poor solubility of fusion protein remained for further optimization (Hoffmann, Weissenborn et al. 2016).

Several efforts have been reported on fusion of heterologous expressed CYP and redox proteins. Fusion construction of CYP51 and Fe-S cluster-containing reductase succeeded with sterol demethylation activity (Choi, Park et al. 2010). CYP176A1 from *Citrobacter braakii*, P450cin catalyzing cineole oxidation, was fused to its native flavodoxin (CinA) using peptides of different lengths to improve electron transfer efficiency (Belsare, Ruff et al. 2014).

### 1.2.5 CYP engineering by direct evolution and semi-rational design

Various CYPs have been subjected to protein engineering to improve their specific activities, regio-selectivities and stabilities by directed evolution, rationally designed mutations based on computation methods, and hybrid combination of these approaches (Girvan and Munro 2016). CYP102A1 BM3, for instance, has been engineered for various substrate such as drugs, alkanes, terpenes, and polycyclic aromatic hydrocarbon (PAH) (Peters, Meinhold et al. 2003, Whitehouse, Bell et al. 2012, Roiban and Reetz 2015). CYP153A7, another example, has been also evolved to catalyze hydroxylation of butanol or alicyclic compounds with high regio- and stereo-selectivity (Yang, Chi et al. 2015, Yang and Li 2015). Cytochrome P450 has also been engineered to improve hydroxylation activity toward fatty acid. CYP102A1 L181K and L75T/L181K mutant showed 13-, 15-fold improvement of catalytic activity toward $C_4$ and $C_6$, respectively (Ost, Miles et al. 2000). CYP102A2 P15S mutant showed 10-fold enhancement of specific activity toward $C_{12}$ (Axarli, Prigipaki et al. 2005). G307 on CYP153A33 was selected as key amino acid for substrate binding, based on sequence alignment with CYP101A1 (Honda Malca, Scheps et al. 2012). CYP153A33 G307A/S233G and

G307A/S120R/P165N/S453N mutant developed for higher activity toward $C_{12}$ and oleic acid, respectively (Duan, Ba et al. 2016, Notonier, Gricman et al. 2016).

Among the methods for generation of mutant library, semi-rational engineering, combination of directed evolution and rational design, merges mechanistic and structural information, as well as computational prediction to select promising target sites, dramatically reduced library size with higher possibility (Lutz 2010, Porter, Rusli et al. 2016, Zorn, Oroz-Guinea et al. 2016). For instance, semi-rational engineering of CYP102A1 allowed equal improvement for propane hydroxylation compared to 10-12 rounds of directed evolution using random and site-saturation mutagenesis (Chen, Snow et al. 2012). Computation tools for rational designs have been developed based on sequence alignment (Gricman, Vogel et al. 2014, Gricman, Vogel et al. 2015), substrate entrance tunnel (Liskova, Bednar et al. 2015), substrate docking simulation (Chen, Snow et al. 2012), and calculation of mutability using combination of both sequence and structural information (Pavelka, Chovancova et al. 2009, Bendl, Stourac et al. 2016).

### 1.2.6 Fatty acid ω-hydroxylase

Among the various fatty acid hydroxylases (Kim and Oh 2013), only CYP can do ω-hydroxylation of fatty acid regioselectively. For instance, CYP4 in mammalian (Hardwick 2008) and CYP86, CYP94 and CYP96 in plant were well characterized as fatty acid ω-hydroxylase (Benveniste, Tijet et al. 1998, Tijet, Helvig et al. 1998, Benveniste, Saito et al. 2006), but their low turnover rates and poor expression levels in *E.coli* are the limitations for application in industry level.

In addition, alkane induced CYPs in CYP52 family also showed similar terminal

hydroxylation activity toward fatty acids as well as alkanes, producing ω-HFAs and α,ω-diols, respectively (Zimmer, Ohkuma et al. 1996, Scheller, Zimmer et al. 1998). A biosynthetic process converting methyl tetradecanoate (200 g/L) to 14-hydroxy tetradecanoic acid (174 g/L) and 1,14-tetradecanedioic acid (6.1 g/L) in 148 h of fermentation was demonstrated in engineered *Candida tropicalis* (Table 1.1) (Lu, Ness et al. 2010). Although such ω-HFA production was mainly attempted using yeast as industrial host system, it is still desirable to use *E.coli* as a host in the case of single hydroxylation reaction since *E.coli* is more competent host microbial system than yeast due to its rapid growth, well-known physiology, and easy genetic manipulation (Steen, Kang et al. 2010). However, to accomplish such development of *E.coli* system, eukaryotic P450s are inappropriate because those are membrane-anchored enzymes localized at the endo-plasmatic reticulum (ER) of the cell, thus additional engineering of the membrane anchored region of P450s is required for functional expression in *E.coli* (Gillam, Baba et al. 1993).

Recently, bacterial CYPs in the CYP153A family such as CYP153A16 from *Mycobacterium marinum*, CYP153A33 from *Marinobacter aquaeolei* and CYP153A34 from *Polaromonas* sp. were characterized as fatty acid ω-hydroxylase that acts on saturated and unsaturated fatty acids(Honda Malca, Scheps et al. 2012). Using CYP153A33 in recombinant *E.coli* system, high ω-regioselective bioconversion of 1.2 g/L of 12-hydroxy dodecanoic acid from 10.0 g/L (50 mM) of dodecanoic acid and 4.0 g/L of 12-hydroxy dodecanoic acid methyl ester from dodecanoic acid methyl ester was achieved by overexpression of AlkL, the fatty acid ester transport (Scheps, Honda Malca et al. 2013), and bioconversion of 2.4 g/L of 16-hydroxy palmitic acid from 2.6 g/L (10 mM) of palmitic acid was also

reported by deletion of fatty acid ω-oxidation degradation pathway (i.e. ΔfadD) and overexpression of a fatty acid transporter FadL (Bae, Park et al. 2014). Despite such

**Table 1.1 Summarization of production of ω-hydroxy fatty acid using CYPs**

| host | CYP | Redox protein (s) | Product | Titer (g/L) | Productivity (g/L/h) | ref |
|---|---|---|---|---|---|---|
| ***Candida tropicalis*** | CYP52 | CaCPR | 14-hydroxy tetradecanoic acid | 174 | 1.17 | (Lu, Ness et al. 2010) |
| ***E.coli*** | CYP153A33 | fused BMR | 12-hydroxy dedecanoic acid | 4 | 0.14 | (Scheps, Honda Malca et al. 2013) |
| ***E.coli*** | CYP153A33 | CamA/CamB | 16-hydroxy hexadecanoic acid | 2.4 | 0.07 | (Bae, Park et al. 2014) |

successful ω-HFA production in *E.coli*, still there are rooms for enhancing both yield and productivity of long chain (C12-C18) ω-HFAs by screening higher catalytically active CYPs among numerous CYP sequences and incorporating an appropriate electron transfer system into CYPs.

### 1.3 Research objectives

In this study, first, CYP153A13 and CYP153A35 were newly cloned from *Alcanivorax borkumensis* SK2 and *Gordonia alkanivorans*, respectively, and ω-hydroxylation activities toward saturated fatty acids were compared with CYP153A33 from *Marinobacter aquaeolei* VT8 previously reported (Honda Malca, Scheps et al. 2012). CYP153A35 exhibited the highest whole-cell activity toward palmitic acid among the CYP153As with putidaredoxin reductase (CamA) and putidaredoxin (CamB). Then, to find out efficient electron transfer system for CYP153A35, firstly, class I P450 system with CamAB requiring NADH, and class VIII self-sufficient system requiring NADPH, i.e., a CYP153A35 gene fused to reductase domain of CYP102A1 (BMR) from *Bacillus megaterium* were compared. Secondly, further improvement in terms of initial productivity of ω-hydroxy palmitic acid was obtained by gene rearrangement and changing promoter strengths to optimize the relative expression levels of CYP153A35 and CamAB in whole-cell. This result highlights a disagreement of evaluations of electron transfer system whole-cell and *in vitro* and suggests careful consideration for data analysis in two systems.

Second, engineering of CYP153A35-BMR was performed to obtain high-performance mutants of ω-hydroxylation activity toward palmitic acid. To select

target amino acids, two computational tools, Modeller 9.11 and CAVER 3.0, were used to identify the amino acid residues involved in recognition and binding of fatty acids, i.e. substrate recognition sites (SRSs), and hence determine fatty acid specificity. Then, using colorimetric HTS method base on O-demethylation activity of P450, mutants were screened and investigated the effects toward palmitic acid. This result highlights altering fatty acid chain length specificity and improvement catalytic activity in ω-hydroxylation reaction.

Finally, linker sequences between CYP153A33 and reductase domain of CYP102A1 were optimized using repeated flexible or rigid sequence randomly. Using developed HTS method, the best mutants were selected and examined compare to native BM3 linker.

# Chapter 2.

# Materials and Methods

## 2.1 Bacterial strains and chemical materials

Saturated fatty acids, ω-hydroxy palmitic acid, purpald and N,O-bis(trimethylsily)trifluoroacetamide (BSTFA) for the derivatization for GC/MS analysis were purchased from Sigma-Aldrich Chemical Co. (St. Louis, MO, USA). All other chemicals were were purchased from Sigma-Aldrich, and Junsei Chemical Co. Ltd. (Tokyo, Japan).

Restriction enzymes, $T_4$ DNA ligase, DNA polymerase, and other DNA modifying enzymes were purchased from Thermo Fermentas (Waltham, MA, USA), New England Biolabs (Ipswich, MA, USA), Takara (Shiga, Japan), Solgent (Korea), and Promega (Madison, WI, USA), and used as recommended by the manufacturers.

*Escherichia coli* DH5α, BL21 (DE3), BW25113 (DE3) were used as hosts for cloning and expression of CYPs. For the culture of cells above, Difco Luria-Bertani (LB) (1% tryptone, 0.5% yeast extract, 1% sodium chloride) and Difco Terrific broth (TB) (1.2% pancreatic digest of casein, 2.4% yeast extract, 0.94% dipotassium phosphate, 0.22% monopotassium phosphate, and 0.4% glycerol) were used (Becton, Dickinson and company, USA).

## 2.2 Construction of CYP and redox protein plasmids

All plasmids and PCR primers of CYPs and redox proteins are listed in Table 2.1 and Table 2.2. *Alcanivorax borkumensis* SK2 and *Gordonia alkanivorans* DSM44369 were obtained from the Korea Collection for Type Cultures (KCTC, Daejeon, South Korea). CYP153A13 (GI:CAL15649.1) from *Alcanivorax borkumensis* SK2 and CYP153A35 (GI:GAA11433.1) from *Gordonia*

*alkanivorans* DSM44369 were amplified by PCR with oligonucleotides. After restriction digestion and T4 DNAase ligation, the plasmid was used to transform competent *E.coli* DH5α cells. Successful cloning was verified by DNA sequencing. Construction method of a self-sufficient fusion protein (pCYP153A35-BMR) with CYP153A35 and reductase domain of CYP102A1 was carried out following previously described procedures (Scheps, Honda Malca et al. 2013). pCW ori$^{+}$ vector was kindly provided by the laboratory of Donghak Kim at Konkuk Univ. pCW-CYP153A35 and pCW-CamA were constructed by *NdeI* and *BglII*. pCamB-CYP153A35, pCamB-CamA, pCamB-CYP153A35-CamA and pCamB-CamA-CYP153A35 encoding cyp153A35 and camAB as an operon were constructed by compatible cohesive ends produced by *SpeI* and *XbaI*. We previously cloned CYP153A33 from *Marinobacter aquaeolei* and fadL from *E. coli* into pCDFmT7 and camA and camB from *Pseudomonas putida* were cloned into pET28a and pETDuet-1

**2.3 Saturation mutagenesis for construction of CYP libraries**

Saturation mutagenesis was performed to search a single mutation among the selected amino acid residues in substrate binding site of CYP153A35. To generate mutant library, PCR was carried out using the vector pET28a(+) harboring the CYP153A35 fused CYP102A1 (pCYP153A35-BMR) as a template and the designed primers shown in Table 2.3. Thermal cycling program consisted of the following reaction conditions: 95 °C for 10 min, 25 cycles [95 °C for 30 s, 50 °C for 30 s, 72 °C for 5 min], and 72 °C for 5min. The PCR products were purified

after DpnI treatment and transformed into *E. coli* DH5α. The plasmids harvested from the *E. coli* DH5α cells were transformed into *E. coli* BL21 (DE3).

1 **Table 2.1 plasmids of CYP and redox protein**

| Plasmids | Description |
|---|---|
| pET28a | pBR322 ori lacI T7 promoter, $Km^R$ |
| pET24ma | P15A ori lacI T7 promoter, $Km^R$ |
| pETduet-1 | pBR322 ori lacI T7 promoter, $Amp^R$ |
| pCDFmT7 | Modified pCDFDuet-1 to harbor only one T7 promoter, CDF ori, $Str^R$ |
| $pCWori^+$ | pBR322 ori lacI tac promoter, $Amp^R$ |
| pCYP153A33 | pET24ma encoding for cyp153A33 |
| pCYP153A13 | pET24ma encoding for cyp153A13 |
| pCYP153A35 | pET24ma encoding for cyp153A35 |
| pCamA | pET28a encoding for camA |
| pCamB | pET28a encoding for camB |
| pCamAB | pETDuet-1 encoding for camA and camB |
| pFadL | pCDFmT7 encoding for fadL |
| pCYP153A35-BMR | pET28a encoding for cyp153A35 fused cyp102A1 reductase |
| pCW-CYP153A35 | $pCWori^+$ encoding for cyp153A35 |
| pCW-camA | $pCWori^+$ encoding for camA |
| pCamB-CYP153A35 | pET24ma encoding for camB-cyp153A35 operon |
| pCamB-CamA | pET24ma encoding for camB-camA operon |
| pCamB-CYP153A35-CamA | pET24ma encoding for camB-cyp153A35-camA operon |
| pCamB-CamA-CYP153A35 | pET24ma encoding for camB -camA-cyp153A35 operon |

1 **Table 2.2 PCR primers used in the construction of CYP and redox prote**

| Name | Sequence (5' to 3') | Details |
|---|---|---|
| 153A13-F | ATAT CATATG TCAACGAGTTCAAGTACAA | Cloning into pET24ma vector using NdeI and XhoI restriction enzymes |
| 153A13-R | ATAT CTCGAG TTTTTTTGCCGTCAATTTAACCATCA | |
| 153A35-F | ATAT CATATG CAGATCCTCGACCGCGTCGT | |
| 153A35-R | ATAT CTCGAG TCATGACCGTGTCTTCGGCGTGA | |
| A35fusion-F | ATAA CCATGG GCATGCAGATCCTCGACCG | Cloning into pET28a vector using NcoI and XhoI restriction enzymes and PCR fused by assembly PCR |
| A35fusion-R | AGCAGACTGTTCAGTGCTAGGTGAAGGAATTGACCGTGTCTTCGG CGTG | |
| BMRfusion-F | ATTCCTTCACCTAGCACTGAAC | |
| BMR-R | ATAT CTCGAG CCCAGCCCACACGTCTTTTG | |
| CYP153A35-bglII-R | ATAT AGATCT TCATGACCGTGTCTTCGGCGTGA | Cloning into pCW ori$^{+}$ vector using NdeI and BglII restriction enzymes |
| CamA-F | ATAT CATATG AACGCAAACGACAACGTGG | |
| CamA-R | ATAT AGATCT TCAGGCACTACTCAGTTCAGCTTTGG | |
| CamB-F | ATAT CATATG TCTAAAGTAGTGTATGTGT | Operon constructed by compatible cohesive ends by restriction enzyme using SpeI and XbaI |
| speI-CamB-R | ATAT GAATTC ACTAGT TTACCATTGCCTATCGGGAACATCGA | |
| rbs-A35-F | CCC TCTAGA AATAATTTTGTTTAACTT | |
| speI-A35-R | ATAT GAATTC ACTAGT TCATGACCGTGTCTTCGGCGTGA | |
| rbs-CamA-F | CCC TCTAGA AATAATTTTGTTTAACTT | |
| speI-CamA-R | ATAT GAGCTC ACTAGT TCAGGCACTACTCAGTTCAGCTTTGG | |

**Table 2.3 Primer sequences used for site-directed mutagenesis**

| Amino acid | | Sequence (5' to 3') |
|---|---|---|
| I123 | F | AACCCTTCATCGTGNNKGGCACTCCC |
| | R | GGGAGTGCCMNNCACGATGAAGGGTT |
| P128 | F | GGCACTCCCCCANNKGGCCTCAGCGTCGA |
| | R | TCGACGTCGAGGCCMNNTGGGGGAGTGCC |
| L130 | F | CACCGGGCNNKAGCGTCGAGATG |
| | R | CATCTCGACGCTMNNGCCCGGTG |
| D131 | F | GGCCTCNNKGTCGAGATGTTCATC |
| | R | ACATCTCGACMNNGAGGCCCG |
| V132 | F | GCCTCGACNNKGAGATGTTCATC |
| | R | GATGAACATCTCMNNGTCGAGGC |
| M134 | F | TCGACGTCGAGNNKTTCATCGCGATG |
| | R | CATCGCGATGAAMNNCTCGACGTCGA |
| I136 | F | GTCGAGATGTTCNNKGCGATGGACC |
| | R | GGTCCATCGCMNNGAACATCTCGAC |
| A219 | F | TGGTCCGATCTCNNKTCCGGCAG |
| | R | CTGCCGGAMNNGAGATCGGACCA |
| Y236 | F | GAGGTGNNKGCGGCAGCCCTG |
| | R | CTGCCGCMNNCACCTCGTCGG |
| A239 | F | TACGCGGCANNKCTGGAGATGACC |
| | R | CATCTCCAGMNNTGCCGCGTACAC |
| L240 | F | GCAGCCNNKGAGATGACCCGTG |
| | R | GGTCATCTCMNNGGCTGCCGC |
| | F | GAGATGNNKCGTGCCTTCAGCG |
| | R | GGCACGMNNCATCTCCAGGGC |

| | | |
|---|---|---|
| T292 | F | GCAACCTGNNKCTGCTGATCGTCG |
| | R | ATCAGCAGMNNCAGGTTGCCGAT |
| L293 | F | GC AAC CTG ACG DYK CTG ATC GTC G |
| | R | CGACGATCAGMRHCGTCAGGTTGC |
| V296 | F | GCTGCTGATCNNKGGCGGAAACG |
| | R | CGTTTCCGCCMNNGATCAGCAGC |
| T301 | F | GGAAACGACNNKACGCGCAACTC |
| | R | GAGTTGCGCGTMNNGTCGTTTCC |
| L344 | F | AGACCCCGNNKGCGTACATGCGA |
| | R | TCGCATGTACGCMNNCGGGGTCT |
| M347 | F | CTCGCGTACNNKCGACGGGTC |
| | R | GACCCGTCGMNNGTACGCGAG |
| F445 | F | TGCAGTCCAACNNKGTCCGTGGTTAC |
| | R | GTAACCACGGACMNNGTTGGACTGCA |

## 2.4 Screening of mutants based colorimetric HTS assay

According to the theoretical calculations, a total of 172 mutant clones are required for each amino acid residue to have 95 % coverage of all 20 possible amino acids (Nov 2012). Therefore, 180 clones for each site were taken and inoculated into two 96-deep well plates, where each well contained 200 µL of LB medium supplemented with 50 µg/mL of kanamycin. The deep-well plate was shaken at 500 rpm and 37 °C for 12 h. Each culture (30 µL) was transferred to a fresh deep-well plate containing 450 µL of TB medium supplemented with 50 µL/mL of kanamycin. After incubating the plate for 1 h at 37 °C, protein expression was induced by adding 0.01 mM IPTG, 0.5 mM ALA and 0.1 mM $FeSO_4$ at 30 °C for 16 h. The cells were harvested by centrifugation at 3500 rpm for 15 min. The cell pellets were thoroughly resuspended with 200 µL of 100 mM potassium phosphate buffer (pH 7.5) and disrupted by sonication. The lysates were centrifuged, and 30 µL of the supernatants were transferred to a new 96-well microplates containing 70 µL of substrate solution (100 mM phosphate buffer (pH7.5), 0.2 mM 16-methoxy palmitic acid, 0.4 mM $NADP^+$, 4 mM glucose, 0.1 U/mL of glucose dehydrogenase. After incubating for 20 min at 37 °C, Purpald (168 mM in 2 M NaOH) was added. After 15 min at room temperate, the absorbance of each well was measured at 550 nm.

## 2.5 Analysis by gas chromatography

Reactions were stopped by adding 0.2 mL $CHCl_3$ and the products were extracted with vigorous vortexing for 1 min. After centrifugation, the organic phase was transferred to an Eppendorf tube, and samples converted to their trimethylsilyl

derivatives by incubation at 50 °C for 20 min with an excess of BSTFA.

Qualitative analysis was performed by a Trace GC Ultra system (Thermo Scientific, Waltham, MA, USA), coupled to an ion trap mass detector ITQ 1100 (GC/MS). The GC injector (250 °C) was operated in a pulsed splitless mode, one microliter of the sample was injected and analyzed using a nonpolar capillary column (5 % phenyl methyl siloxane capillary 30 m × 0.25 mm i.d. × 0.25 μm film thickness, TR-5MS), and the GC oven started at 50 °C for 1 min, and was then increased by 15 °C/min to 250 °C, holding at this temperature for 10 min. Samples were transferred through a heated transfer line (275 °C) to an ion source (230 °C) in mass detector. Mass spectra were obtained by electron impact ionization at 70 eV.

Quantitative analysis was performed by an HP 6890 Series (Agilent Technologies, Santa Clara, CA, USA) with flame ionization detector (GC/FID). Two microliters of the sample was injected by split mode (split ratio 20:1) and analyzed using a nonpolar capillary column (5 % phenyl methyl siloxane capillary 30 m × 0.32 mm i.d. × 0.25 μm film thickness, HP-5). The GC oven temperature program was the same as that of the GC/MS. Each peak was identified by comparison of the GC chromatogram with that of an authentic reference. Errors in the analysis were corrected for by using heptadecanoic acid as the internal standard.

**2.6 Quantification of intracellular cofactors using LC-MS**

To quantify intracellular redox cofactors such as NAD(H) and NADP(H), *E.coli* BW25113 was incubated at 30 °C for 16 h. After harvest cells, quenching was done by mixing with methanol pre-chilled at -48 °C, and centrifuge for 10 min at 13000 rpm. The pellets were dissolved using 3 mL of MeOH, frozen in liquid nitrogen,

and allowed to thaw on ice three times. Extracted metabolite samples were analyzed using UPLC/triple quadrupole mass spectrometry (QQQ-MS) (Thermo Scientific, Waltham, MA, USA). The analysis was carried out following described procedures (Sung, Jung et al. 2015).

**2.7 Homology modeling and docking simulations**

The structure of CYP153A35 was obtained by homology modeling using Modeller 9.11 (Sali and Blundell 1993). CYP153A7 (PDB ID: 3RWL from *Sphingopyxis macrogoltabida*) used as a template has 53 % protein sequence identity with CYP153A35. The substrate entrance channels were investigated using CAVER 3.0 (Chovancova, Pavelka et al. 2012). Coordinates of Fe atom in heme were fixed as starting points. AutoDock Vina 1.1.2 (Trott and Olson 2010) and MGLTools 1.5.6 were used for docking simulation. Grid spacing, exhaustiveness and energy range were set as default, which were 20Å, 8, 5, respectively. Among the 20 docking poses generated from docking simulations, the one with the minimum docking energy value was selected. Docking results were evaluated via binding energy score and distance between terminal carbon of palmitic acid and Fe on heme.

# Chapter 3.

# ω-Hydroxylation using bacterial P450s (CYP153As)

### 3.1 Sequence alignment analysis of target CYP153As

CYP153A family was known to catalyze ω-hydroxylation reaction toward saturated and unsaturated fatty acids (Honda Malca, Scheps et al. 2012). To explore ω-hydroxylase activity of CYP153As toward fatty acids, two CYP153A sequences were selected by a BLAST search of GeneBank protein database using CYP153A33 protein sequence as a template, which showed the highest activity toward palmitic acid among the reported fatty acid ω-hydroxylases. From the search, the most promising two enzyme candidates were selected. One was CYP153A16 from *A. borkumensis,* which was well known as alkane ω-hydroxylase (van Beilen, Funhoff et al. 2006) with 80 % sequence identity. Another was putative CYP153A from *G. alkanivorans*, which showed 68% sequence identity with CYP153A33. Later, CYP153A from *G. alkanivorans* was classified as CYP153A35 (Nelson 1998).

Amino acid sequence analysis revealed a high sequence similarity and two distinct characteristics (Figure 3.1). First, the residues at the entrance of the substrate access channel are diverse, which may differentiate their substrate specificity and binding affinity according to alkyl chain length, methyl and carboxylic acid moiety. Second, CYP153 family contains a conserved sequence of NXXLLIVGGNDTT in the central I-helix implying that these residues might be responsible for high ω-regioselectivity of CYP153A.

### 3.2 Cloning of cyp153As and codon optimization of cyp153A13

Firstly, genetic sequence information of cyp153A13 and cyp153A35 was obtained from NCBI database (Figure 3.2). Two cyp153As were newly cloned to

pET24ma expression vector. CYP153A35 was well expressed functionally in *E.coli* BL21


**Figure 3.1 Sequence alignment of select regions of CYP153A family members.**

(A) Identification of critical residues of substrate access channel in CYP153A

(B) Conserved amino acid sequences in the central I-helix

whereas CYP153A13 was poor expressed. To improve the expression level of CYP153A13, the cyp153A13 gene was newly synthesized for codon optimization (Bioneer, Korea). The sequence of synthesized gene sub-cloned into T-vector was confirmed by sequencing (Figure 3,3).

### 3.3 Substrate specificity of three CYP153As *in vitro*

The hydroxylation activities of the three CYP153As for $C_{12:0}$–$C_{16:0}$ fatty acids were measured *in vitro* using CamAB as electron transfer partners. The specific activity of each enzyme system is shown in Figure 3.4. CYP153A35 showed the similar substrate specificity with CYP153A33 (Honda Malca, Scheps et al. 2012) such that the specific activity for myristic acid was the highest. It was seven times and 2.7 times higher than those for lauric acid and palmitic acid, respectively. In contrast, CYP153A13 had a broad substrate specificity towards $C_{12:0}$–$C_{16:0}$. Especially, the specific activity of CYP153A13 toward palmitic acid was two times higher than those of CYP153A33 and CYP153A35.

In terms of the regioselectivity, both CYP153A13 and CYP153A35 had high ω-regioselectivity similar to CYP153A33. (>92% of the total product, Table 3.1, Figure 3.5, 3.6)

### 3.4 Determination of kinetic parameters of CYP153As

Additional experiments confirmed that CYP153A13 was more active toward palmitic acid than CYP153A33 and CYP153A35 (Table 3.2). The turnover number (*kcat*) of CYP153A13 was 3.5 times and two times higher than that of CYP153A33 and CYP153A35, respectively. On the other hand, the Michaelis constant ($K_M$) of

>gi|193248874|dbj|AB426724.1| Gordonia alkanivorans goaBAC gene for cytochrome P450, complete cds

ATGCAGATCCTCGACCGCGTCGTTGAGACGGTGCAGGCGAACATCCCGCTGGACCGTCAGG
TTCAGGGCCTCCAGCTCTTCCACAAGACGCGTGCTCGCCTGCTCGGCGAGTCGCGGCCGGA
AACCTATGTGGAGCAGCCTATCCCGCCGGTCAACGAAGTCGGTCTGGACGAGATCGACATG
AGCAACCCGTTCATGTACCGGCAGGGGCAGTGGGTTCCCTACTTCGCTCGCCTCCGCGCCG
AGGCGCCGGTCCACTATCAGCCGGAAAGCCGGTTCGGCCCGTTCTGGTCGATCACCCGCTA
CGACGACATCATGACAGTCGACAAGGACCACGAGACCTTCTCGGCCGAACCCTTCATCGTG
ATCGGCACTCCCCCACCGGGCCTCGACGTCGAGATGTTCATCGCGATGGACCCGCCGCGGC
ATGACGAGCAGCGTCGCGCCGTTCAGGGCGTCGTCGCCCCGAAGAATCTCAAGGAGATGGA
AGGGCTGATCCGGGAACGCGTGTGCGAGGTTCTCGACAACCTTCCCGTCGGCGAACCGTTC
AATTGGGTCGATCGCGTTTCGGTCGAGATCACCGCCCGGACCCTGGCGACCATCCTCGACT
TCCCGTACGAGCAGCGGCGCAGTCTCGTCCGCTGGTCCGATCTCGCGTCCGGCAGCGAAGA
GGCCACCGGCGGCGCCAGCGATCCCGACGAGGTGTACGCGGCAGCCCTGGAGATGACCCGT
GCCTTCAGCGCGCTGTGGCACGACAAGGCCGCACGACGCGCCGCCGGCGAGGCACCGGGAT
TCGACCTCATCAGCATGCTGCAGTCCGATCCGAAGACCGCCGACCTAGTGAAGCGTCCGAT
GGAGTTCATCGGCAACCTGACGCTGCTGATCGTCGGCGGAAACGACACCACGCGCAACTCG
ATGTCGGGCGGTGTCTACGCACTGAACAAGTTCCCCGCCGAGTTCGAGAAGCTCAAGGCTG
ATCCGAGCCTGATCCCGAACATGGTGTCGGAGATCATCCGCTGGCAGACCCCGCTCGCGTA
CATGCGACGGGTCGCGAAGAAGGATGCGATTCTCAACGGCCAATTCATCCGCAAGGGCGAC
AAGCTGGTGATGTGGTACGCCTCGGGCAACCGGGACGAGACCAAGTTCGACAGCCCCGACG
AACTCATCATCGACCGGCCGAACGCCCGCAACCACATGGCATTCGGTTTCGGTGTGCACCG
GTGCATGGGCAACCGTCTCGCCGAACTGCAGCTGCGCATCCTCTGGGAAGAACTGCTGCAG
CGCTTCGATGACATCAAGGTCATCGAGGAACCCGAGTACGTGCAGTCCAACTTCGTCCGTG
GTTACAGCAAGCTGATGGTCGAACTCACGCCGAAGACACGGTCATGA

**Figure 3.2 Genetic sequence information of cyp153A35**

ATGTCAACGAGTTCAAGTACAAGTAATGACATTCAGGCAAAAATAATAAACGCCACATCTA
AAGTCGTCCCAATGCATCTGCAGATCAAAGCATTAAAAAACCTGATGAAGGTGAAACGGAA
GACAATTGGCACTTCCCGCCCACAGGTGCATTTTGTTGAAACCGACTTGCCTGACGTGAAT
GATTTGGCGATAGAAGATATCGATACGAGCAACCCTTTTTTATACCGACAAGGTAAAGCGA
ATGCCTACTTTAAGCGGTTGCGTGATGAAGCGCCGGTCCACTATCAGAAAAATTCTGCTTT
TGGGCCGTTCTGGTCGGTTACAAGGTACGAAGATATTGTCTTCGTAGACAAGAGCCATGAT
CTATTTTCAGCCGAGCCCCAAATTATTCTCGGTGACCCTCCGGAAGGCCTGTCTGTTGAAA
TGTTCATCGCTATGGATCCGCCCAAGCACGACGTACAGCGTCGGGCAGTCCAGGGTGTTGT
TGCGCCTAAAAATCTGAAAGAAATGGAGGGACTGATCCGCAAAAGAACCGGGGACGTACTG
GACAGCCTGCCGTTGGACACTCCGTTTAACTGGGTGCCTGTGGTGTCAAAAGAACTGACCG
GGCGGATGCTTGCTTCACTGTTAGATTTCCCGTATGACGAACGCGAAAAACTGGTTGGTTG
GAGTGATCGACTCTCCGGCGCGTCCTCGGCAACCGGCGGCGAGTTTACTAATGAAGATGTA
TTTTTTGATGACGCTGCAGATATGGCCTGGGCTTTCTCCAAACTTTGGCGTGATAAAGAGG
CCCGTCAAAAAGCAGGTGAAGAGCCGGGCTTCGATCTTATCTCTATGCTTCAGAGTAATGA
AGACACAAAAGATCTGATTAATCGTCCTTTAGAATTCATTGGTAATCTCGCGTTACTGATT
GTTGGAGGTAATGATACTACGCGTAACTCAATGAGCGGGGGAGTGCTGGCTCTCAATCAGT
TCCCCGAGCAGTTTGAGAAGCTAAAAGCGAACCCAAAGCTGATCCCCAATATGGTCTCTGA
AATCACTCGCTGGCAAACCCCGCTTGCATATATGCGCCGTGTTGCCAAGCAGGATGTGGAG
CTGAATGGACAGACCATCAAGAAGGGTGATCGCGTACTGATGTGGTATGCGAGCGGCAACC
AGGATGAGAGAAAATTCGAGAATCCAGAGCAATTTATTATAGATCGCAAAGATACGCGTAA
CCATGTGAGCTTTGGTTATGGAGTTCACAGATGTATGGGCAACCGCCTTGCCGAACTGCAG
CTGCGTATTCTGTGGGAAGAGCTTTTGCCACGCTTTGAAAACATAGAAGTAATTGGTGAAC
CGGAGAGAGTGCAATCGAATTTTGTAAGGGGGTATTCCAAAATGATGGTTAAATTGACGGC
AAAAAAATAA

**Figure 3.3 Genetic sequence information of codon optimized cyp153A13**

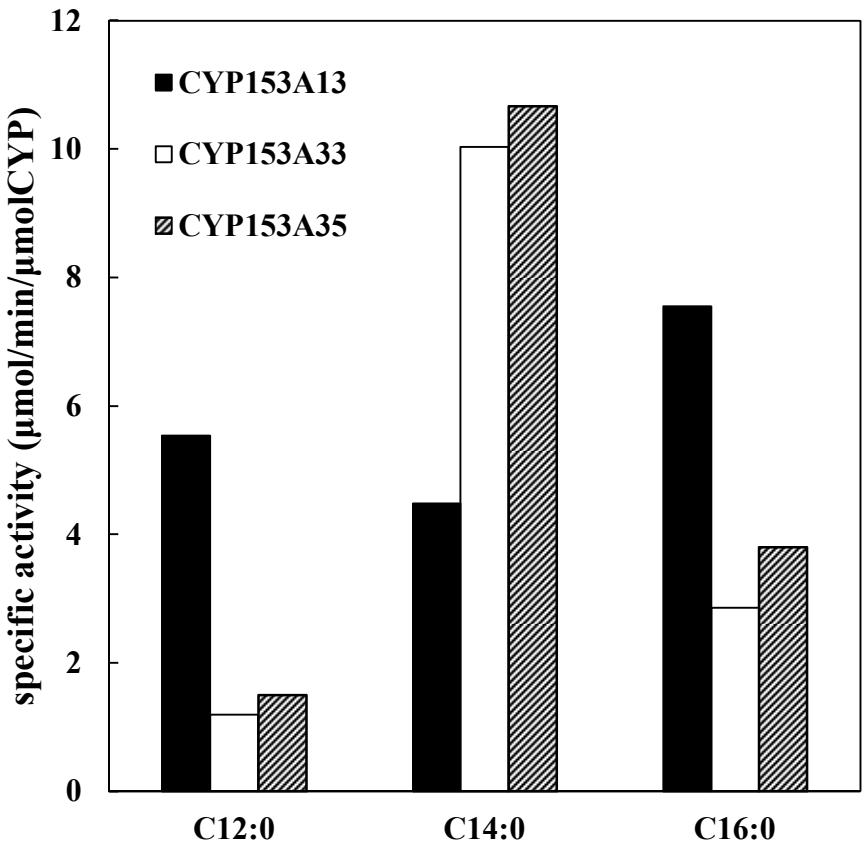


**Figure 3.4 Specific activity of CYP153As for fatty oxidation reaction using purified enzyme.**

Reaction mixture contained 2 μM P450, 10 μM CamA, 20 μM CamB, 0.5 mM substrate, 2 % DMSO, 0.5 mM NADH with cofactor regeneration.

**Table 3.1 Product distributions in oxidation reactions catalyzed by CYP153As**

| | $C_{12:0}$ | | $C_{14:0}$ | | $C_{16:0}$ | |
|---|---|---|---|---|---|---|
| **Enzyme** | **(ω-1)-OH** | **ω-OH** | **(ω-1)-OH** | **ω-OH** | **(ω-1)-OH** | **ω-OH** |
| **CYP153A13** | **-** | **100** | **7.2** | **92.8** | **2.9** | **97.1** |
| **CYP153A33** | **-** | **100** | **4.0** | **96.0** | **-** | **100** |
| **CYP153A35** | **-** | **100** | **-** | **100** | **-** | **100** |

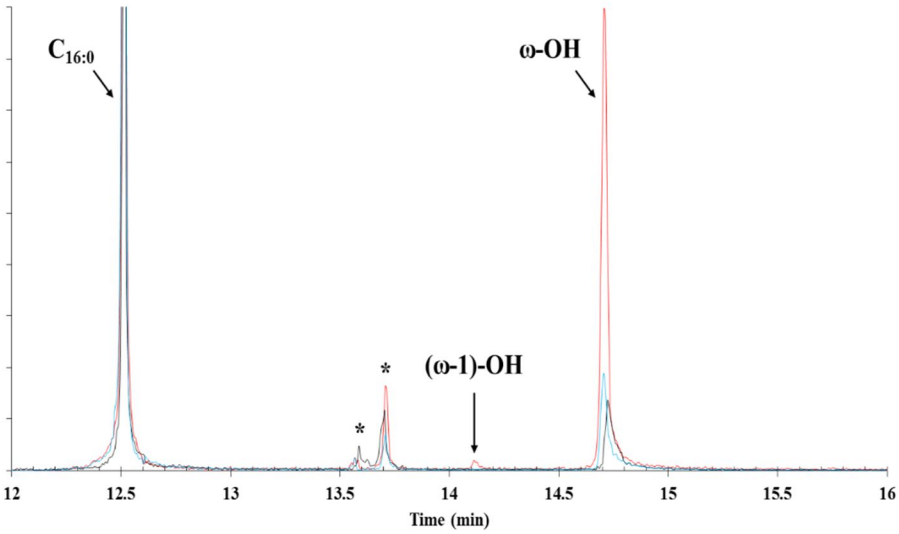


**Figure 3.5 GC/MS total ion current (TIC) of CYP153A-catalyzed reactions with palmitic acid.**

CYP153A13 (red line), CYP153A33 (black line), and CYP153A35 (blue line). Abbreviations: C16:0, palmitic acid; (ω-1)-OH, 15-hydroxy palmitic acid; ω-OH, 16-hydroxy palmitic acid; * impurity

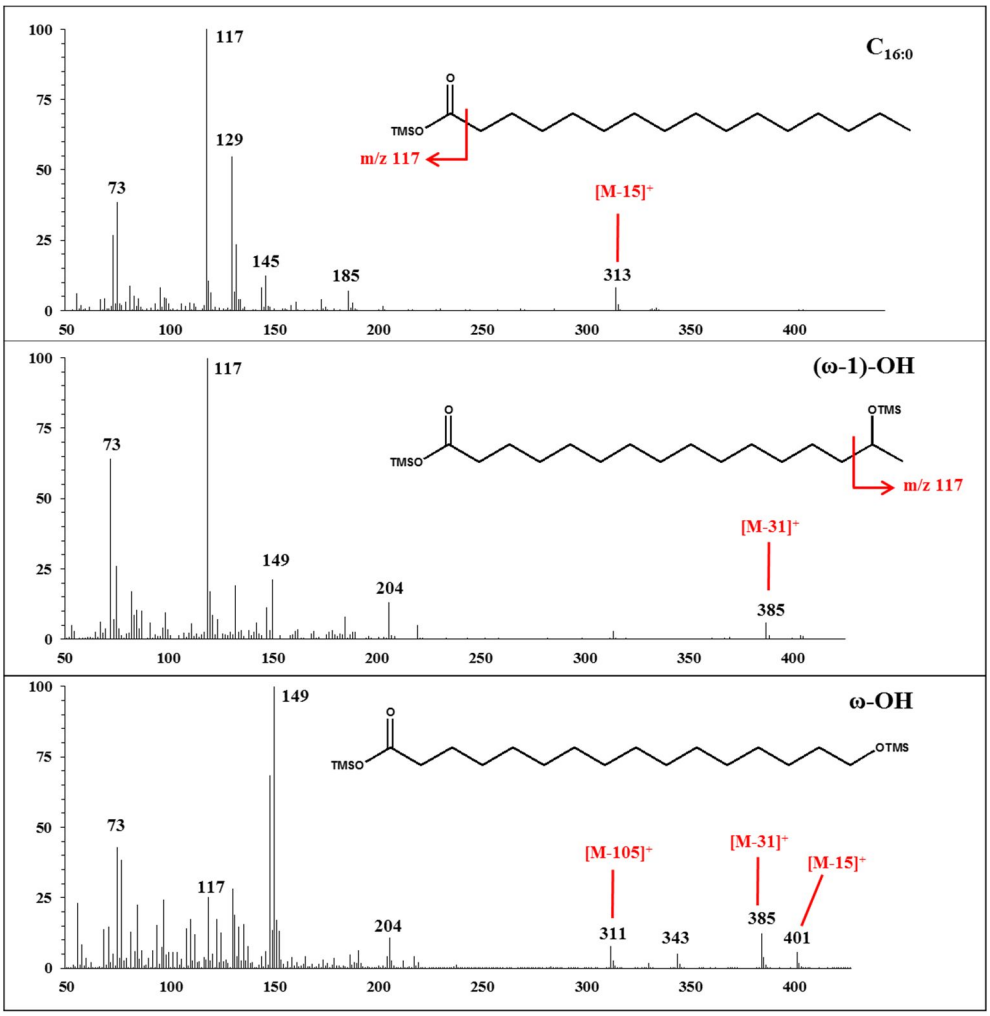


**Figure 3.6 Mass spectra of TMS derivatives of (hydroxylated) palmitic acid.**

The common fragment ion m/z =73 occurs upon the loss of one TMS ester group. The fragment ion m/z =149, typical of polysylated compounds, involves the loss of a methyl radical from one silyl group and its interaction with another TMS ester group. Characteristic peaks of each derivatives are indicated in the corresponding mass spectrum.

CYP153A13 was 1.5 times higher than that of CYP153A33 and similar to that of CYP153A35. In terms of catalytic efficiency, the specificity constant, $k_{cat}/K_M$, of CYP153A13 was the highest among the three CYP153As.

### 3.5 Substrate specificities of CYP153As in whole-cell reaction

To apply CYP153A for large scales industrial process, using isolated enzyme has disadvantages for maintaining enzyme stability and supply of expensive nicotinamide cofactors (Woodley 2006). Therefore, the activities of three CYP153As were re-evaluated with individual whole-cell reaction co-expressing CamAB as redox partners. pCYP153A13, pCYP153A33 and pCYP153A35 were all transformed with pCamAB into *E.coli* DL (Δ*fad*D, pFadL), generating A13-AB1, A33-AB1 and A35-AB1 strains, respectively. To minimize the changes in enzyme concentration by cell growth and to maintain NADH cofactor regeneration, a resting cell reaction in the presence of glucose (1 % *w/v*) and fatty acid (1 mM of each $C_{12:0}$–$C_{16:0}$ fatty acid) in phosphate buffer solution (pH 7.5) was used for fatty acid hydroxylation. To compare the initial reaction rate, the reaction media were sampled every two hours for several points in time.

Interestingly, the activities of CYP153As using whole-cell were completely different from those using purified enzymes (Figure 3.7). The resting cell assay revealed that the specific ω-hydroxylation activities of CYP153A35 and CYP153A33 for palmitic acid in *in vitro* reaction were almost the same. A35-AB1 strain resulted 193 μM/h and 176 μM/h productivities toward $C_{14:0}$ and $C_{16:0}$, which were 2.5 times and 1.6 times higher than those of A33-AB1 strain (78 μM/h for $C_{14:0}$ and 109 μM/h for $C_{16:0}$).

**Table 3.2 Kinetic constants of CYP153A13, CYP153A33 and CYP153A35 towards palmitic acid.**

| Enzyme | $K_M$ (mM) | $k_{cat}$ ($min^{-1}$) | $k_{cat}/K_M$ ($min^{-1}mM^{-1}$) |
|---|---|---|---|
| **CYP153A13** | **0.35 ±0.05** | **16.35 ±3.15** | **46.71 ±3.0** |
| **CYP153A33** | **0.24 ±0.03** | **4.63 ±1.22** | **19.3 ±1.1** |
| **CYP153A35** | **0.39 ±0.05** | **7.12 ±3.02** | **17.9 ±2.8** |

* 1 μM CYP153A, 5 μM CamA and 10 μM CamB were used for measurement.

On the other hand, the productivity of A35-AB1 strain with $C_{12:0}$ was twice lower than that of A33-AB1 strain. Therefore, A33-AB1 strain was the best for the production of 12-hydroxy lauric acid, whereas A35-AB1strain resulted the highest yield for the production of 14-hydroxy myristic acid and 16-hydroxy palmitic acid. Second, A13-AB1 strain showed only 70 μM/h, 55 μM/h, 60 μM/h productivities of the corresponding ω-hydroxylated products of $C_{12:0}$, $C_{14:0}$ and $C_{16:0}$, respectively. It was somewhat unexpected result because CYP153A13 in *in vitro* reaction showed the highest specific activity toward lauric acid and palmitic acid. To figure out the differences between the whole-cell activities and specific activities of CYP153As in *in vitro* reaction, the quantification of active P450 enzyme concentration was carefully carried out by CO-binding and SDS-PAGE gel analysis (Table 3.3, Figure 3.8) (Omura and Sato 1964), after the cell suspensions were concentrated to final $OD_{600}$ of 20. The functional expression level of CYP153A35 was the highest among the three CYP153As, hence supporting the results of the highest whole-cell activity toward palmitic acid. Whereas CYP153A13 showed the lowest functional expression level, suggesting that protein solubility and functional protein expression level are key determinants to achieve high yield of ω-hydroxylation of fatty acids. In results, CYP153A13 was unsuitable for the production of ω-hydroxy palmitic acid for whole-cell reaction system even though it showed good specific activity, and further yield improvement experiments using whole-cell system was proceeded with CYP153A35.

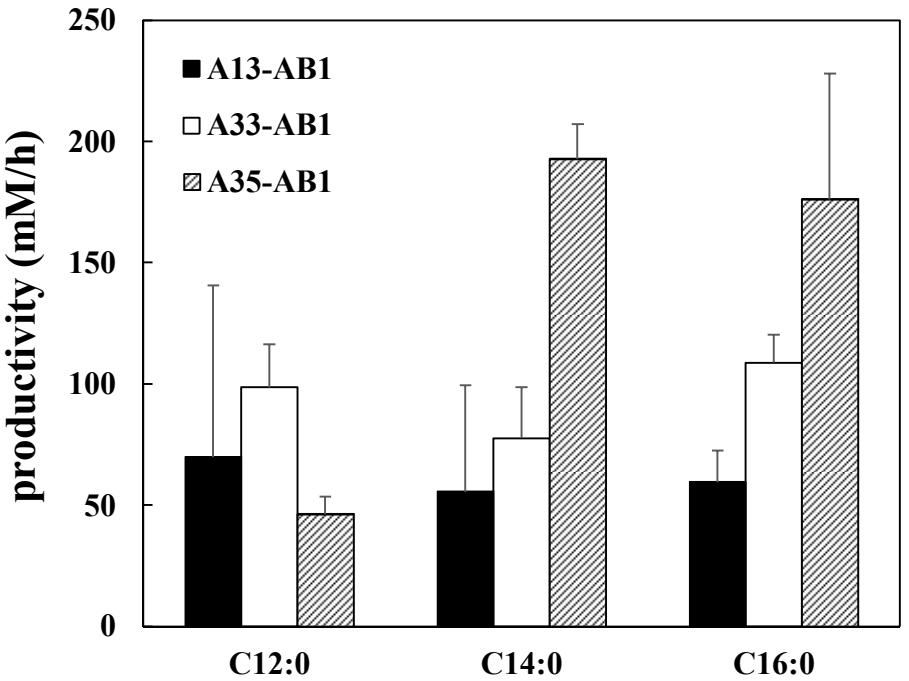


**Figure 3.7 Whole cell reaction of CYP153As for fatty oxidation reaction**

Whole cell reaction of CYP153A13, CYP153A33 and CYP153A35 was performed with 1 mM each fatty acid. The ODs at 600 nm of the cell suspensions were 20.

**Table 3.3 Concentration of CYP153As based on CO binding assay**

| Strain | A13-AB1 | A33-AB1 | A35-AB1 |
|---|---|---|---|
| [P450] ($nmol/g_{DCW}$) [a] | 11.0 | 49.8 | 90.0 |

[a] Values were obtained by triplicate experiments with standard deviations within ≤10%

**(A)**

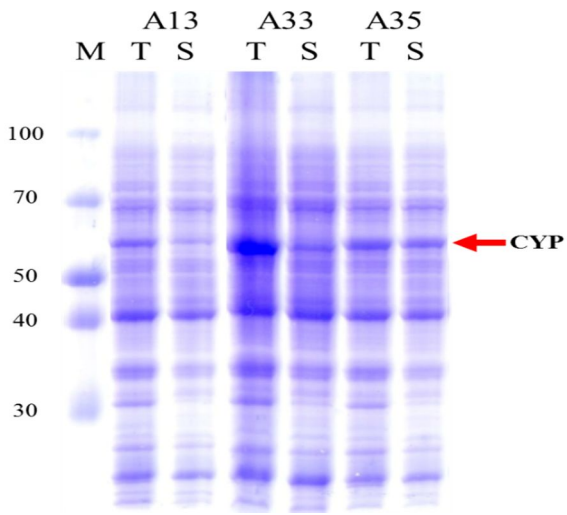


**(B)**

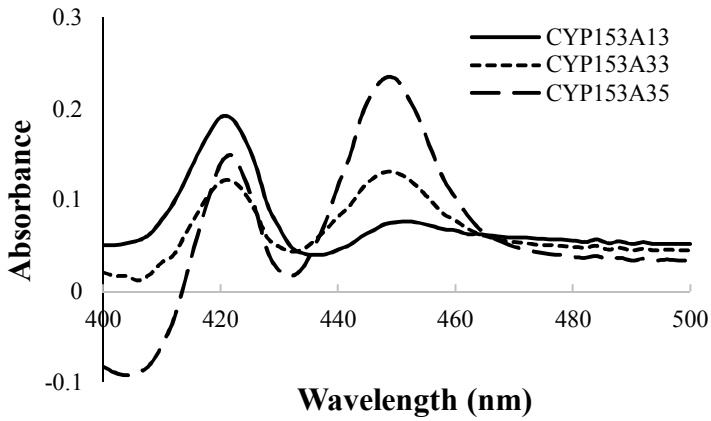


**Figure 3.8 Expression of CYP153As in *E.coli* BL21**

(A) Detection of P450 expression using SDS-PAGE (*M*, mid-range marker; *T*, total; *S*, soluble)

(B) CO-binding spectra of CYP153A13, CYP153A33, and CYP153A35. Solid line, CYP153A13; dotted line, CYP153A33; dashed line, CYP153A35.

# Chapter 4.

# Comparison and optimization of CYP electron transfer system

## 4.1 Hydroxylation activity of CYP153A35 with different redox systems

### 4.1.1 Electron transfer efficiency of CamAB and self-sufficient system

Among various electron transfer systems for CYP reactions, class I (CYP153A35 and CamAB) and class VIII (CYP153A35-BMR fusion) were selected for CYP153A35. In CYP153A35 and CamAB system, electron transfer occurs following the sequence of NADH → FAD (CamA) → 2Fe-2S (CamB) → Heme (P450), whereas in CYP153A35-BMR fusion system, where cyp153A35 was fused to the reductase domain of cyp102A1 without using any additional linker, initial electron donor would be NADPH and follows NADPH → FAD (BMR) → FMN (BMR) → Heme (P450). The fusion protein was functionally expressed (Figure 4.1) and purified to examine the activity toward palmitic acid. The product formation rate of CYP153A35-BMR in *in vitro* reaction was five times higher than that of CYP153A35+CamAB for palmitic acid, whereas a NAD(P)H consumption rate is rather similar (Table 4.1), indicating that coupling efficiency for electron transfer of CYP153A35-BMR is four times higher than that of CYP153A35+CamAB.

### 4.1.2 Comparison of yield of CamAB and self-sufficient system

A35-BMR strain was also constructed by transforming pCYP153A35-BMR into *E.coli* DL (Δ*fad*D, ::pFadL) and whole-cell reactions were compared. The final product yield of A35-AB1 and A35-BMR at 1 mM palmitic acid for 6 h reaction time were 98 % and 65 %, respectively (Figure 4.2), indicating that the class VIII self-sufficient system is no longer better than class I system in whole-

cell reaction, which is rather surprising and contradictory to our current understanding. To our

**(A)**

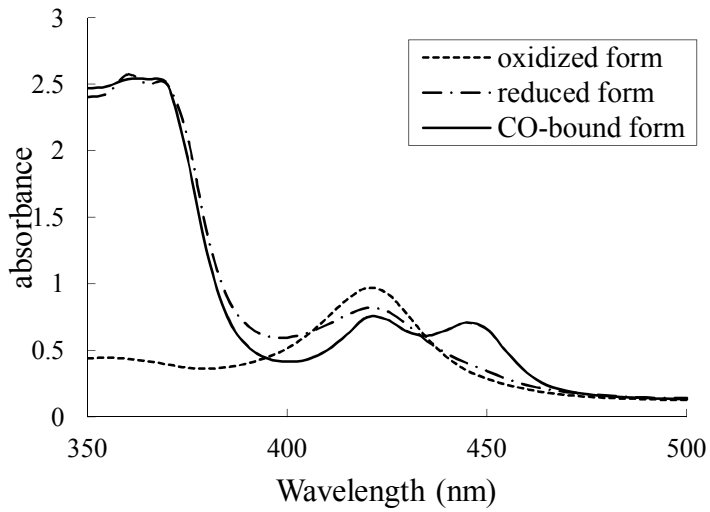


**(B)**

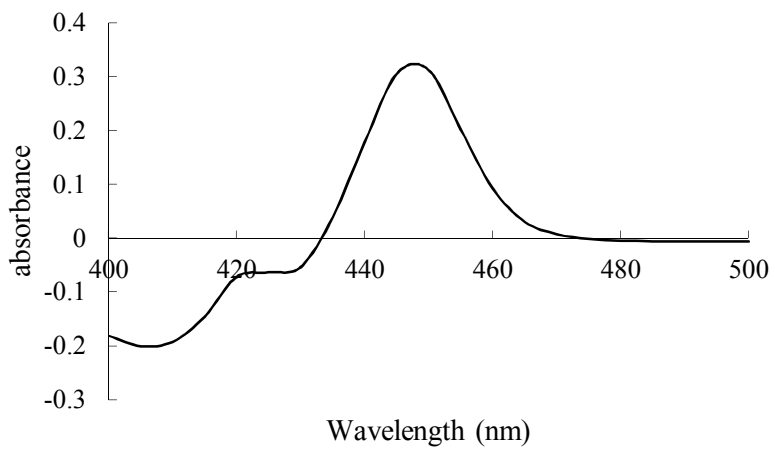


**Figure 4.1 UV-visible absorbance spectra of purified CYP153A35-BMR**

(A) Dotted line, oxidized form; dashed line, reduced form with dithionite; solid line, CO-difference spectra

(B) CO-binding spectra of CYP153A35-BMR

**Table 4.1 NAD(P)H consumption, product formation, and coupling efficiency of CYP153A35 by different electron transfer system toward fatty acid[a]**

| | CamA/CamB | | | fused CYP102A1 reductase | | |
|---|---|---|---|---|---|---|
| **Substrate** | **NADH consumption rate (uM/min)** | **Product formation rate [b] (uM/min)** | **Coupling efficiency (%)** | **NADPH consumption rate (uM/min)** | **Product formation rate (uM/min)** | **Coupling efficiency (%)** |
| **$C_{12:0}$** | **13.9** | **nd [c]** | **- [d]** | **23** | **nd [b]** | **- [c]** |
| **$C_{14:0}$** | **22** | **1.1** | **5.0** | **31.3** | **8.5** | **27.1** |
| **$C_{16:0}$** | **21.1** | **1.3** | **6.0** | **27.8** | **6.6** | **23.7** |

[a] Values were obtained by triplicate experiment with standard deviations within ≤10 %

[b] Product was ω-hydroxy fatty acid

[c] not determined

[d] no calculation

surprise, the evaluation of functional CYP153A35 concentrations between the two systems based on CO binding assay showed almost the same amount of P450s (Table 4.2). This is one of the rare cases of showing such that CYP+CamAB system is better than its own self-sufficient CYP system in whole-cell reaction.

To explain this results, the concentrations of NAD(H) and NADP(H) in *E.coli* BW25113(DE3) were measured (Table 4.3). According to our analysis, total amount of NADH is about twice higher than NADPH in *E.coli* BW25113, suggesting that the concentration of electron donor in CamAB system would be twice higher than that in self-sufficient system in whole-cell.

## 4.2 Optimization for CYP153A35 and CamAB

### 4.2.1 Specific activity depends on ratio of CYP153A35 and CamAB *in vitro*

Rate-limiting step in P450 reaction is often the transfer of the second electron to an oxy-P450-substrate complex, thus the oxidation rate of P450 was seriously affected by the relative ratios of P450 to redox partners (Girhard, Klaus et al. 2010). To enhance the oxidation rates of CYP153A35, optimization of the expression ratios of the redox partners was investigated through varying concentrations of each redox protein in *in vitro* reaction system. As somewhat expected, it was observed that the relative concentrations of CamAB versus CYP153A35 showed a significant effect on the activity of CYP153A35 toward palmitic acid (Table 4.4). For example, the increase in CamA concentration from 1:1:10 (P450:CamA:CamB) up to a ratio of 1:5:10 resulted an almost two times improved product yield of ω-

hydroxylation from 7.5% up to 15.7 % at 0.2 mM palmitic acid, respectively, whereas the increase in

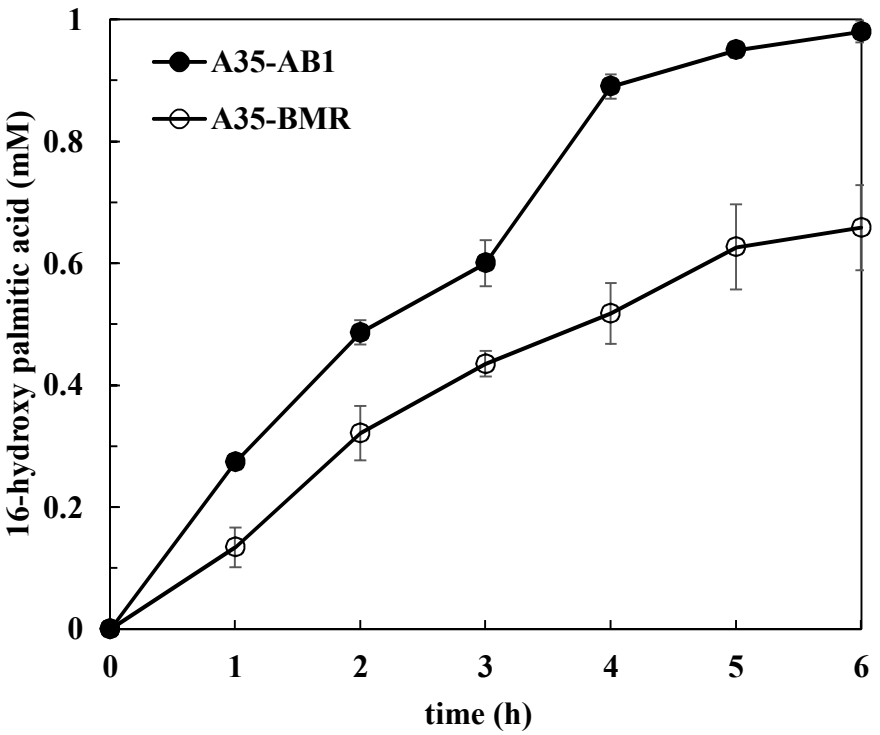


**Figure 4.2 Resting cell reaction for the production of 16-hydroxy fatty acid using A35-AB1 and A35-BMR strains**

Reaction was performed with 1 mM palmitic acid. The OD at 600 nm of the cell suspensions were 20.

**Table 4.2 Concentration of CYP153A35 and CYP153A35-BMR based on CO binding assay**

| Strain | A13-AB1 | A35-BMR |
|---|---|---|
| [P450] (nmol/$g_{DCW}$) [a] | 90.0 | 84.4 |

[a] Values were obtained by triplicate experiments with standard deviations within ≤10 %

**Table 4.3 Quantification of NAD(H) and NADP(H) in *E.coli* BW25113(DE3)**

| | $NAD^+$ | NADH | $NADP^+$ | NADPH |
|---|---|---|---|---|
| **Conc. ($\mu mol/g_{DCW}$) [a]** | **9.38** | **0.56** | **1.0** | **0.3** |

[a] Values were obtained by triplicate experiments with standard deviations within ≤10 %

CamB concentration ratio from 1:2:5 to 1:2:20 resulted much higher folds increased product yield of ω-hydroxylation from 3.7 % up to 30.7 %, respectively, suggesting that CamB concentration is a bottleneck for the *in vitro* activity reconstitution of CYP153A35. Finally, the product yield of ω-hydroxylation increased up to 66.2 % at 0.2 mM palmitic acid when the ratio of CYP153A35:CamA:CamB was optimized to 1:5:20.

### 4.2.2 Controlling of protein expression of CYP153A35 with CamAB

In order to maintain the same ratio of the three proteins in *E.coli* cell system with that obtained from *in vitro* system, several gene arrangements and promoter strength change were investigated and their effects on the production of ω-hydroxy palmitic acid were evaluated. To achieve this, several expression vectors were constructed. Since CamB concentration should be much higher than CamA and CYP153A35, camB was located in upfront position after T7 promoter, and camA and cyp153A35 were sequentially situated. Furthermore, relatively weak tac promoter was used for achieving lower expression level of CamA and CYP153A35. Four expression systems, A35-AB2 (Δ*fad*D, pFadL, pCamB-CYP153A35-CamA), A35-AB3 (Δ*fad*D, pFadL, pCamB-CamA-CYP153A35), A35-AB4 (Δ*fad*D, pFadL, pCamB-CYP153A35, pCW-CamA) and A35-AB5 (Δ*fad*D, pFadL, pCamB-CamA, pCW-CYP153A35) were constructed and compared using A35-AB1 (Δ*fad*D, pFadL, pCYP153A35, pCamAB) as a control (Figure 4.3).

**Table 4.4 Production of ω-hydroxy palmitic acid by CYP153A35 and CamAB system with varying ratios of redox partner proteins**

| P450:CamA:CamB [μM] | Product yield (%)[a] |
|---|---|
| 1:1:1 | nd[b] |
| 1:1:5 | nd |
| 1:1:10 | 7.5 |
| 1:1:20 | 28.1 |
| 1:2:5 | 3.7 |
| 1:2:10 | 4.5 |
| 1:2:20 | 10.7 |
| 1:5:1 | 2.2 |
| 1:5:5 | 7.0 |
| 1:5:10 | 15.7 |
| 1:5:20 | 66.2 |

[a] Product yield was determined with 0.2 mM palmitic acid after 1 h. Values were obtained by triplicate experiment with standard deviations within ≤10 %

[b] not determined

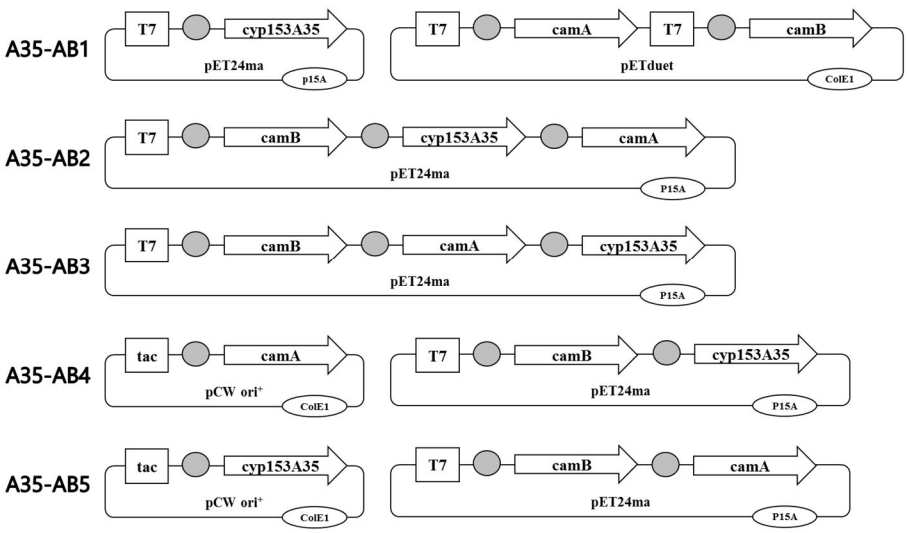


**Figure 4.3 Schematic representation of the plasmid systems used for modulating CYP153A35 and CamAB**

The gray dot upstream of the target genes represents Shine-Dalgarno sequences.

### 4.2.3 Comparison of productivity and yield of various constructs

As shown in Figure 4.4, A35-AB2 resulted the highest product yield for ω-hydroxy palmitic acid in batch flask reaction at 5 mM of palmitic acid, which is 66% improvement compared A35-AB1 with two vectors using each T7 promoter for the three genes. The cases of A35-AB2 and A35-AB3 showed that only gene arrangement can make a difference in 50 % product yield of ω-hydroxylation reaction. The quantification of CYP153A35 concentration was also carried out by CO-binding in each system (Table 4.5). To our surprise, despite the low product yield of A35-AB1 strain, the functional expression level of CYP153A35 was the highest in A35-AB1 strain. In addition, although the product yield of A35-AB1 was only 20% higher than that of A35-AB5, the measured concentration of CYP153A35 in A35-AB1strain was ten times higher than that of CYP153A35 in A35-AB5, suggesting that excess CYPA35 expressed in A35-AB1strain does not function properly for the production of ω-hydroxy palmitic acid. The lack of correlation between the concentration of CYP153A35 and the production of ω-hydroxy palmitic acid indicates that optimal ratio between CYP153A35 and CamAB to achieve high electron transfer efficiency is more important to obtain the maximal production of ω-hydroxy palmitic acid.

### 4.2.4 Fed-batch reaction

In order to evaluate such rankings of product yield and productivity are maintained in fed-batch reaction with glucose feeding and pH control at pH 7.5, A35-AB1 and A35-AB2 strain were compared using 20 mM (5.1 g/L) of palmitic acid initial substrate concentration for 30 h reaction time. Surprisingly again, their

rankings

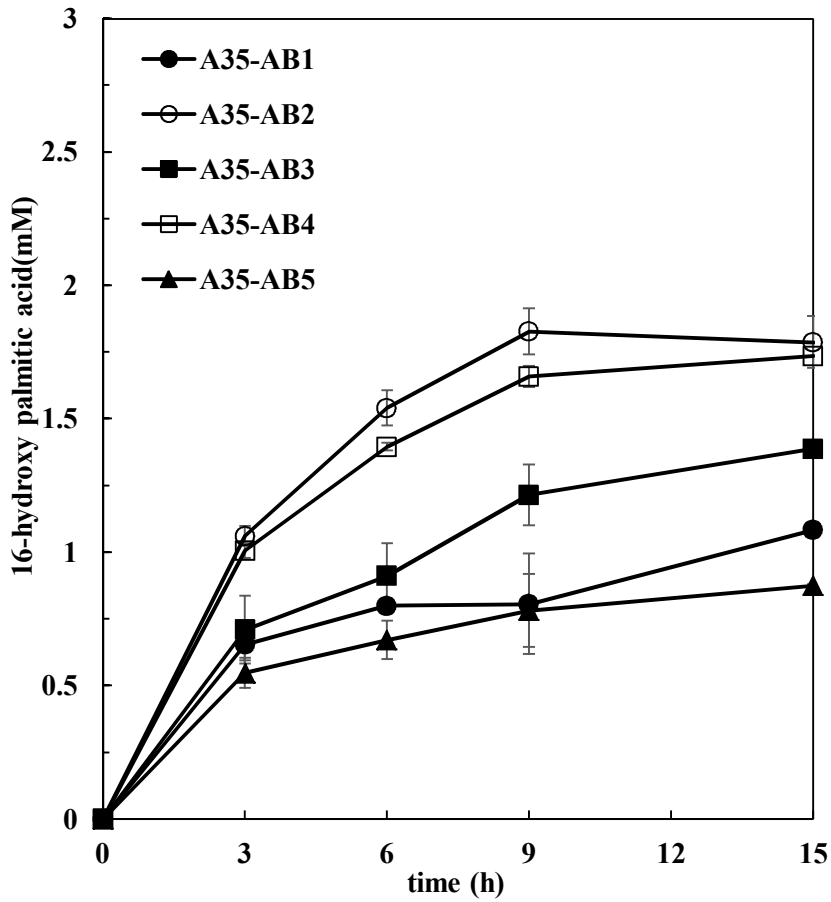


**Figure 4.4 Reaction profiles of the different expression systems for CYP153A35 and CamAB**

Reactions were performed with 5 mM palmitic acid

**Table 4.5 Concentration of CYP153A35 based on CO binding assay**

| Strain | A35-AB1 | A35-AB2 | A35-AB3 | A35-AB4 | A35-AB5 |
|---|---|---|---|---|---|
| [P450] ($nmol/g_{DCW}$) [a] | 90.0 | 55.1 | 16.5 | 44.0 | 9.2 |

[a] Values were obtained by triplicate experiments with standard deviations within ≤10 %

of final product yields in batch reaction were different in fed-batch reactions. A35-AB1 strain resulted the highest product yield of 17.0 mM (4.6 g/L) of ω-hydroxy palmitic acid (Figure 4.6) and 154 mg/L/h of the productivity, which are 1.9 times increased product yield of 8.8 mM (2.4 g/L) and 2.3 times enhanced productivity (66 mg/L/h) compared to A33-AB1strain (Bae, Park et al. 2014). Whereas A35-AB2 strain only produced 11.1 mM (3.0 g/L) of ω-hydroxy palmitic acid, although the initial productivity within 6 h was 1.2 times higher than that of A35-AB1 strain, suggesting that CYP expression level and stability become more important for long time fed-batch production of ω-hydroxy fatty acids. This result also indicated that comparison of mutants in batch type reaction does not always agree with the evaluation in fed-batch reaction in the case of CYPA35 reaction for higher product concentrations. This is one example of P450 reaction why it is very tricky to perform a correct evaluation of P450 reaction system.

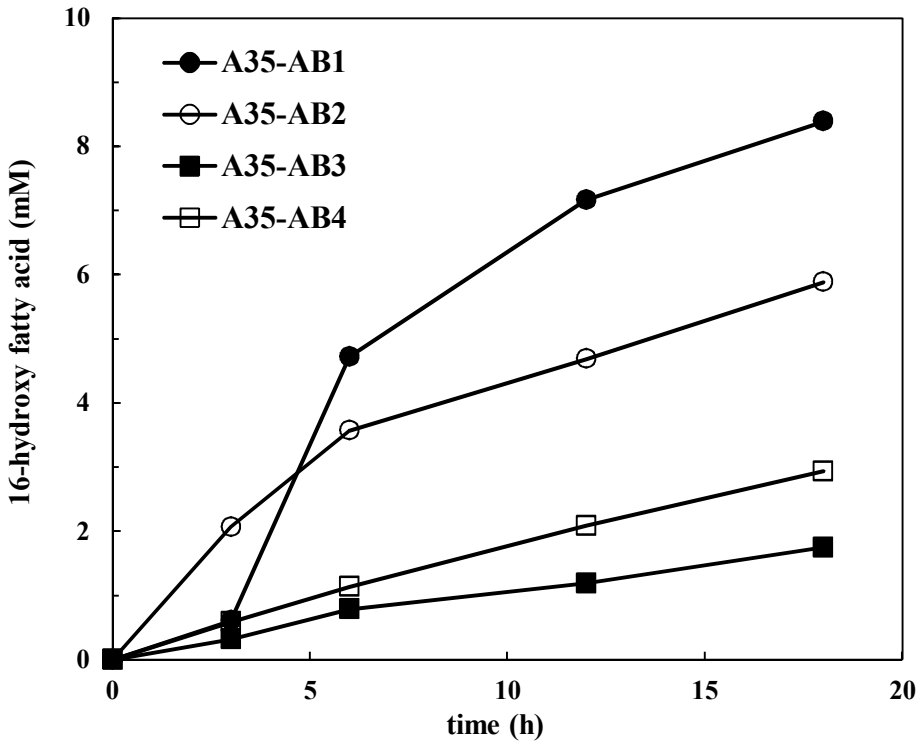


**Figure 4.5 Fed-batch reaction time profiles of the different expression systems for production of 16-hydroxy palmitic acid**

Reactions were performed with 10 mM palmitic acid. 0.4 % glucose was added every 6 h.

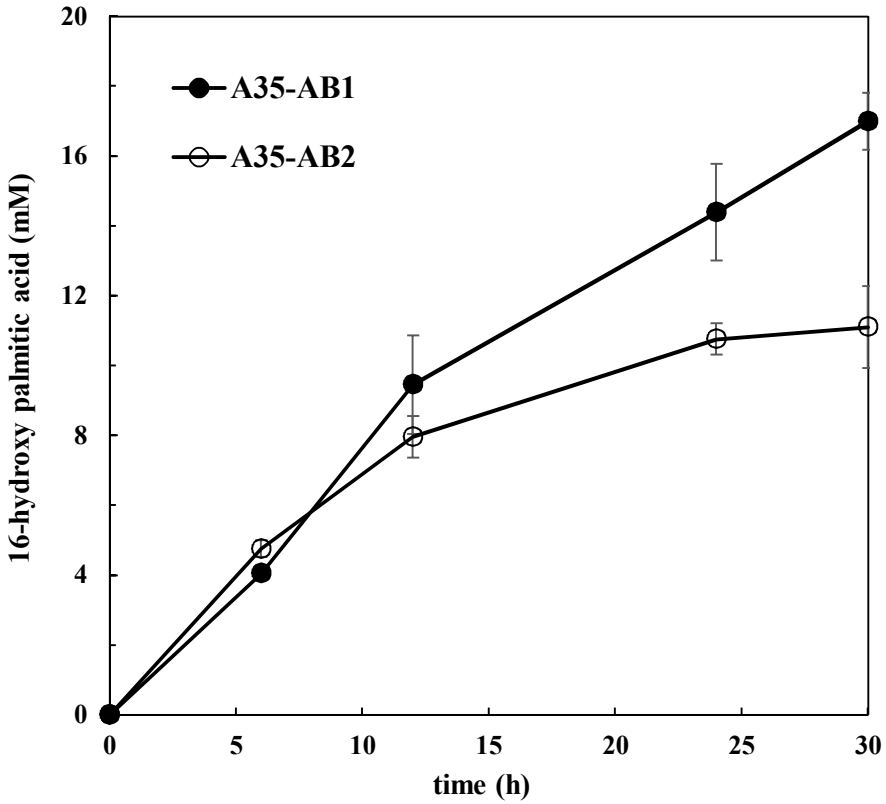


**Figure 4.6 Fed-batch reaction time profiles of A35-AB1 and A35-AB2 for production of 16-hydroxy palmitic acid**

Reactions were performed with 20 mM palmitic acid using A35-AB1 and A35-AB2 strains.

### 4.3 Optimization for CYP153A13 and CamAB

#### 4.3.1 Specific activity depends on ratio of CYP153A13 and CamAB *in vitro*

Similar to CYP153A35 and CamAB system, the optimization of the expression ratios of the redox partners was investigated through varying concentrations of each redox protein in *in vitro* reaction system to enhance the oxidation rates of CYP153A13. As somewhat expected, it was observed that the relative concentrations of CamB showed a significant effect on the activity of CYP153A13 toward palmitic acid (Table 4.4). Although the increase in CamA concentration did not affect ω-hydroxylation activity of CYP153A13, the increase in CamB concentration ratio from 1:1:1 to 1:1:10 resulted 5.1 times improvement of ω-hydroxylation activity of CYP153A13, suggesting that CamB concentration is a bottleneck for the *in vitro* activity reconstitution of CYP153A13.

#### 4.3.2 Controlling of protein expression of CYP153A13 with CamAB

In order to maintain the same ratio of the three proteins in *E.coli* cell system with that obtained from *in vitro* system, several gene arrangements and promoter strength change were investigated and their effects on the production of ω-hydroxy palmitic acid were evaluated. To achieve this, several expression vectors were constructed. Since CamB concentration should be much higher than CamA and CYP153A13, camB was located in upfront position after T7 promoter, and cyp153A13 and camA were sequentially situated. Furthermore, relatively weak tac promoter was used for achieving lower expression level of CamA and CYP153A13. Three expression systems, A13-AB2 (Δ*fad*D, pFadL, pCamB-

CYP153A13-CamA), A13-AB3

**Table 4.6 Production of ω-hydroxy palmitic acid by CYP153A13 and CamAB system with varying ratios of redox partner proteins**

| P450:CamA:CamB [μM] | Relative activity (%)[a] |
|---|---|
| **1:1:1** | **100** |
| **1:1:5** | **306** |
| **1:1:10** | **514** |
| **1:2:1** | **112** |
| **1:2:5** | **380** |
| **1:2:10** | **539** |
| **1:5:5** | **331** |
| **1:5:10** | **464** |
| **1:5:20** | **595** |

[a] Product yield was determined with 0.5 mM palmitic acid after 2 h.

(Δ*fad*D, pFadL, pCamB-CYP153A13, pCW-CamA) and A35-AB4 (Δ*fad*D, pFadL, pCamB-CamA, pCW-CYP153A13) were constructed and compared using A13-AB1 (Δ*fad*D, pFadL, pCYP153A13, pCamAB) as a control (Figure 4.7).

### 4.3.3 Comparison of productivity and yield of various constructs

As shown in Figure 4.8, A13-AB2 resulted the highest product yield for ω-hydroxy palmitic acid in batch flask reaction at 1 mM palmitic acid, which is 50 % improvement compared A13-AB1 with two vectors using each T7 promoter for the three genes. The quantification of CYP153A13 concentration was also carried out by CO-binding in each system (Table 4.7). To our surprise, the solubility of CYP153A13 increased as cyp153A13 gene located after camB under T7 promoter, which might cause week expression of CYP153A13 (Figure 4.9). In addition, although the product yield of A13-AB1 was only 20% higher than that of A13-AB4, the measured concentration of CYP153A13 in A13-AB1 strain was ten times higher than that of CYP153A13 in A13-AB5, suggesting that the functional expression of CYP153A13 caused the enhancement of production of ω-hydroxy palmitic acid.

### 4.3.4 Fed-batch reaction

In order to evaluate such rankings of product yield and productivity are maintained in fed-batch reaction with glucose feeding and pH control at pH 7.5, A13-AB1, A13-AB2 and A13-AB3 strain were compared using 10 mM (2.6 g/L) palmitic acid initial substrate concentration for 24 h reaction time. Surprisingly again, their rankings of final product yields in batch reaction were different in fed-

batch reactions. A13-AB3 strain resulted the highest product yield of 4.8 mM (1.3 g/L) ω-hydroxy palmitic

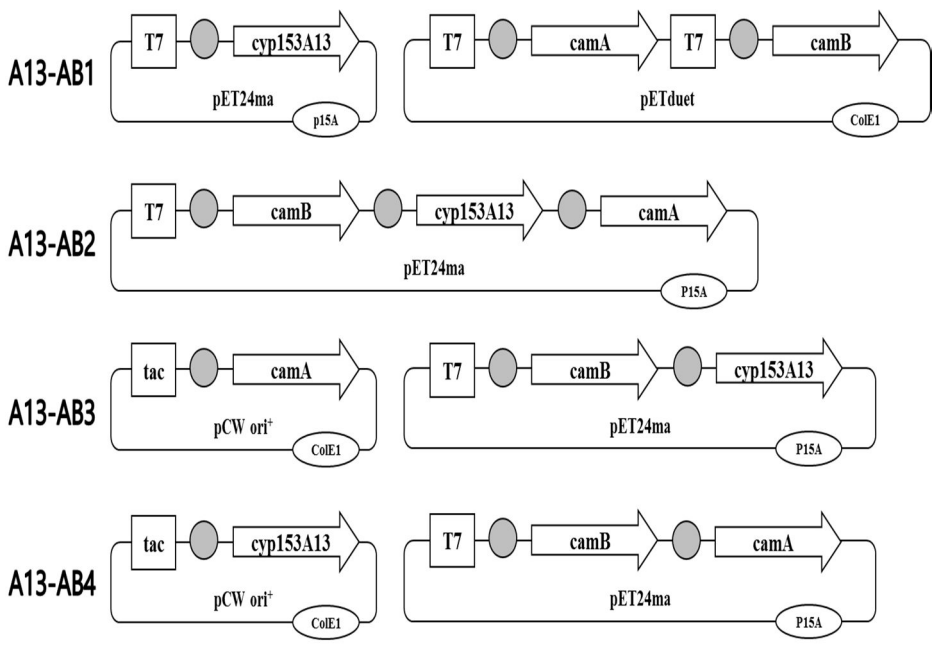


**Figure 4.7 Schematic representation of the plasmid systems used for modulating CYP153A13 and CamAB**

The gray dot upstream of the target genes represents Shine-Dalgarno sequences.

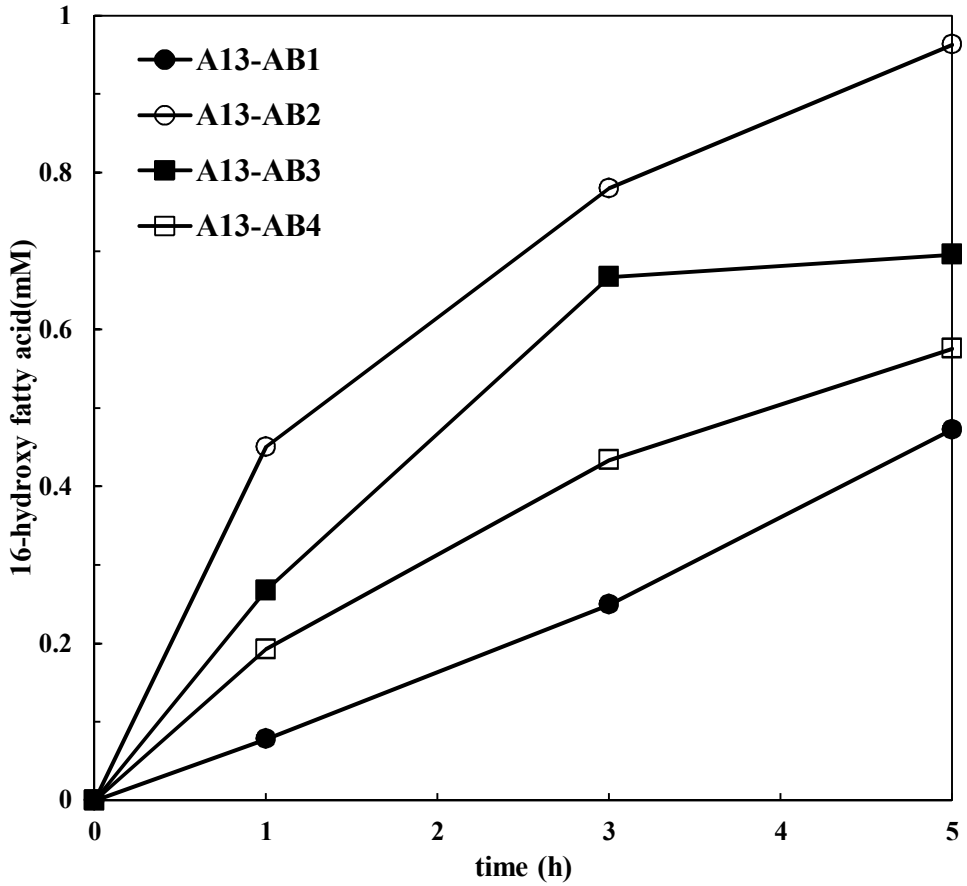


**Figure 4.8 Reaction profiles of the different expression systems for CYP153A13 and CamAB**

Reactions were performed with 1 mM palmitic acid

**Table 4.7 Concentration of CYP153A13 based on CO binding assay**

| Strain | A13-AB1 | A13-AB2 | A13-AB3 | A13-AB4 |
|---|---|---|---|---|
| [P450] ($nmol/g_{DCW}$) | 11.0 | 20.6 | 35.8 | 13.4 |

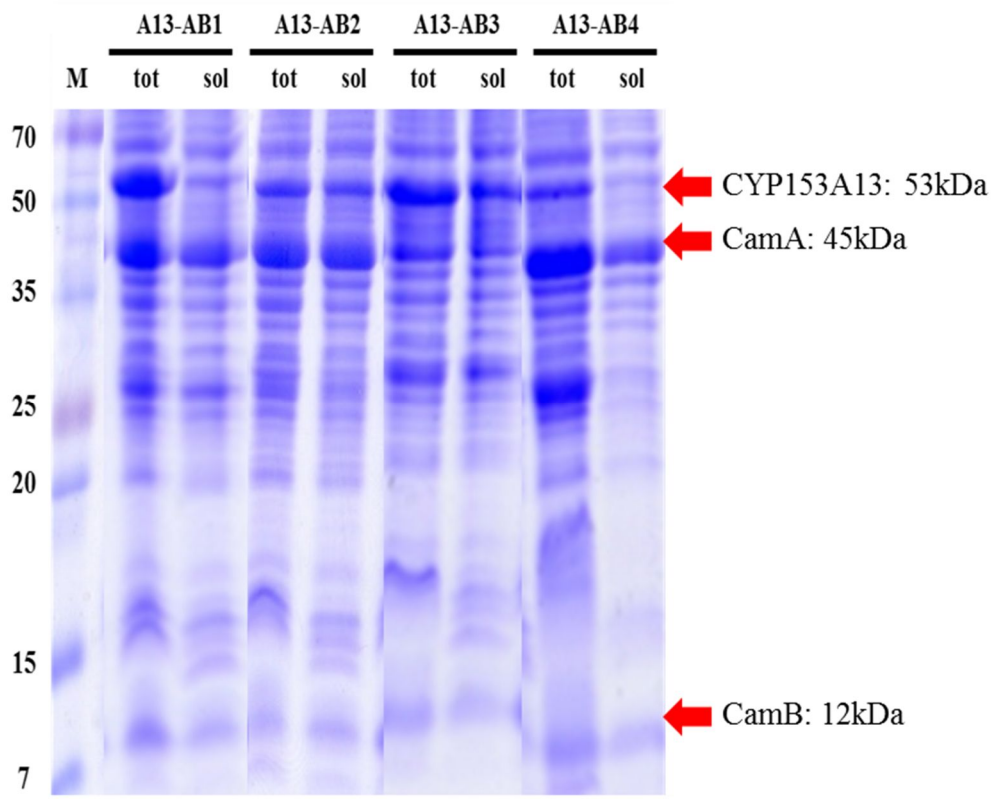


**Figure 4.9 SDS-PAGE of CYP153A13 and CamAB in various expression systems.**

acid (Figure 4.10) and 54 mg/L/h of the productivity, which are 8.8 times increased product yield of 0.54 mM (0.15 g/L) and 9 times enhanced productivity (6.1 mg/L/h) compared to A13-AB1strain. Whereas A13-AB2 strain produced 4 mM (1.1 g/L) ω-hydroxy palmitic acid. It was also proved that P450 expression level and stability become more important for long time fed-batch production of ω-hydroxy fatty acids using CYP153A13.

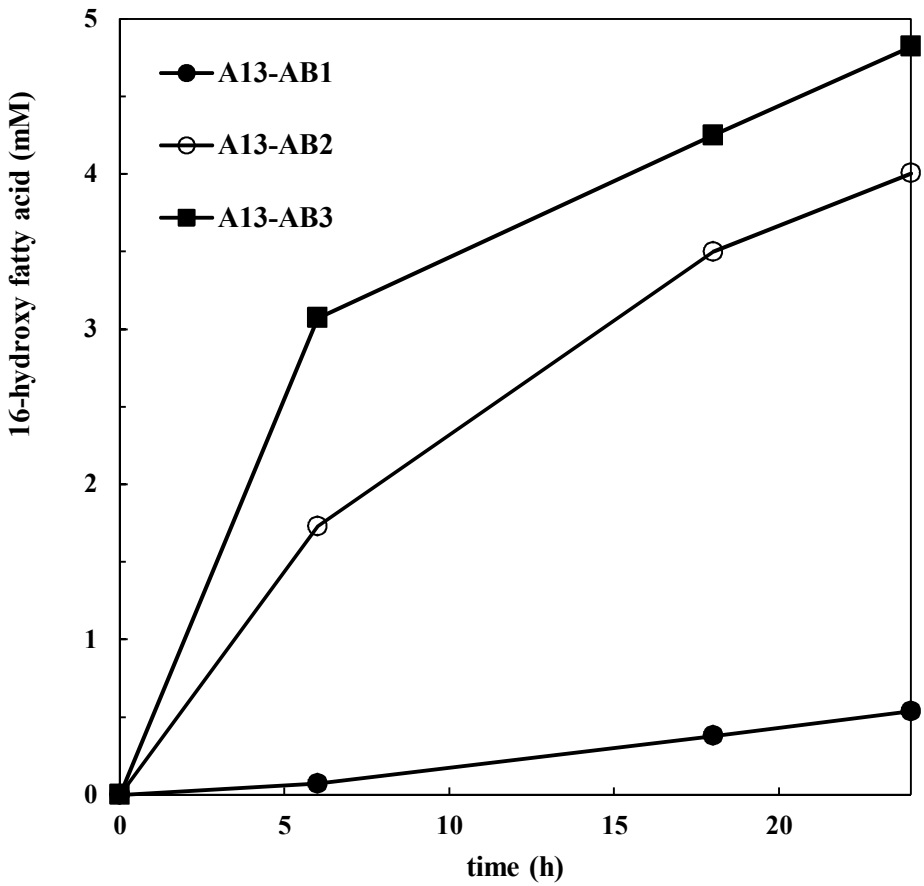


**Figure 4.10 Fed-batch reaction time profiles for production of 16-hydroxy palmitic acid**

Reactions were performed with 10 mM palmitic acid using A13-AB1, A13-AB2, and A13-AB3 strains.

# Chapter 5.

# Engineering CYP153A35 by site-directed /saturation mutagenesis

### 5.1 Selection of mutation sites of CYP153A35 for semi-rational design

Enhancing catalytic activity and changing substrate specificity of cytochrome P450 are mainly achieved by mutations within its active site (Nickerson, HarfordCross et al. 1997, Meinhold, Peters et al. 2005, Yang and Li 2015). To explore such possibility, firstly, we constructed a homology model of CYP153A35 by using CYP153A7 as the template which has a 56% protein sequence identity. Nextly, substrate access routes of CYP153A35 were predicted by CAVER3.0 which approximates the channels involved in movements of its substrates and products from the inner active site to the protein surface (Petrek, Otyepka et al. 2006, Cojocaru, Winn et al. 2007). We set the starting point as 3 Å above the iron of the heme in the CYP153A35 structure. The only one route passing through between the BC-loop and F/G helix was identified and it is also described as Substrate Recognition Sites (SRSs) as shown in Figure 5.1 (Gotoh 1992, Sirim, Widmann et al. 2010). All the residues which might be involved in the recognition and binding of palmitic acid shown in Figure 5.2 are located in SRSs: SRS1: Ile123, Pro128, Leu130, Asp131, Val132, Met134 and Ile136; SRS2: Ala219; SRS3: Tyr236, Ala239, Leu240, and Thr243; SRS4: Thr292, Leu293, Val296 and Thr301; SRS5: Leu344 and Met347; and SRS6: F445 (Table 5.1)

### 5.2 Development of high-throughput screening assay

Direct on-site screening P450 libraries by detecting the hydroxylated products in the reaction mixture is quite desirable and can dramatically reduce the time for mutation experiments. Among the several high-throughput screening (HTS)

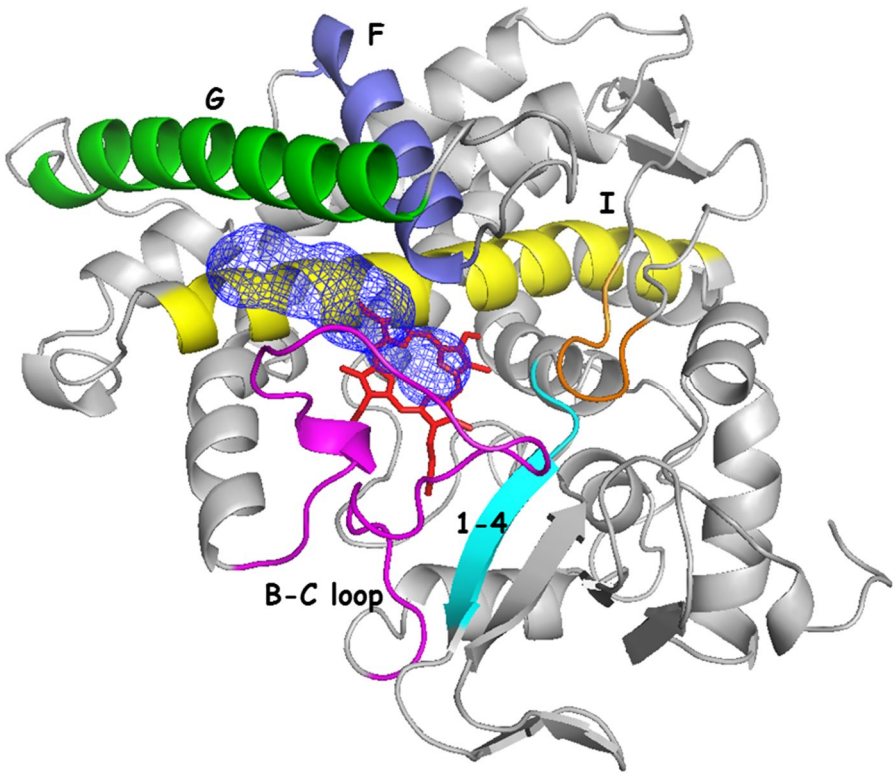


**Figure 5.1 A route for recognition and binding of fatty acid predicted using CAVER3.0**

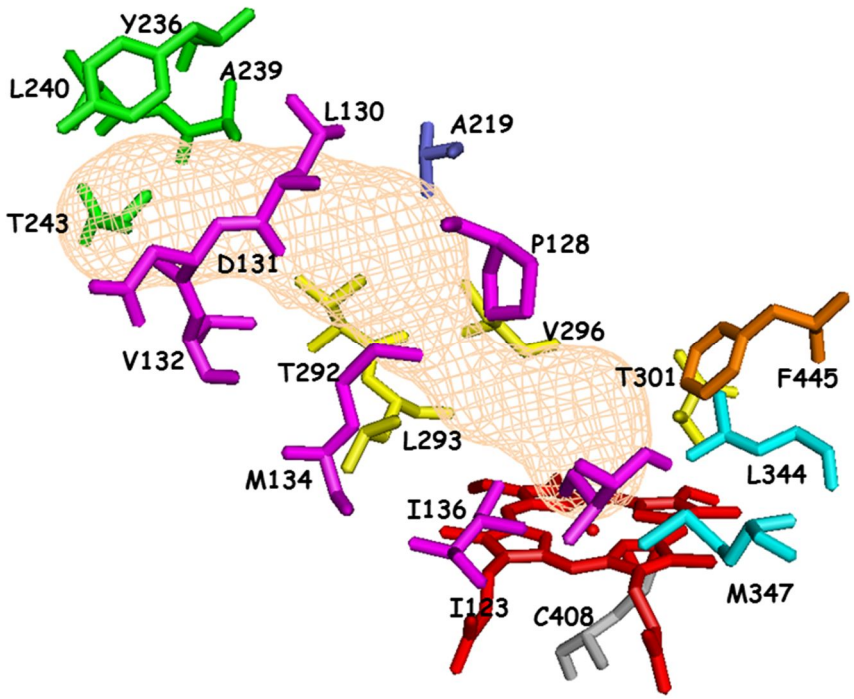


**Figure 5.2 Spatial overview of 19 selected amino acid residues for site-directed saturation mutagenesis**

Those are related with the substrate binding site of palmitic acid in CYP153A35

| SRS | residues | location |
|---|---|---|
| 1 | I123, P128, L130, D131, V132, M134, I136 | BC-loop |
| 2 | A219 | C-terminal of αF |
| 3 | Y236, A239, L240, T243 | N-terminal of αG |
| 4 | T292, L293, V296, T301 | N-terminal of αI |
| 5 | L344, M347 | β3 |
| 6 | F445 | β5 |

**Table 5.1 List of 19 residues and those of location on SRSs of CYP153A35**

methods for P450 mutation (Schwaneberg, Otey et al. 2001, Celik, Speight et al. 2005, Yang and Li 2015), detection of O-demethylation activity of P450 using a surrogate substrate is a well-known and very sensitive method (Meinhold, Peters et al. 2006, Choi, Yang et al. 2015, Yang, Chi et al. 2015). We have followed the same principle of detection of stoichiometrically released aldehyde from the surrogate substrate, i.e. 16-methoxy palmitate, as shown in Figure 5.3a and CYP reaction will generate 16-hydroxy palmitic acid and formaldehyde equivalently. The amount of formaldehyde produced can be detected by reacting with Purpald to give a purple product and following UV absorbance of at 550 nm using a microplate reader (Meinhold, Peters et al. 2006). This assay showed a linear relationship between 15 μM and 1 mM of formaldehyde (Figure 5.3b).

### 5.3 Site direct saturation mutagenesis of CYP153A35-BMR

Using CYP153A35 fused with CYP102A1 reductase domain as a template, we constructed 19 individual libraries generated by single-site saturation mutagenesis of all the amino acid residues in the substrate binding sites except Cys408 which provides a thiolate ligand to the heme iron. After screening of 3420 clones each 180 clones for putative 19 mutation sites, two mutants substituted at Asp131 in SRS1 were found to exhibit improved activities while no mutants in other sites exhibited higher activity than those of wild-type (Figure 5.4a). Using saturated mutation library at Asp131 position, the correlation between the O-demethylation activity of 16-methoxy palmitic acid and the hydroxylation activity of palmitic acid was confirmed by the data generated by the colorimetric UV assay and GC analysis (Figure 5.4b), respectively, because using a surrogate screening always has a

danger

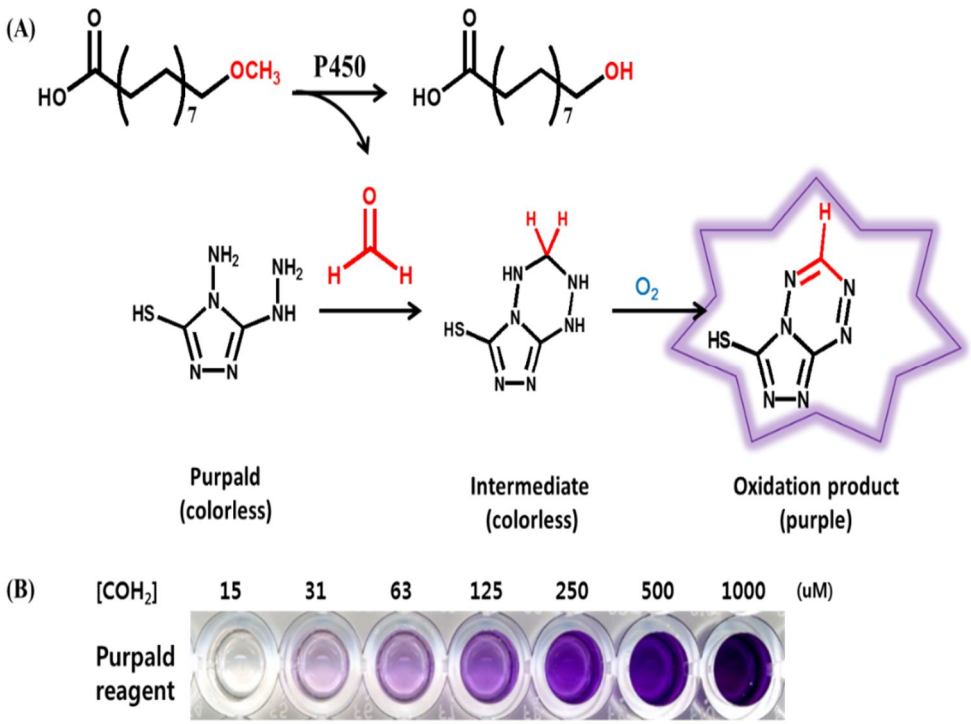


**Figure 5.3 Scheme of high-throughput screening assay**

(A) Principle of the colorimetric HTS assay using 16-methoxy palmitic acid. The formaldehyde produced turns dark purple in the presence of Purpald. (B) Detection limits of the Purpald assay ranged from 15 μM to 1 mM

**(A)**

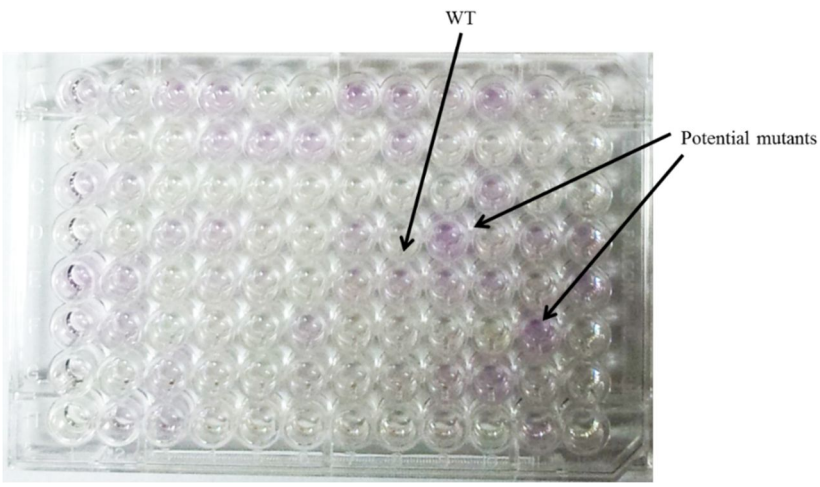


**(B)**

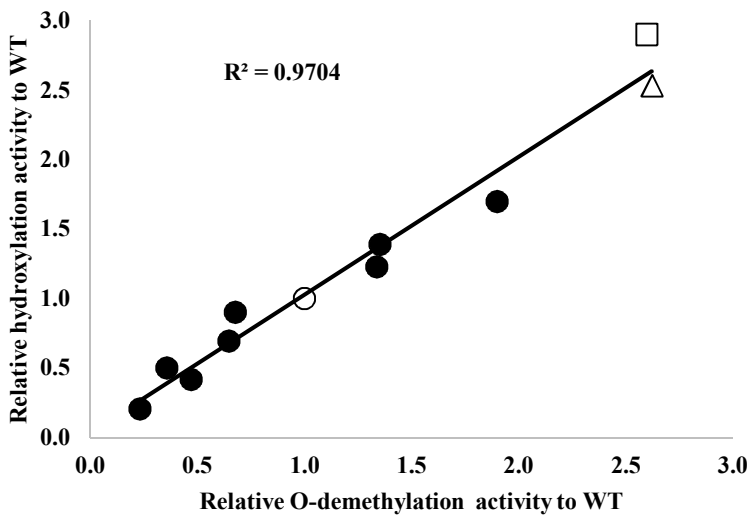


**Figure 5.4 Representative example of 96-well plate after using high-throughput colorimetric assay** (A) The stronger purple color indicating higher concentration of the purple product. (B) The hydroxylation activity toward palmitic acid correlated with the O-demethylation activity toward 16-methoxy palmitic acid. ○ : wild-type, □ : D131S, △ : D131F

of identifying mutants that are more active on the surrogate substrate but not the target substrate. The result suggests that the surrogate substrate-based HTS assay is very reliable to substitute for real screening of terminal hydroxylation.

### 5.4 Evaluation of hydroxylation activity of screened mutants *in vitro*

Using DNA sequencing, we found that Asp131 of the wild type CYP153A35-BMR was replaced with Ser or Phe, respectively, and the two mutants were purified for further characterization (Figure 5.5). Total turnover numbers (TTN) for terminal hydroxylation of the fatty acids of chain length $C_{12:0}$ - $C_{16:0}$ were measured in Table 5.2. In order to compare the changes in the substrate specificity of fatty acids D131F and D131S mutants were subjected to the hydroxylation reactions with$C_{12:0}$ - $C_{16:0}$ fatty acids. The degrees of enhancement for different chain length fatty acids were different. The TTN of D131S mutant for palmitic acid was increased by 16.5-fold, whereas those for lauric acid and myristic acid was increased by 2.2- and 7.6-fold, respectively, indicating that Asp131 in SRS1 exerts a critical effect on the binding of palmitic acid in its active site.

To understand the mechanisms for the enhancement of hydroxylation activity of the mutants, the kinetic constants of the purified mutants were measured toward palmitic acid (Table 5.3). Compared to the wild type, D131S and D131F mutants showed 2.8-fold and 2.6- fold decreased $K_M$ values of palmitic acid, respectively, suggesting the improved palmitic acid binding affinity of the mutants. In addition, the turnover number ($k_{cat}$) of D131S and D131F mutants increased remarkably by a factor of 6.7 and 4.7, respectively. In result, the overall catalytic efficiencies ($k_{cat}/K_M$) of D131S and D131F mutants increased by 17-folds and 13-folds

compared to that

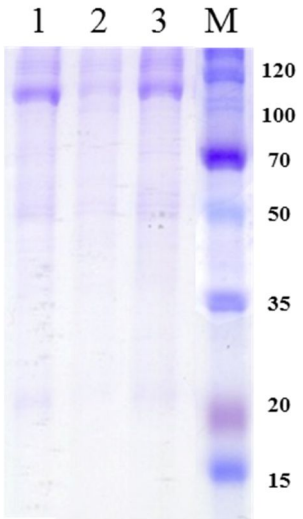


**Figure 5.5 SDS-PAGE of purified CYP153A35-BMR wild-type and mutants**

*M*, broad-range marker; *1*, wild-type; *2*, D131S mutant; *3*, D131F mutants

**Table 5.2 Total turnover numbers of CYP153A35 wild-type and mutants for various fatty acids**

| Enzyme | $C_{12:0}$ | | $C_{14:0}$ | | $C_{16:0}$ | |
|---|---|---|---|---|---|---|
| | TTN[a] | folds | TTN | folds | TTN | folds |
| WT | 14.1 ± 8.8 | -[b] | 20.6 ±13.9 | - | 10.3 ±6.1 | - |
| D131F | 28.8 ± 14.4 | 2.0 | 125.1 ± 22.8 | 6.1 | 134.8 ±9.4 | 13.1 |
| D131S | 31.4 ± 18.5 | 2.2 | 156.9 ± 22.1 | 7.6 | 169.6 ±17.4 | 16.5 |

[a] Total turnover numbers determined as μmol product/ μmol protein. The reactions were carried out with CYP (1 μM), an NADPH regeneration system (0.4 mM $NADP^+$, 4 mM glucose, 0.1 U/mL of glucose dehydrogenase) and fatty acids (0.2 mM) in 100 mM potassium phosphate buffer (pH 7.5) for 30 min at 37°C.

[b] no calculation

**Table 5.3 Kinetic constants of CYP153A35 wild-type and mutants towards palmitic acid**[a]

| Enzyme | $K_M$ (mM) | $k_{cat}$ ($min^{-1}$) | $k_{cat}/K_M$ ($min^{-1}mM^{-1}$) |
|---|---|---|---|
| **WT** | **0.42 ±0.12** | **6.91 ±0.87** | **16.5** |
| **D131F** | **0.15 ±0.08** | **32.53 ±5.23** | **214.1** |
| **D131S** | **0.16 ±0.06** | **45.98 ±5.90** | **281.4** |

[a] The substrate concentration ranged from 50 μM to 1 mM

of the wild-type.

### 5.5 Evaluation of hydroxylation activity of screened mutants in whole-cell reaction

Because *in vitro* evolution always correlate to *in vivo* production, the effects of the mutants were investigated in resting cell reaction. The D131S mutant resulted the best product yield with 0.5 mM of 16-hydroxy palmitic acid, which is the 55% improvement compared wild-type (0.32 mM of 16-hydroxy palmitic acid) (Figure 5.6), despite 35% decrease of the expression level compared wild-type (Table 5.4).

### 5.6 Docking simulation of fatty acids

*In silico* docking simulation of fatty acid into the homology model of wild-type CYP153A35 and D131S mutant were performed using Autodock Vina to understand the reason for the changes in specific activities of different chain-length fatty acids. As shown in Figure 5.7, Asp131 is located in the substrate access channel, suggesting that the carboxylic moiety of Asp131 can have a potential hindering effect on both recognition and binding of fatty acid in the CYP153A35 binding pocket. By replacing this negative charged amino acid residue with either Ser or Phe, the hydroxylation activity for the fatty acids was greatly increased (Table 5.2). In addition, Asp131 is very close to the carboxylic acid moiety of palmitic acid (2.9 Å, Figure 5.7c), compared to those of myristic acid (5.7 Å, Figure 5.7b) and those of lauric acid (11.4 Å, Figure 5.7a), thus the effect of Asp131 appears to be the strongest for palmitic acid and to be reduced as chain-length of fatty acid becomes shorter. Similar report was published for BM3 mutant

such that R47E mutants lost its catalytic activity toward arachidonic acid, but still maintained some activities toward shorter chain fatty acids (Graham-Lorence, Truan et al. 1997, Oliver, Modi et al. 1997).

On the other hand, the substitution of Ser for Asp showed that the hydroxyl moiety of Ser stabilized the binding of palmitic acid, which might situate the terminal carbon of palmitic acid closer to heme (Figure 5.8). In general, hydroxyl group-containing amino acid such as Tyr51 in BM3 can interact with the carboxyl group of fatty acid in the entrance of substrate channel and the residue is well conserved (Noble, Miles et al. 1999). In the case of D131F mutant, the phenyl moiety of Phe would make somewhat hydrophobic surface of the substrate channel in CYP153A35, enabling to become a fatty acid recognition and binding site (Ravichandran, Boddupalli et al. 1993, Girvan and Munro 2016).

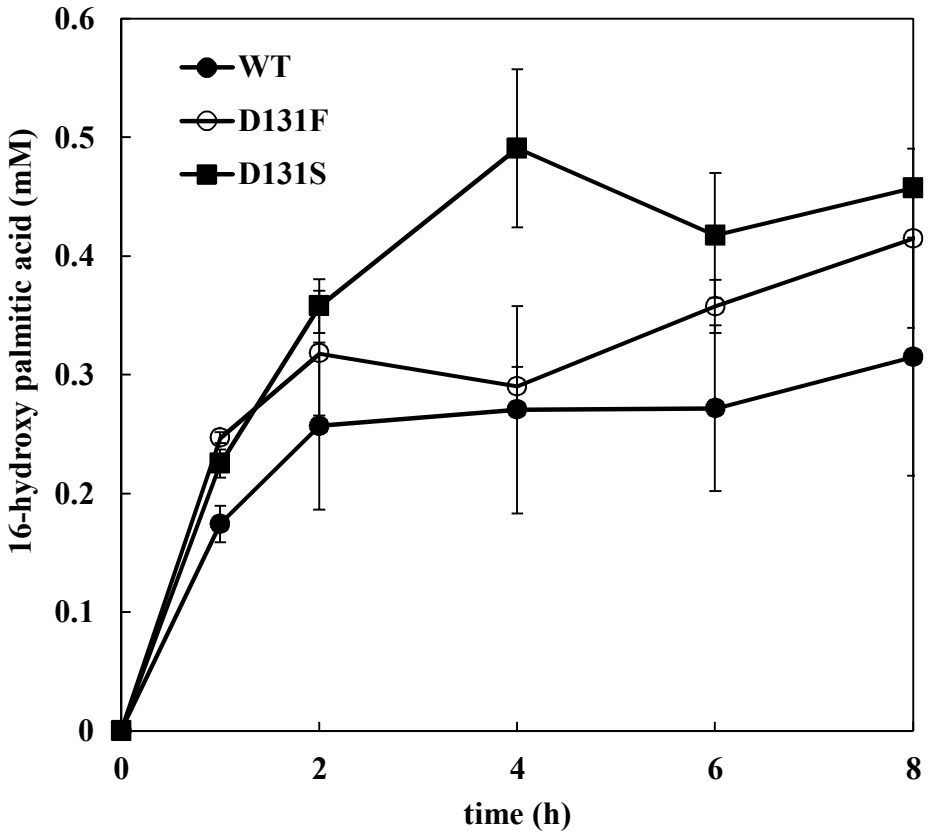


**Figure 5.6 Reaction profile of wild-type and mutants**

Resting cell reaction profiles for the production of 16-hydroxy fatty acid with 2 mM of palmitic acid using CYP153A35-BMR wild type and mutants. The OD at 600nm of the cell suspensions were 20.

**Table 5.4 Concentration of CYP153A35-BMR wild-type and mutants based on CO binding assay**

| Strain | Wild-type | D131F | D131S |
|---|---|---|---|
| **[P450] (nmol/$g_{DCW}$)** [a] | **67.3** | **62.3** | **43.4** |

[a] Values were obtained by triplicate experiments with standard deviations within ≤10%

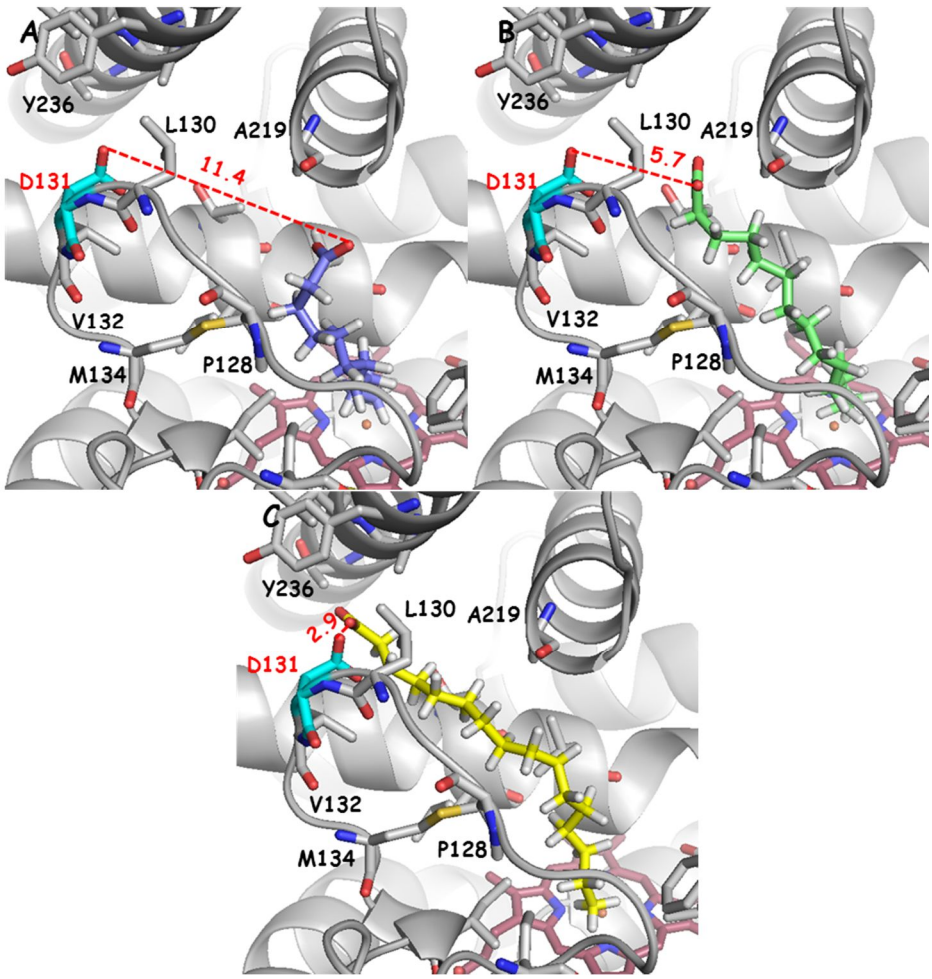


**Figure 5.7 Docking of fatty acid into the active sites of wild-type.**

(a) Lauric acid; (b) Myrisitic acid; (c) Palmitic acid. Distance between Asp131 and carboxylic moiety of fatty acids (in angstrom) are denoted by red dashed lines.

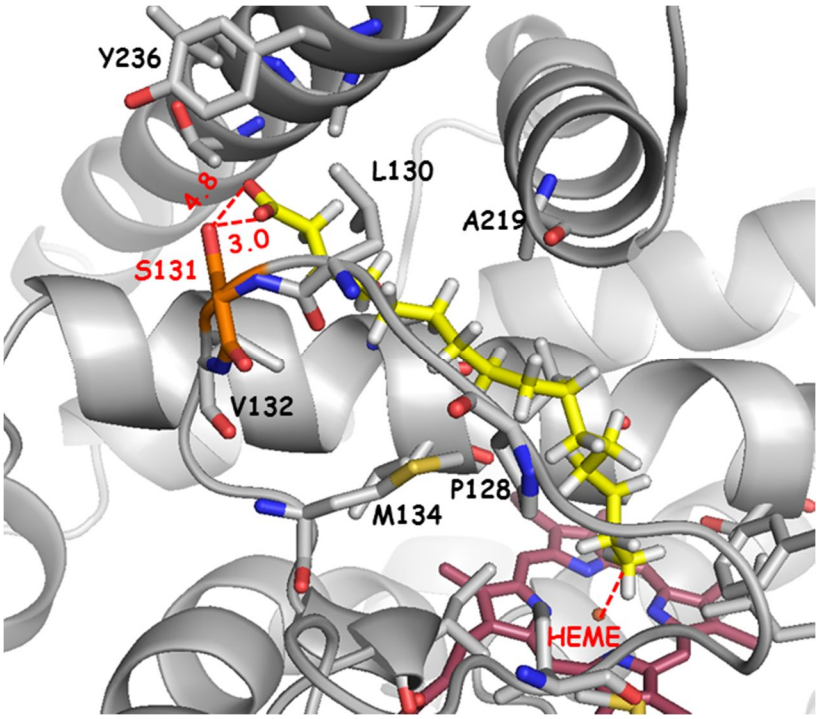


**Figure 5.8 Docking of palmitic acid into the active sites of D131S mutant.**

Distance between Ser131 and carboxylic moiety of fatty acids (in angstrom) are denoted by red dashed lines.

# Chapter 6.

# Linker design for artificial self-sufficient CYP

## 6.1 Design of random linker sequence libraries for artificial self-sufficient fatty acid ω-hydroxylase

Natural self-sufficient CYPs are composed with N-terminal heme domain and C-terminal reductase domain, and 20~30 amino acids act as linker to connect two domains (Figure 6.1a) (Munro, Girvan et al. 2007). Therefore, artificial self-sufficient CYPs were generally constructed by fusion interest class I type P450 to reductase domain of self-sufficient CYP using genetic techniques (Nodate, Kubota et al. 2006, Choi, Jung et al. 2012, Scheps, Honda Malca et al. 2013, Zuo, Zhang et al. 2016). However, the impact of fusion protein was smaller than expected due to stability and coupling efficiency (Hoffmann, Weissenborn et al. 2016). To optimize the linker sequence between fatty acid ω-hydroxylase and reductase domain of P450 BM-3 (Figure 6.1b), repeated flexible or rigid sequence are designed randomly (Figure 6.2a). Gly-rich sequences (GGGGS) provide flexibility and α-helix sequences contribute orientations of the fused domains direction and specific conformations to two domains (Arai, Ueda et al. 2001). EAAAK peptide sequence used for α-helix conformation. After cloning of linker fragment to CYP153A33-BMR plasmid, 8 clones were selected randomly and plasmid prep were performed. After bglII digestion, DNA gel electrophoresis was carried out, and 73% cloning efficiency was confirmed (Figure 6.2b). To evaluation the quality of library, 10 clones were selected, and DNA sequencing was performed (Table 6.1). The linker sequences were encoded (GGGGS)m(EAAAK)n (m, n = 1-12), hence the total number of variants was 4096. The number of transformants actually screened was calculated based on previously proposed algorithms (Reetz, Kahakeaw et al. 2008). To ensure a 0.95 probability of full coverage, the required library size was 12270.

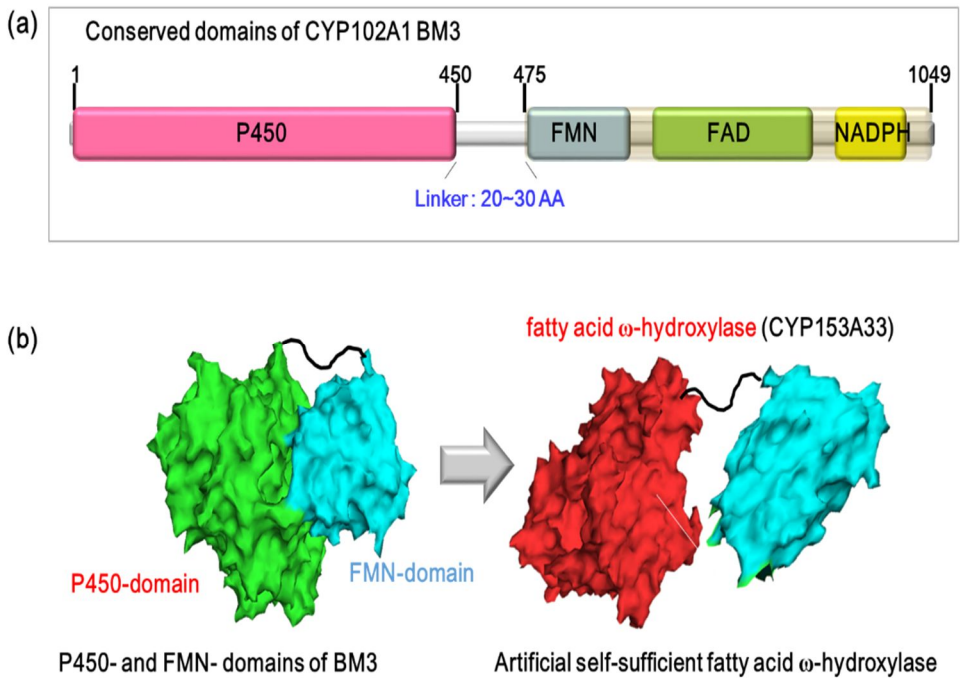


**Figure 6.1 Construction of artificial self-sufficient CYP**

(a) Composition of self-sufficient CYP (P450-linker-CPR) (b) fatty acid ω-hydroxylase fusion protein

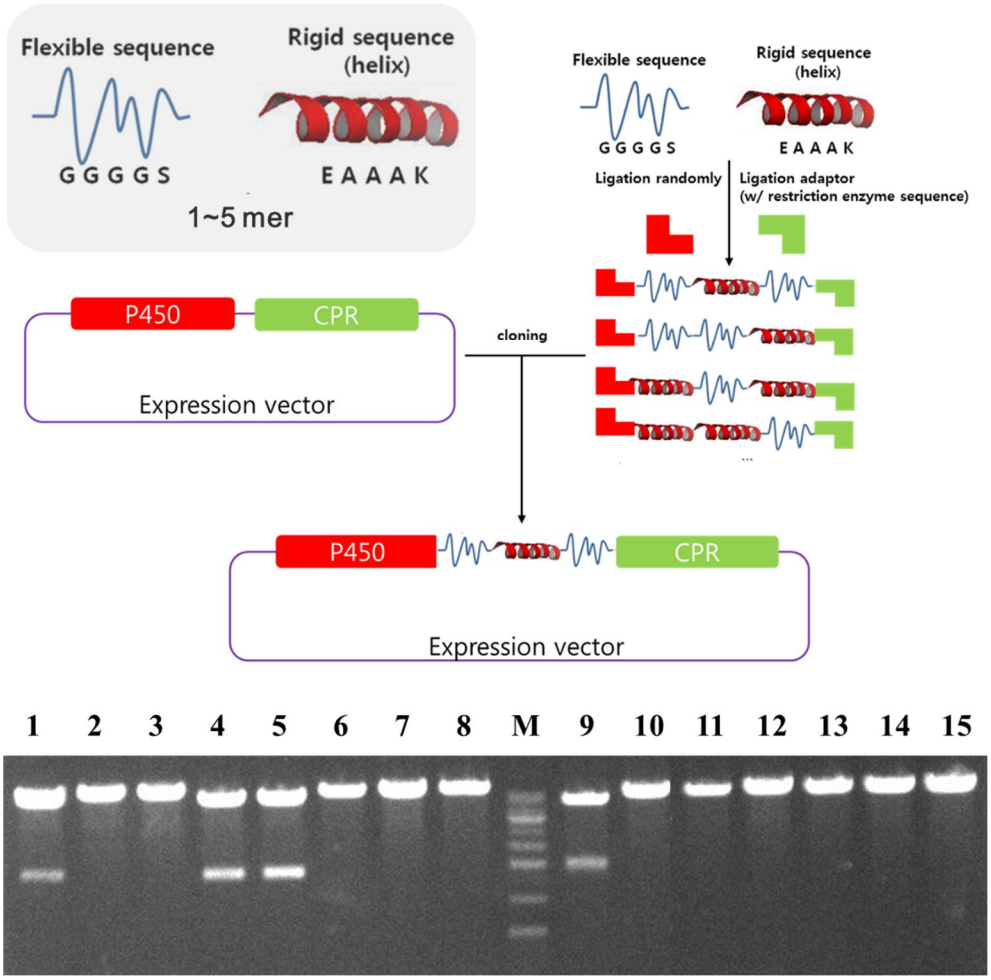


**Figure 6.2 Strategy for construction of library using flexible or rigid (helix) linker sequence randomly**

(a) Strategy for construction of library using flexible or rigid (helix) linker sequence randomly (b) Quality control of linker library using restriction enzyme; After BglII digestion, samples run on a DNA gel electrophoresis with 0.7% agarose. Lane 2,3, 6-8, and 10-15 indicate successful cloning of linker sequence, whereas Lane 1,4,5, and 9 show negative control.

**Table 6.1 Quality control of linker library using DNA sequencing**

| | Linker sequence | No. of repetitive sequence |
|---|---|---|
| 1 | ELEEAAAK GAS | 1 |
| 2 | ELEGGGGS GAS | 1 |
| 3 | ELEEAAAK EAAAK GAS | 2 |
| 4 | ELEGGGGS EAAAK EAAAK EAAAK GAS | 4 |
| 5 | ELEGGGGS EAAAK GGGGS EAAAK GGGGS GAS | 5 |
| 6 | ELEEAAAK EAAAK EAAAK EAAAK EAAAK EAAAK GAS | 6 |
| 7 | ELEGGGGS EAAAK GGGGS EAAAK EAAAK EAAAK GGGGS GAS | 7 |
| 8 | ELEGGGGS GGGGS EAAAK GGGGS GGGGS EAAAK EAAAK GAS | 7 |
| 9 | ELEGGGGS GGGGS GGGGS EAAAK EAAAK EAAAK GGGGS GGGGS EAAAK GGGGS GAS | 10 |
| 10 | ELEEAAAK GGGGS EAAAK EAAAK GGGGS EAAAK EAAAK EAAAK EAAAK EAAAK GGGGS GGGGS GAS | 12 |

### 6.2 Evaluation of mutants for production of ω-hydroxy palmitic acid

After screening of 400 clones using HTS method (Section 2.4), five mutants were selected (Table 6.2 and 6.3). All mutants have EAAAK at the both ends of the linker as well as with high frequency, which suggest that α-helix forming sequences are more efficient for structural orientations of the fusion. The effects of the mutants were investigated in resting cell reaction with 1 mM of palmitic acid, following BM3 linker used as control. A33-BMR showed the highest conversion yield with 47.5 %, and H9 mutant was the best among the selected mutant with 32.2 % of conversion yield (Table 6.4). The quantification of P450 concentration was carried out by CO-binding assay. Most mutants showed lower expression level than A33-BMR, in addition, poor solubility (Figure 6.3). To compare the activities of the enzyme in resting cells, thereby excluding the expression level, specific activities were calculated by normalizing the *in vivo* conversion yield to the P450 concentration. The analysis revealed that the H11 mutants showed the highest specific activity, which 50% higher than BM3 native linker, and the specific activity of the H9 mutants was 20% higher than those of A33-BMR.

**Table 6.2 DNA sequences of selected linker mutants**

| mutants | DNA sequences |
|---|---|
| H9 | GAGCTCGAGGAAGCCGCAGCGAAAGAAGCCGCAGCGAA AGGAGCTAGC |
| H11 | GAGCTCGAGGAAGCCGCAGCGAAAGGTGGCGGTGGCAG CGGTGGCGGTGGCAGCGGTGGCGGTGGCAGCGAAGCCGC AGCGAAAGGAGCTAGC |
| D3 | GAGCTCGAGGAAGCCGCAGCGAAAGAAGCCGCAGCGAA AGAAGCCGCAGCGAAAGGTGGCGGTGGCAGCGAAGCCG CAGCGAAAGGTGGCGGTGGCAGCGAAGCCGCAGCGAAA GGAGCTAGC |
| C10 | GAGCTCGAGGAAGCCGCAGCGAAAGAAGCCGCAGCGAA AGGTGGCGGTGGCAGCGGTGGCGGTGGCAGCGGTGGCGG TGGCAGCGAAGCCGCAGCGAAAGAAGCCGCAGCGAAAG AAGCCGCAGCGAAAGAAGCCGCAGCGAAAGGAGCTAGC |
| C12 | GAGCTCGAGGAAGCCGCAGCGAAAGGTGGCGGTGGCAG CGAAGCCGCAGCGAAAGGTGGCGGTGGCAGCGAAGCCG CAGCGAAAGAAGCCGCAGCGAAAGAAGCCGCAGCGAAA GGTGGCGGTGGCAGCGAAGCCGCAGCGAAAGGTGGCGG TGGCAGCGAAGCCGCAGCGAAAGGAGCTAG |

* red: rigid sequence, blue: flexible sequence, and gray: adaptor sequence

**Table 6.3 Amino acid sequences of selected linker mutants**

| mutants | Amino acid sequences |
|---|---|
| H9 | ELEEAAAK EAAAKGAS |
| H11 | ELEEAAAK GGGGS GGGGS GGGGS EAAAKGAS |
| D3 | ELEEAAAK EAAAK EAAAK GGGGS EAAAK GGGGS EAAAKGAS |
| C10 | ELEEAAAK EAAAK GGGGS GGGGS GGGGS EAAAK EAAAK EAAAK EAAAKGAS |
| C12 | ELEEAAAK GGGGS EAAAK GGGGS EAAAK EAAAK EAAAK GGGGS EAAAK GGGGS EAAAKGAS |

* red: rigid sequence, blue: flexible sequence, and gray: adaptor sequence

| Strain | ω-hydroxy palmitic acid (μM) [a] | Conc. of P450 (nmol/$g_{DCW}$) [b] | Specific activity (μmol/μmol) [c] | Relative specific activity (%) |
|---|---|---|---|---|
| A33-BMR | 475 | 22.8 | 83.3 | 100 |
| H9 | 322 | 12.8 | 100.6 | 120 |
| H11 | 275 | 8.8 | 125 | 150 |
| D3 | 152 | 8.8 | 69.1 | 83 |
| C10 | 82 | 4.8 | 68.3 | 82 |
| C12 | 62 | 4.0 | 62 | 74 |

**Table 6.4 Yields of ω-hydroxy palmitic acid using linker mutants**

[a] The reactions were carried out with 1 mM of palmitic acid for 6 h. The OD at 600nm of the cell suspensions were 20.

[b] Concentration of P450 was measured by CO binding assay

[c] Specific activity calculated as μmol product/μmol CYP *in vivo*.

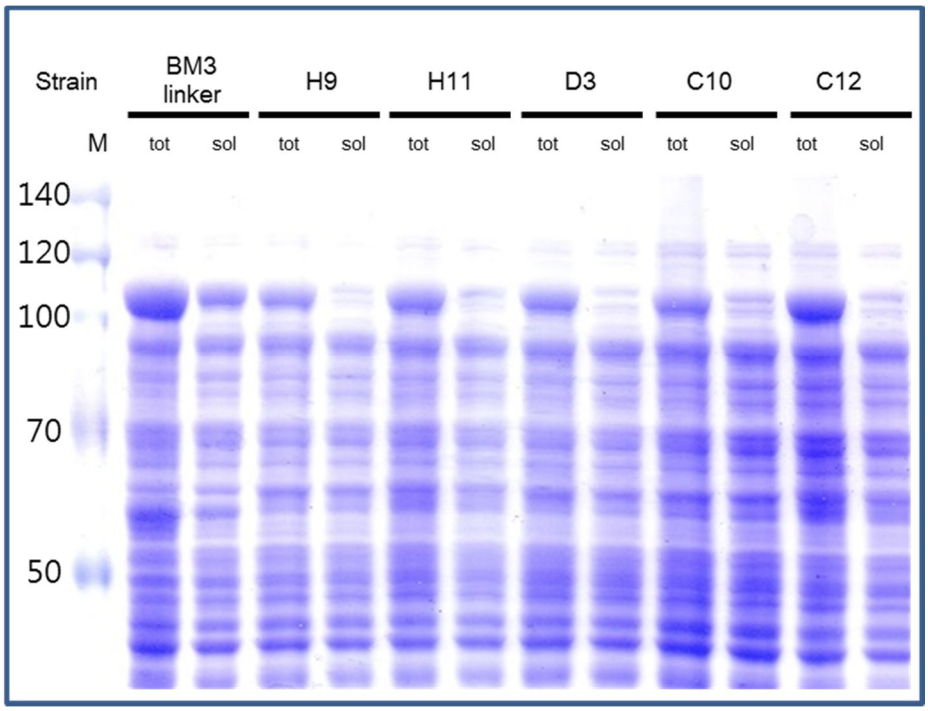


**Figure 6.3 SDS-PAGE of linker mutants and CYP153A33-BMR**

# Chapter 7.

# Overall discussion and further suggestion

## 7.1 Overall discussion

Since the first CYP153A1 was found in *Acinetobacter calcoaceticus* cultured on minimal medium with hexadecane as carbon source (Asperger, Naumann et al. 1981), CYP153 enzymes have been well known to catalyze ω-hydroxylation toward aliphatic, alicyclic, and alkyl-substituted compounds with high regio- and stereo-selectivity (Funhoff, Salzmann et al. 2007). Recently, it was discovered that CYP153A16, CYP153A33 and CYP153A34 could catalyze ω-hydroxylation toward saturated and unsaturated fatty acids (Honda Malca, Scheps et al. 2012) as well as alkanes and alcohols (Scheps, Malca et al. 2011). In this study, we have confirmed that CYP153A13 previously characterized as alkane ω-hydroxylase (Funhoff, Salzmann et al. 2007) also showed a good fatty acid ω-hydroxylase activity with 16.4 $\pm$3.15 $min^{-1}$ of turnover number toward palmitic acid. Its specific activity was 3.5 times higher than that of CYP153A33 (4.6 $\pm$1.22 $min^{-1}$) which showed the highest fatty acid ω-hydroxylase activity in the previous reports (Table 3.1) (Honda Malca, Scheps et al. 2012). Although the ω-hydroxylation activity of CYP153A13 was superior, the productivity of ω-hydroxy palmitic acid using whole cell system was only 55% of that of CYP153A33 (Figure 3.5) caused by its low expression level: Compared to 50 nmol/$g_{CDW}$ of CYP153A33, the expression level of CYP153A13 was only 11 nmol/$g_{CDW}$(Table 3.2). Similarly, the expression level of self-sufficient CYP153A13-Red was only 10% of that of CYP102A1 (i.e. BM3) in *E.coli* BL21 (DE3) which is well known for its high soluble expression (Bordeaux, de Girval et al. 2014), indicating that solublization and functional expression of CYP153A13 would be a critical to achieve high product yields and become a big challenge for application in industry.

Although the CYP153A35 from *Gordonia alkanivorans* was not yet characterized as ω-hydroxylase, *Gordonia alkanivorans* strain was identified as indigenous diesel-degrading strain (Young, Lin et al. 2005), and three alkanal monooxygenase genes related to hydrocarbon degradation were suggested by genome sequencing (Wang, Jin et al. 2014), suggesting that CYP153A35 is very likely to show ω-hydroxylation activity toward fatty acids. In this study, ω-hydroxylation activity of CYP153A35 for palmitic acid and its highest productivity of ω-hydroxy palmitic acid were observed with high expression level in *E.coli* (90 nmol/$g_{CDW}$) (Figure 3.5, Table 3.2).

Among the various electron transfer system for P450 (Hannemann, Bichet et al. 2007), CamAB system and BM3 diflavin reductase fusion system were applied to CYP153A35 for the production of ω-hydroxy palmitic acid. The two systems were often compared and evaluated for hydroxylation of isoflavonoids and fatty acids *in vitro* and *in vivo* (Choi, Jung et al. 2012, Scheps, Honda Malca et al. 2013, Choi, Jung et al. 2014, Sung, Jung et al. 2015). In general, the self-sufficient type CYP showed superior electron coupling transfer efficiency over CYP+CamAB system in the optimized condition *in vitro*, since the self-sufficient system has the characteristics of intra-molecular electron transfer system. However, in the case of *in vivo*, the situation becomes a little bit different depending upon CYPs, since the amount of functional CYP and ratios of the expressed redox partner proteins vary depending on the promoter strength, plasmid copy number, induction strategy and concentration of reducing power NAD(P)H. Although CYP153A35-BMR showed the electron transfer efficiency four times higher than CYP153A35+CamAB *in vitro* (Table 4.1), the result of the whole cell reactions showed that CYP153A35-

BMR is no longer the better system for P450 reaction (Figure 4.2). There are two hypotheses to explain this result; 1) different cofactor dependency between CYP153A35+CamAB system and CYP153A35-BMR system resulting from the difference in the concentration of NADH and NADPH in the cells, and 2) significant reduction of the effective reaction (electron transfer in the case of P450 reaction) volume for CamAB system and different functional CYP expression level. First, CamA is the NADH dependent reductase, whereas BM3 reductase has NADPH dependency. According to our analysis (Table 4.3), total amount of NADH is about twice higher than NADPH in *E.coli* BW25113, suggesting that the concentration of electron donor in CamAB system would be twice higher than that in self-sufficient system *in vivo*.

Second, *in vitro* CYP activity is often compared in micro-centrifuge tubes with a volume of 100 μL reaction buffer, whereas the volumes of a *E.coli* cell and a CYP protein are is approximately $10^{-9}$ μL and $10^{-16}$ μL, assuming a cylinder and a round ball, respectively (Harpaz, Gerstein et al. 1994). Then, the effective reaction (electron transfer) volume for class VIII self-sufficient CYP is $10^{-16}$ μL and it does not change although the CYP reaction goes to *in vivo* cell reaction. However, in the case of class I CYP with CamAB, the concentrations of CYP as well as CamAB in the 100 μL reaction buffer increase dramatically when they go to *in vivo* cell system. Therefore, if the initial enzyme concentration is fixed as a constant, the effective reaction (electron transfer) volume is reduced by $10^{11}$ fold, enhancing the same degree of density of the enzyme, i.e. concentration. Although this is a very rough calculation of the fold changes in the effective electron transfer efficiency based on the reduction in effective reaction volume, CYP153A35+ CamAB system

has some genuine advantages (ca. $10^{11}$ fold) in effective volume effect over CYP153A35-BMR system when it goes to *in vivo* whole cell reaction (Figure 7.1). In result, although CYP153A35-BMR system appears to be a superior to CYP153A35+CamAB system *in vitro*, it may not be true anymore in *in vivo* cell system.

For further enhancement of class I system, the oxidation rate of CYP was compared according to the relative ratios of CYP and redox partners, and usage of different redox partners in the previous reports (Bell, Dale et al. 2010, Girhard, Klaus et al. 2010, Yang, Bell et al. 2010). The results suggested that the amount or the type of ferredoxin protein is the most important factor for the CYP oxidation. Despite importance of ferredoxin, gene order of three proteins among P450 and CamAB in the expression system was not considered in detail (Bell, Harford-Cross et al. 2001, Kim, Cryle et al. 2007, Ringle, Khatri et al. 2013). In this study, it was confirmed that the concentration of ferredoxin protein, CamB, is significant for P450 oxidation *in vitro*, and the different product yields of five mutants (Figure 4.4) suggested that understanding the relationship between CYP153A35 and its redox partners in the whole cell system is a key to improve its specific activity and productivity. However, CYP expression level and stability become more important when it goes to long term production using fed-batch fermentation. Therefore, the optimization of three components for class I CYP reaction *in vivo* should be considered carefully for further improvement for CYP biotransformation. The results in this study emphasized that correct evaluation of P450 reaction system is really difficult, since many factors such as *in vitro*/*in vivo* reaction, the expression ratio of CYP to electron partners, induction strategy, functional expression and

protein stability are involved for the evaluation.

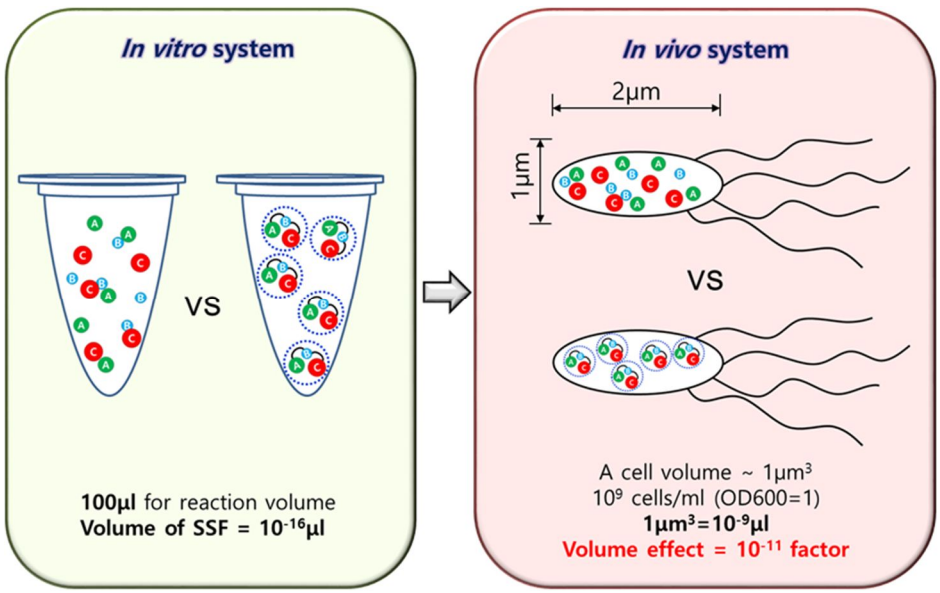


**Figure 7.1 Scheme for reduced volume effect on in whole-cell system**

## 7.2 Further suggestion

From the chapter 5, we figured out Asp131 cause instable binding of fatty acid, especially palmitic acid, due to closeness. Therefore, elimination of negative charged amino acid, such as aspartic acid, glutamic acid, in active site of fatty acid hydroxylase might improve the hydroxylation activity of enzyme. To verify this idea, the structure of CYP153A33, which is also fatty acid ω-hydroxylase, was predicted and cavies were scanned. In CYP153A33, there are three negative charged amino acid, Glu137, Glu142, and Glu242, were selected (Figure 7.2), and alanine scanning experiments were performed. Using whole cell system with CamAB as redox proteins, relative activities of CYP153A33 wild-type and mutants were evaluated (Table 7.2). As a results, E137A mutant showed slight improvement for both myricitic acid and palmitic acid, and E142A mutant showed only enhancement for palmitic acid. Later, three mutants were also evaluated for lauric acid hydroxylation, and E142A mutants showed twice higher yield using 2 mM lauric acid (data not shown), thus those mutants are need for further characterization *in vitro*.

**Table 7.1 Summarization of production of ω-hydroxy fatty acid using CYPs**

| host | CYP | Redox protein(s) | Product | Yield (g/L) | Productivity (g/L/h) | ref |
|---|---|---|---|---|---|---|
| ***Candida tropicalis*** | CYP52 | CaCPR | 14-hydroxy tetradecanoic acid | 174 | 1.17 | (Lu, Ness et al. 2010) |
| ***Candida tropicalis*** | CYP52 | CaCPR | 16-hydroxy hexadecanoic acid | 24 | - | (Lu, Ness et al. 2010) |
| ***Candida tropicalis*** | CYP52 | CaCPR | 18-hydroxy octadecanoic acid | 12 | - | (Lu, Ness et al. 2010) |
| ***E.coli*** | CYP153A33 | fused BMR | 12-hydroxy dedecanoic acid | 4 | 0.14 | (Scheps, Honda Malca et al. 2013) |
| ***E.coli*** | CYP153A33 | CamA/CamB | 16-hydroxy hexadecanoic acid | 2.4 | 0.07 | (Bae, Park et al. 2014) |
| ***E.coli*** | CYP153A35 | CamA/CamB | 16-hydroxy hexadecanoic acid | 4.6 | 0.15 | This study |

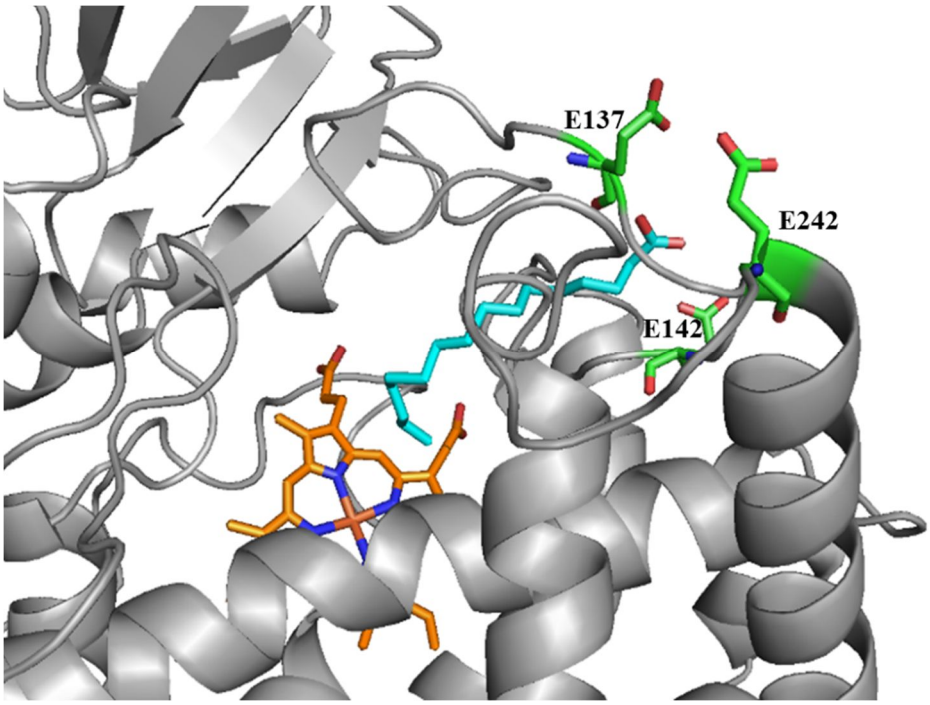


**Figure 7.2 Docking of palmitic acid into the active sites of CYP153A33**

**Table 7.2 Relative activity of CYP153A33 wild-type and mutants**

| mutants | Relative activity (%) | |
|---|---|---|
| | C14 | C16 |
| WT | 100 | 100 |
| E137A | 121 | 128 |
| E142A | 93 | 140 |
| E242A | 54 | 82 |

# Bibliography

Anzenbacher, P. and E. Anzenbacherova (2001). "Cytochromes P450 and metabolism of xenobiotics." Cell Mol Life Sci **58**(5-6): 737-747.

Arai, R., H. Ueda, A. Kitayama, N. Kamiya and T. Nagamune (2001). "Design of the linkers which effectively separate domains of a bifunctional fusion protein." Protein Engineering **14**(8): 529-532.

Asperger, O., A. Naumann and H.-P. Kleber (1981). "Occurrence of cytochrome P-450 in Acinetobacter strains after growth on n-hexadecane." FEMS Microbiology Letters **11**(4): 309-312.

Axarli, I., A. Prigipaki and N. E. Labrou (2005). "Engineering the substrate specificity of cytochrome P450 CYP102A2 by directed evolution: production of an efficient enzyme for bioconversion of fine chemicals." Biomol Eng **22**(1-3): 81-88.

Axelson, M. and K. D. Setchell (1981). "The excretion of lignans in rats -- evidence for an intestinal bacterial source for this new group of compounds." FEBS Lett **123**(2): 337-342.

Bae, J. H., B. G. Park, E. Jung, P. G. Lee and B. G. Kim (2014). "fadD deletion and fadL overexpression in Escherichia coli increase hydroxy long-chain fatty acid productivity." Appl Microbiol Biotechnol **98**(21): 8917-8925.

Bell, S. G., A. Dale, N. H. Rees and L. L. Wong (2010). "A cytochrome P450 class I electron transfer system from Novosphingobium aromaticivorans." Appl Microbiol Biotechnol **86**(1): 163-175.

Bell, S. G., C. F. Harford-Cross and L. L. Wong (2001). "Engineering the CYP101 system for in vivo oxidation of unnatural substrates." Protein Eng **14**(10): 797-802.

Bell, S. G., F. Xu, E. O. Johnson, I. M. Forward, M. Bartlam, Z. Rao and L. L. Wong (2010). "Protein recognition in ferredoxin-P450 electron transfer in the class

I CYP199A2 system from Rhodopseudomonas palustris." J Biol Inorg Chem **15**(3): 315-328.

Belsare, K. D., A. J. Ruff, R. Martinez, A. V. Shivange, H. Mundhada, D. Holtmann, J. Schrader and U. Schwaneberg (2014). "P-LinK: A method for generating multicomponent cytochrome P450 fusions with variable linker length." Biotechniques **57**(1): 13-20.

Bendl, J., J. Stourac, E. Sebestova, O. Vavra, M. Musil, J. Brezovsky and J. Damborsky (2016). "HotSpot Wizard 2.0: automated design of site-specific mutations and smart libraries in protein engineering." Nucleic Acids Res.

Benveniste, I., T. Saito, Y. Wang, S. Kandel, H. W. Huang, F. Pinot, R. A. Kahn, J. P. Salaun and M. Shimoji (2006). "Evolutionary relationship and substrate specificity of Arabidopsis thaliana fatty acid omega-hydroxylase." Plant Science **170**(2): 326-338.

Benveniste, I., N. Tijet, F. Adas, G. Philipps, J. P. Salaun and F. Durst (1998). "CYP86A1 from Arabidopsis thaliana encodes a cytochrome P450-dependent fatty acid omega-hydroxylase." Biochemical and Biophysical Research Communications **243**(3): 688-693.

Bernhardt, R. and V. B. Urlacher (2014). "Cytochromes P450 as promising catalysts for biotechnological application: chances and limitations." Applied Microbiology and Biotechnology **98**(14): 6185-6203.

Bordeaux, M., D. de Girval, R. Rullaud, M. Subileau, E. Dubreucq and J. Drone (2014). "High-cell-density cultivation of recombinant Escherichia coli, purification and characterization of a self-sufficient biosynthetic octane omega-hydroxylase." Applied Microbiology and Biotechnology **98**(14): 6275-6283.

Bouwstra, J. A., G. S. Gooris, F. E. R. Dubbelaar, A. M. Weerheim, A. P. IJzerman and M. Ponec (1998). "Role of ceramide 1 in the molecular organization of the stratum corneum lipids." Journal of Lipid Research **39**(1): 186-196.

Brodie, B. B., J. Axelrod, J. R. Cooper, L. Gaudette, B. N. Ladu, C. Mitoma and S. Udenfriend (1955). "Detoxication of Drugs and Other Foreign Compounds by Liver Microsomes." Science **121**(3147): 603-604.

Celik, A., R. E. Speight and N. J. Turner (2005). "Identification of broad specificity P450(CAM) variants by primary screening against indole as substrate." Chemical Communications(29): 3652-3654.

Chen, M. M. Y., C. D. Snow, C. L. Vizcarra, S. L. Mayo and F. H. Arnold (2012). "Comparison of random mutagenesis and semi-rational designed libraries for improved cytochrome P450 BM3-catalyzed hydroxylation of small alkanes." Protein Engineering Design & Selection **25**(4): 171-178.

Cho, S. H. and V. DeFlorio (1996). Process of preparing ω-hydroxy acids, Google Patents.

Choi, K.-Y., H.-Y. Park and B.-G. Kim (2010). "Characterization of bi-functional CYP154 from Nocardia farcinica IFM10152 in the O-dealkylation and ortho-hydroxylation of formononetin." Enzyme and Microbial Technology **477**: 327-334.

Choi, K. Y., E. Jung, D. H. Jung, B. R. An, B. P. Pandey, H. Yun, C. Sung, H. Y. Park and B. G. Kim (2012). "Engineering of daidzein 3'-hydroxylase P450 enzyme into catalytically self-sufficient cytochrome P450." Microb Cell Fact **11**: 81.

Choi, K. Y., E. Jung, H. Yun, Y. H. Yang and B. G. Kim (2014). "Engineering class I cytochrome P450 by gene fusion with NADPH-dependent reductase and S. avermitilis host development for daidzein biotransformation." Appl Microbiol

Biotechnol **98**(19): 8191-8200.

Choi, K. Y., T. J. Kim, S. K. Koh, C. H. Roh, B. P. Pandey, N. Lee and B. G. Kim (2009). "A-ring ortho-specific monohydroxylation of daidzein by cytochrome P450s of Nocardia farcinica IFM10152." Biotechnol J **4**(11): 1586-1595.

Choi, K. Y., H. Y. Park and B. G. Kim (2010). "Characterization of bi-functional CYP154 from Nocardia farcinica IFM10152 in the O-dealkylation and ortho-hydroxylation of formononetin." Enzyme and Microbial Technology **47**(7): 327-334.

Choi, K. Y., Y. H. Yang and B. G. Kim (2015). "Regioselectivity-driven evolution of CYP102D1 for improved synthesis of 3 '-ortho-dihydroxyisoflavone." Enzyme and Microbial Technology **71**: 20-27.

Choi, M. J. and H. I. Maibach (2005). "Role of ceramides in barrier function of healthy and diseased skin." American Journal of Clinical Dermatology **6**(4): 215-223.

Chovancova, E., A. Pavelka, P. Benes, O. Strnad, J. Brezovsky, B. Kozlikova, A. Gora, V. Sustr, M. Klvana, P. Medek, L. Biedermannova, J. Sochor and J. Damborsky (2012). "CAVER 3.0: a tool for the analysis of transport pathways in dynamic protein structures." PLoS Comput Biol **8**(10): e1002708.

Clomburg, J. M., M. D. Blankschien, J. E. Vick, A. Chou, S. Kim and R. Gonzalez (2015). "Integrated engineering of beta-oxidation reversal and omega-oxidation pathways for the synthesis of medium chain omega-functionalized carboxylic acids." Metabolic Engineering **28**: 202-212.

Cojocaru, V., P. J. Winn and R. C. Wade (2007). "The ins and outs of cytochrome P450s." Biochimica Et Biophysica Acta-General Subjects **1770**(3): 390-401.

De Mot, R. and A. H. Parret (2002). "A novel class of self-sufficient cytochrome P450 monooxygenases in prokaryotes." Trends Microbiol **10**(11): 502-508.

Denisov, I. G., T. M. Makris, S. G. Sligar and I. Schlichting (2005). "Structure and chemistry of cytochrome P450." Chem Rev **105**(6): 2253-2277.

Dodhia, V. R., A. Fantuzzi and G. Gilardi (2006). "Engineering human cytochrome P450 enzymes into catalytically self-sufficient chimeras using molecular Lego." Journal of Biological Inorganic Chemistry **11**(7): 903-916.

Downing, D. T. (1992). "Lipid and protein structures in the permeability barrier of mammalian epidermis." J Lipid Res **33**(3): 301-313.

Duan, Y., L. Ba, J. Gao, X. Gao, D. Zhu, R. M. de Jong, D. Mink, I. Kaluzna and Z. Lin (2016). "Semi-rational engineering of cytochrome CYP153A from Marinobacter aquaeolei for improved omega-hydroxylation activity towards oleic acid." Appl Microbiol Biotechnol.

Fairhead, M., S. Giannini, E. M. J. Gillam and G. Gilardi (2005). "Functional characterisation of an engineered multidomain human P450 2E1 by molecular Lego." Journal of Biological Inorganic Chemistry **10**(8): 842-853.

Funhoff, E. G., J. Salzmann, U. Bauer, B. Witholt and J. B. van Beilen (2007). "Hydroxylation and epoxidation reactions catalyzed by CYP153 enzymes." Enzyme and Microbial Technology **40**(4): 806-812.

Gillam, E. M., T. Baba, B. R. Kim, S. Ohmori and F. P. Guengerich (1993). "Expression of modified human cytochrome P450 3A4 in Escherichia coli and purification and reconstitution of the enzyme." Arch Biochem Biophys **305**(1): 123-131.

Girhard, M., T. Klaus, Y. Khatri, R. Bernhardt and V. B. Urlacher (2010).

"Characterization of the versatile monooxygenase CYP109B1 from Bacillus subtilis." Appl Microbiol Biotechnol **87**(2): 595-607.

Girvan, H. M. and A. W. Munro (2016). "Applications of microbial cytochrome P450 enzymes in biotechnology and synthetic biology." Curr Opin Chem Biol **31**: 136-145.

Gotoh, O. (1992). "Substrate Recognition Sites in Cytochrome-P450 Family-2 (Cyp2) Proteins Inferred from Comparative Analyses of Amino-Acid and Coding Nucleotide-Sequences." Journal of Biological Chemistry **267**(1): 83-90.

Gotoh, O. (1992). "Substrate recognition sites in cytochrome P450 family 2 (CYP2) proteins inferred from comparative analyses of amino acid and coding nucleotide sequences." J Biol Chem **267**(1): 83-90.

Graham-Lorence, S., G. Truan, J. A. Peterson, J. R. Falck, S. Wei, C. Helvig and J. H. Capdevila (1997). "An active site substitution, F87V, converts cytochrome P450 BM-3 into a regio- and stereoselective (14S,15R)-arachidonic acid epoxygenase." J Biol Chem **272**(2): 1127-1135.

Gricman, L., C. Vogel and J. Pleiss (2015). "Identification of universal selectivity-determining positions in cytochrome P450 monooxygenases by systematic sequence-based literature mining." Proteins **83**(9): 1593-1603.

Gricman, Ł., C. Vogel and J. Pleiss (2014). "Conservation analysis of class-specific positions in cytochrome P450 monooxygenases: functional and structural relevance." Proteins: Structure, Function, and Bioinformatics **82**(3): 491-504.

Haftek, M., S. Callejon, Y. Sandjeu, K. Padois, F. Falson, F. Pirot, P. Portes, F. Demarne and V. Jannin (2011). "Compartmentalization of the human stratum corneum by persistent tight junction-like structures." Experimental Dermatology

**20**(8): 617-621.

Hannemann, F., A. Bichet, K. M. Ewen and R. Bernhardt (2007). "Cytochrome P450 systems--biological variations of electron transport chains." Biochim Biophys Acta **1770**(3): 330-344.

Hardwick, J. P. (2008). "Cytochrome P450 omega hydroxylase (CYP4) function in fatty acid metabolism and metabolic diseases." Biochemical Pharmacology **75**(12): 2263-2275.

Harpaz, Y., M. Gerstein and C. Chothia (1994). "Volume changes on protein folding." Structure **2**(7): 641-649.

Hoffmann, S. M., M. J. Weissenborn, L. Gricman, S. Notonier, J. Pleiss and B. Hauer (2016). "The Impact of Linker Length on P450 Fusion Constructs: Activity, Stability and Coupling." Chemcatchem **8**(8): 1591-1597.

Hoffmann, S. M., M. J. Weissenborn, Ł. Gricman, S. Notonier, J. Pleiss and B. Hauer (2016). "The Impact of Linker Length on P450 Fusion Constructs: Activity, Stability and Coupling." ChemCatChem **8**(8): 1591-1597.

Honda Malca, S., D. Scheps, L. Kuhnel, E. Venegas-Venegas, A. Seifert, B. M. Nestl and B. Hauer (2012). "Bacterial CYP153A monooxygenases for the synthesis of omega-hydroxylated fatty acids." Chem Commun (Camb) **48**(42): 5115-5117.

Hrycay, E. G. and S. M. Bandiera (2015). "Monooxygenase, peroxidase and peroxygenase properties and reaction mechanisms of cytochrome P450 enzymes." Adv Exp Med Biol **851**: 1-61.

Jacobs, E. and M. Metzler (1999). "Oxidative metabolism of the mammalian lignans enterolactone and enterodiol by rat, pig, and human liver microsomes." J Agric Food Chem **47**(3): 1071-1077.

Jang, H. Y., K. Singha, H. H. Kim, Y. U. Kwon and J. B. Park (2016). "Chemo-enzymatic synthesis of 11-hydroxyundecanoic acid and 1,11-undecanedioic acid from ricinoleic acid." Green Chemistry **18**(4): 1089-1095.

Kim, D., M. J. Cryle, J. J. De Voss and P. R. Ortiz de Montellano (2007). "Functional expression and characterization of cytochrome P450 52A21 from Candida albicans." Arch Biochem Biophys **464**(2): 213-220.

Kim, K. R. and D. K. Oh (2013). "Production of hydroxy fatty acids by microbial fatty acid-hydroxylation enzymes." Biotechnol Adv **31**(8): 1473-1485.

Kusunose, M., M. J. Coon and E. Kusunose (1964). "Enzymatic Omega-Oxidation of Fatty Acids .1. Products of Octanoate Decanoate + Laurate Oxidation." Journal of Biological Chemistry **239**(5): 1374-&.

Labinger, J. A. (2004). "Selective alkane oxidation: hot and cold approaches to a hot problem." Journal of Molecular Catalysis a-Chemical **220**(1): 27-35.

Labinger, J. A. and J. E. Bercaw (2002). "Understanding and exploiting C-H bond activation." Nature **417**(6888): 507-514.

Li, H. and T. L. Poulos (1997). "The structure of the cytochrome p450BM-3 haem domain complexed with the fatty acid substrate, palmitoleic acid." Nat Struct Biol **4**(2): 140-146.

Li, H. and T. L. Poulos (1999). "Fatty acid metabolism, conformational change, and electron transfer in cytochrome P-450(BM-3)." Biochim Biophys Acta **1441**(2-3): 141-149.

Liskova, V., D. Bednar, T. Prudnikova, P. Rezacova, T. Koudelakova, E. Sebestova, I. K. Smatanova, J. Brezovsky, R. Chaloupkova and J. Damborsky (2015). "Balancing the Stability-Activity Trade-Off by Fine-Tuning Dehalogenase Access

Tunnels." Chemcatchem **7**(4): 648-659.

Lu, W. H., J. E. Ness, W. C. Xie, X. Y. Zhang, J. Minshull and R. A. Gross (2010). "Biosynthesis of Monomers for Plastics from Renewable Oils." Journal of the American Chemical Society **132**(43): 15451-15455.

Lutz, S. (2010). "Beyond directed evolution--semi-rational protein engineering and design." Curr Opin Biotechnol **21**(6): 734-743.

McCann, S. E., L. U. Thompson, J. Nie, J. Dorn, M. Trevisan, P. G. Shields, C. B. Ambrosone, S. B. Edge, H. F. Li, C. Kasprzak and J. L. Freudenheim (2010). "Dietary lignan intakes in relation to survival among women with breast cancer: the Western New York Exposures and Breast Cancer (WEB) Study." Breast Cancer Res Treat **122**(1): 229-235.

McKenna, E. J. and M. J. Coon (1970). "Enzymatic omega-oxidation. IV. Purification and properties of the omega-hydroxylase of Pseudomonas oleovorans." J Biol Chem **245**(15): 3882-3889.

Meagher, L. P., G. R. Beecher, V. P. Flanagan and B. W. Li (1999). "Isolation and characterization of the lignans, isolariciresinol and pinoresinol, in flaxseed meal." J Agric Food Chem **47**(8): 3173-3180.

Meinhold, P., M. W. Peters, M. M. Chen, K. Takahashi and F. H. Arnold (2005). "Direct conversion of ethane to ethanol by engineered cytochrome P450 BM3." Chembiochem **6**(10): 1765-1768.

Meinhold, P., M. W. Peters, A. Hartwick, A. R. Hernandez and F. H. Arnold (2006). "Engineering cytochrome P450BM3 for terminal alkane hydroxylation." Advanced Synthesis & Catalysis **348**(6): 763-772.

Metzger, J. O. and U. Bornscheuer (2006). "Lipids as renewable resources: current

state of chemical and biotechnological conversion and diversification." Applied Microbiology and Biotechnology **71**(1): 13-22.

Munro, A. W., H. M. Girvan and K. J. McLean (2007). "Cytochrome P450--redox partner fusion enzymes." Biochim Biophys Acta **1770**(3): 345-359.

Murkies, A., F. S. Dalais, E. M. Briganti, H. G. Burger, D. L. Healy, M. L. Wahlqvist and S. R. Davis (2000). "Phytoestrogens and breast cancer in postmenopausal women: a case control study." Menopause **7**(5): 289-296.

Nelson, D. R. (1998). "Cytochrome P450 nomenclature." Methods Mol Biol **107**: 15-24.

Nickerson, D. P., C. F. HarfordCross, S. R. Fulcher and L. L. Wong (1997). "The catalytic activity of cytochrome P450(cam) towards styrene oxidation is increased by site-specific mutagenesis." Febs Letters **405**(2): 153-156.

Noble, M. A., C. S. Miles, S. K. Chapman, D. A. Lysek, A. C. MacKay, G. A. Reid, R. P. Hanzlik and A. W. Munro (1999). "Roles of key active-site residues in flavocytochrome P450 BM3." Biochem J **339 ( Pt 2)**: 371-379.

Nodate, M., M. Kubota and N. Misawa (2006). "Functional expression system for cytochrome P450 genes using the reductase domain of self-sufficient P450RhF from Rhodococcus sp NCIMB 9784." Applied Microbiology and Biotechnology **71**(4): 455-462.

Notonier, S., L. Gricman, J. Pleiss and B. Hauer (2016). "Semi-rational protein engineering of CYP153A M. aq.-CPR BM3 for efficient terminal hydroxylation of short to long chain fatty acids." ChemBioChem.

Oliver, C. F., S. Modi, W. U. Primrose, L. Y. Lian and G. C. Roberts (1997). "Engineering the substrate specificity of Bacillus megaterium cytochrome P-450

BM3: hydroxylation of alkyl trimethylammonium compounds." Biochem J **327 ( Pt 2)**: 537-544.

Omura, T. and R. Sato (1964). "The Carbon Monoxide-Binding Pigment of Liver Microsomes. I. Evidence for Its Hemoprotein Nature." J Biol Chem **239**: 2370-2378.

Ost, T. W., C. S. Miles, J. Murdoch, Y. Cheung, G. A. Reid, S. K. Chapman and A. W. Munro (2000). "Rational re-design of the substrate binding site of flavocytochrome P450 BM3." FEBS Lett **486**(2): 173-177.

Pandey, B. P., N. Lee, K. Y. Choi, J. N. Kim, E. J. Kim and B. G. Kim (2014). "Identification of the specific electron transfer proteins, ferredoxin, and ferredoxin reductase, for CYP105D7 in Streptomyces avermitilis MA4680." Appl Microbiol Biotechnol.

Pavelka, A., E. Chovancova and J. Damborsky (2009). "HotSpot Wizard: a web server for identification of hot spots in protein engineering." Nucleic Acids Res **37**(Web Server issue): W376-383.

Peters, M. W., P. Meinhold, A. Glieder and F. H. Arnold (2003). "Regio- and enantioselective alkane hydroxylation with engineered cytochromes P450 BM-3." J Am Chem Soc **125**(44): 13442-13450.

Petrek, M., M. Otyepka, P. Banas, P. Kosinova, J. Koca and J. Damborsky (2006). "CAVER: a new tool to explore routes from protein clefts, pockets and cavities." BMC Bioinformatics **7**: 316.

Porter, J. L., R. A. Rusli and D. L. Ollis (2016). "Directed Evolution of Enzymes for Industrial Biocatalysis." Chembiochem **17**(3): 197-203.

Ravichandran, K. G., S. S. Boddupalli, C. A. Hasermann, J. A. Peterson and J.

Deisenhofer (1993). "Crystal structure of hemoprotein domain of P450BM-3, a prototype for microsomal P450's." Science **261**(5122): 731-736.

Reetz, M. T., D. Kahakeaw and R. Lohmer (2008). "Addressing the numbers problem in directed evolution." Chembiochem **9**(11): 1797-1804.

Ringle, M., Y. Khatri, J. Zapp, F. Hannemann and R. Bernhardt (2013). "Application of a new versatile electron transfer system for cytochrome P450-based Escherichia coli whole-cell bioconversions." Applied Microbiology and Biotechnology **97**(17): 7741-7754.

Robin, A., V. Kohler, A. Jones, A. Ali, P. P. Kelly, E. O'Reilly, N. J. Turner and S. L. Flitsch (2011). "Chimeric self-sufficient P450cam-RhFRed biocatalysts with broad substrate scope." Beilstein Journal of Organic Chemistry **7**: 1494-1498.

Roh, C., S. H. Seo, K. Y. Choi, M. Cha, B. P. Pandey, J. H. Kim, J. S. Park, D. H. Kim, I. S. Chang and B. G. Kim (2009). "Regioselective hydroxylation of isoflavones by Streptomyces avermitilis MA-4680." J Biosci Bioeng **108**(1): 41-46.

Roiban, G. D. and M. T. Reetz (2015). "Expanding the toolbox of organic chemists: directed evolution of P450 monooxygenases as catalysts in regio- and stereoselective oxidative hydroxylation." Chemical Communications **51**(12): 2208-2224.

Rufer, C. E. and S. E. Kulling (2006). "Antioxidant activity of isoflavones and their major metabolites using different in vitro assays." J Agric Food Chem **54**(8): 2926-2931.

Sali, A. and T. L. Blundell (1993). "Comparative protein modelling by satisfaction of spatial restraints." J Mol Biol **234**(3): 779-815.

Schürer, N. and P. M. Elias (1991). The biochemistry and function of stratum

corneum lipids, Academic Press Inc. San Diego, CA.

Scheller, U., T. Zimmer, D. Becher, F. Schauer and W. H. Schunck (1998). "Oxygenation cascade in conversion of n-alkanes to alpha,omega-dioic acids catalyzed by cytochrome P450 52A3." J Biol Chem **273**(49): 32528-32534.

Scheps, D., S. Honda Malca, S. M. Richter, K. Marisch, B. M. Nestl and B. Hauer (2013). "Synthesis of omega-hydroxy dodecanoic acid based on an engineered CYP153A fusion construct." Microb Biotechnol **6**(6): 694-707.

Scheps, D., S. H. Malca, H. Hoffmann, B. M. Nestl and B. Hauer (2011). "Regioselective omega-hydroxylation of medium-chain n-alkanes and primary alcohols by CYP153 enzymes from Mycobacterium marinum and Polaromonas sp. strain JS666." Org Biomol Chem **9**(19): 6727-6733.

Schwaneberg, U., C. Otey, P. C. Cirino, E. Farinas and F. H. Arnold (2001). "Cost-effective whole-cell assay for laboratory evolution of hydroxylases in Escherichia coli." Journal of Biomolecular Screening **6**(2): 111-117.

Scott, I. R., D. J. K. Crawford and A. V. Rawlings (1993). Synthesis of cosmetic ingredient, Google Patents.

Sevrioukova, I. F., H. Y. Li, H. Zhang, J. A. Peterson and T. L. Poulos (1999). "Structure of a cytochrome P450-redox partner electron-transfer complex." Proceedings of the National Academy of Sciences of the United States of America **96**(5): 1863-1868.

Sirim, D., M. Widmann, F. Wagner and J. Pleiss (2010). "Prediction and analysis of the modular structure of cytochrome P450 monooxygenases." Bmc Structural Biology **10**.

Song, J. W., E. Y. Jeon, D. H. Song, H. Y. Jang, U. T. Bornscheuer, D. K. Oh and J.

B. Park (2013). "Multistep enzymatic synthesis of long-chain alpha,omega-dicarboxylic and omega-hydroxycarboxylic acids from renewable fatty acids and plant oils." Angew Chem Int Ed Engl **52**(9): 2534-2537.

Steen, E. J., Y. Kang, G. Bokinsky, Z. Hu, A. Schirmer, A. McClure, S. B. Del Cardayre and J. D. Keasling (2010). "Microbial production of fatty-acid-derived fuels and chemicals from plant biomass." Nature **463**(7280): 559-562.

Stephan, M. M. S. and B. Mohar (2006). "Simple preparation of highly pure monomeric omega-hydroxycarboxylic acids." Organic Process Research & Development **10**(3): 481-483.

Sung, C., E. Jung, K. Y. Choi, J. H. Bae, M. Kim, J. Kim, E. J. Kim, P. I. Kim and B. G. Kim (2015). "The production of omega-hydroxy palmitic acid using fatty acid metabolism and cofactor optimization in Escherichia coli." Appl Microbiol Biotechnol.

Thompson, J. D., D. G. Higgins and T. J. Gibson (1994). "CLUSTAL W: improving the sensitivity of progressive multiple sequence alignment through sequence weighting, position-specific gap penalties and weight matrix choice." Nucleic Acids Res **22**(22): 4673-4680.

Thompson, L. U. (1998). "Experimental studies on lignans and cancer." Baillieres Clin Endocrinol Metab **12**(4): 691-705.

Tijet, N., C. Helvig, F. Pinot, R. Le Bouquin, A. Lesot, F. Durst, J. P. Salaun and I. Benveniste (1998). "Functional expression in yeast and characterization of a clofibrate-inducible plant cytochrome P-450 (CYP94A1) involved in cutin monomers synthesis." Biochem J **332 ( Pt 2)**: 583-589.

Trott, O. and A. J. Olson (2010). "AutoDock Vina: improving the speed and

accuracy of docking with a new scoring function, efficient optimization, and multithreading." J Comput Chem **31**(2): 455-461.

Urlacher, V. B. and M. Girhard (2012). "Cytochrome P450 monooxygenases: an update on perspectives for synthetic application." Trends Biotechnol **30**(1): 26-36.

van Beilen, J. B., E. G. Funhoff, A. van Loon, A. Just, L. Kaysser, M. Bouza, R. Holtackers, M. Rothlisberger, Z. Li and B. Witholt (2006). "Cytochrome P450 alkane hydroxylases of the CYP153 family are common in alkane-degrading eubacteria lacking integral membrane alkane hydroxylases." Appl Environ Microbiol **72**(1): 59-65.

Vandamme, E. J. and W. Soetaert (2002). "Bioflavours and fragrances via fermentation and biocatalysis." Journal of Chemical Technology and Biotechnology **77**(12): 1323-1332.

Wang, X., D. Jin, L. Zhou, L. Wu, W. An and L. Zhao (2014). "Draft Genome Sequence of Gordonia alkanivorans Strain CGMCC6845, a Halotolerant Hydrocarbon-Degrading Bacterium." Genome Announc **2**(1).

Weber, P. G., J. W. J. Lambers, H. S. Koger and J. Verweij (2000). Phytosphingosine-based ceramide I analogs, Google Patents.

Wertz, P. W., M. C. Miethke, S. A. Long, J. S. Strauss and D. T. Downing (1985). "The composition of the ceramides from human stratum corneum and from comedones." J Invest Dermatol **84**(5): 410-412.

Whitehouse, C. J., S. G. Bell and L. L. Wong (2012). "P450(BM3) (CYP102A1): connecting the dots." Chem Soc Rev **41**(3): 1218-1260.

Woodley, J. M. (2006). "Microbial biocatalytic processes and their development." Adv Appl Microbiol **60**: 1-15.

Yamamoto, A., S. Serizawa, M. Ito and Y. Sato (1991). "Stratum-Corneum Lipid Abnormalities in Atopic-Dermatitis." Archives of Dermatological Research **283**(4): 219-223.

Yang, W., S. G. Bell, H. Wang, W. Zhou, N. Hoskins, A. Dale, M. Bartlam, L. L. Wong and Z. Rao (2010). "Molecular characterization of a class I P450 electron transfer system from Novosphingobium aromaticivorans DSM12444." J Biol Chem **285**(35): 27372-27384.

Yang, Y., Y. T. Chi, H. H. Toh and Z. Li (2015). "Evolving P450pyr monooxygenase for highly regioselective terminal hydroxylation of n-butanol to 1,4-butanediol." Chem Commun (Camb) **51**(5): 914-917.

Yang, Y. and Z. Li (2015). "Evolving P450pyr Monooxygenase for Regio- and Stereoselective Hydroxylations." Chimia (Aarau) **69**(3): 136-141.

Yokota, T. and A. Watanabe (1993). Process for producing ω-hydroxy fatty acids, Google Patents.

Young, C. C., T. C. Lin, M. S. Yeh, F. T. Shen and J. S. Chang (2005). "Identification and kinetic characteristics of an indigenous diesel-degrading Gordonia alkanivorans strain." World Journal of Microbiology & Biotechnology **21**(8-9): 1409-1414.

Zhou, H. and Y. Zhou (2005). "SPEM: improving multiple sequence alignment with sequence profiles and predicted secondary structures." Bioinformatics **21**(18): 3615-3621.

Zimmer, T., M. Ohkuma, A. Ohta, M. Takagi and W. H. Schunck (1996). "The CYP52 multigene family of Candida maltosa encodes functionally diverse n-alkane-inducible cytochromes P450." Biochem Biophys Res Commun **224**(3): 784-

789.

Zorn, K., I. Oroz-Guinea, H. Brundiek and U. T. Bornscheuer (2016). "Engineering and Application of Enzymes for Lipid Modification, an Update." Prog Lipid Res.

Zuo, R., Y. Zhang, J. C. Huguet-Tapia, M. Mehta, E. Dedic, S. D. Bruner, R. Loria and Y. Ding (2016). "An artificial self-sufficient cytochrome P450 directly nitrates fluorinated tryptophan analogs with a different regio-selectivity." Biotechnol J **11**(5): 624-632.

# APPENDIX

## AI. Ortho-Hydroxylation of Mammalian Lignan Enterodiol by Cytochrome P450s from *Actinomycetes sp.*

### AI.1 Abstract

An animal lignin, i.e. enterodiol (END), is known to be formed by conversion of secoisolariciresinol from flaxseed by intestinal bacteria. Thirteen bacteria strains were examined for their hydroxylation activity for END. Among them, *Streptomyces avermitilis* MA-4680 and *Nocardia facinica* IFM10152 showed the highest hydroxylation activity for END. Reaction products profiling using GC/MS revealed that four products mono-hydroxylated in aliphatic position (Al-OH-END) and three products mono-hydroxylated in aromatic ring (Ar-OH-END) were found in *S. avermitilis* MA-4680, whereas only two Ar-OH-ENDs were detected in the case of *N. facinica* IFM10152. From 15mg/L of END, 900ug/L of Al-OH-END and 210ug/L of 4-hydroxy END (4-OH-END) were produced by *S. avermitilis* MA-4680, and 300ug/L of 2-hydroxy END (2-OH-END) and 480ug/L of 4-OH-END were obtained by *N. facinica* IFM10152. To find out the P450s are responsible for the substrate specificity to END, 33 P450s from *S. avermitilis* MA-4680 and 26 P450s from *N. facinica* IFM10152 were cloned and compared with coexpression of putidaredoxin reductase(camA) and putidaredoxin(camB) from *Pseudomonas putida* as redox partners in *E.coli*. As a result, Nfa45180 showed the highest hydroxylation activity especially for ortho-hydroxylation in aromatic ring *in vivo*. The results of the docking simulation of END into the homology model of Nfa45180 explained the reason for regio-specificity of the hydroxylation. To our knowledge, this is the first report of regioselective hydroxylation of END using

microorganism P450s.

**AI.2 Introduction**

Lignan, one of phytoestogens, biosynthesized in human body from the plant lignans uptaken through our diet has drawn great attention due to their estrogenic, anticarcinogenic, antioxidant effects on our body (Thompson 1998, Murkies, Dalais et al. 2000, McCann, Thompson et al. 2010). Among such animal lignans, enterodiol (END) is known to be formed by conversion of secoisolariciresinol from flaxseed by intestinal bacteria. Flax-seed contains several plant lignans such as secoisolariciresinol ,matairesinol, isolariciresinol, and pinoresinol (Meagher, Beecher et al. 1999). Secoisolariciresinol and matairesinol are known to be digested by intestinal bacteria and finally converted into the mammalian lignans enterodiol (END) and enterolactone (ENL). Subsequently, the final metabolites of such lignans are excreted in the liver of rats and humans (Axelson and Setchell 1981). Moreover, it has been reported that END gives rise to seven monohydroxylated metabolites upon incubation with microsomes from rat, pig, and human liver (Jacobs and Metzler 1999). Recently, hydroxylated compounds have attracted considerable scientific interests due to their health related qualities. Hydroxylated phytoestrogens such as asdaidzein or genistein have potent antioxidant properties that contribute to their cholesterol-lowering effects, cardiovascular protection, antitumor effects, and anticarcinogenic properties (Rufer and Kulling 2006). Regiospecific hydroxylation of aromatic compounds by chemical synthesis is difficult and involves diverse reaction steps. The conversion of aromatic hydrocarbons into hydroxylated aromatic hydrocarbons, i.e., inserting an oxygen atom into a carbon-hydrogen bond, in microorganism is one of the key

features of oxidative metabolism of many aromatic compounds. There have been few reports about lignin hydroxylation by human P450 in *E.coli* (Rufer and Kulling 2006). In addition, microbial biotransformation of phytoestrogen has also been studied, aiming for regio- and stereoselective hydroxylation using cytochrome P450 from *Actinomycetes sp.* (Choi, Kim et al. 2009, Roh, Seo et al. 2009, Choi, Jung et al. 2012, Pandey, Lee et al. 2014)

In this study, microorganisms participating in hydroxylations of END were screened among 13 *Streptomyces sp.*, *Bacillus sp.*, and *Nocardia sp.* as they are known to have several cytochrome P450 monoxygease enzymes (CYPs) which are involved in mono-hydroxylation both on aliphatic and aromatic molecules. And the hydroxylation products were discovered from the extracts from whole cell reaction of *S. avermitilis* MA-4680 and *N. facinica* IFM10152, and the structures of the products were identified by GC/MS. Finally, three CYPs from *S. avermitilis* MA-4680 and four CYPs from *N. facinica* IFM10152 showed the activity for hydroxylation of END. Especially, CYP154 (Nfa45180) from *N. facinica* IFM10152 showed the highest activity for ortho-specific hydroxylation of END.

## AI.3 Material and Method

### Chemicals and biochemicals

Enterodiol was purchased from Sigma-Aldrich Chemical Co. (St. Louis, MO, USA) and N,O-bis(trimethylsily)trifluoroacetamide for the derivatization for GC/MS analysis was obtained from Fluka (Buchs, Switzerland). All other chemicals were of the highest grade.

**Bacterial Strains and culture condition**

*Streptomyces spp.* including *S. avermitilis* MA-4680 were obtained from the Korea Collection for Type Cultures (KCTC, Daejeon, South Korea). Various kinds of *Bacillus spp.* were obtained from the Microbial Resources Center (SNU, South Korea). *N. farcinica* IFM10152 was provided by the Research Center for Pathogenic Fungi and Microbial Toxicoses, Chiba University, Japan . All microbes were cultured in an appropriate nutrient medium and under recommended culture conditions (Microbial Resources Center, SNU; Korea Collection for Type Cultures). *Streptomyces spp.* were cultured in 30℃ in $R5^-$ liquid broth. Various kinds of *Bacillus spp.* were cultured in 30 ℃ in Luria-Bertani(LB) medium. *N. farcinica* IFM10152 was grown in 37℃ in Bacto™ Brain Heart Infusion Broth from BD Bioscience, Sparks, Md, USA.

**Co-expression of cytochrome P450s and redox partners CamA/CamB in *E.coli* and cell distruption for UV absorbance CO-binding spectra**

The 33 P450 genes from *S. avermitilis* MA-4680 and 26 P450 genes from *N. farcinica* IFM10152 were cloned into expression vector pET28a(+) and protein soluble expression was confirmed with CO binding spectra.(Choi, Park et al. 2010). The expression vector, pETDuet-1 (Novagen) was used for the cloning of camA and camB(Roh, Seo et al. 2009). The plasmids of both P450 and redox partners were transformed together into *E.coli* BL21(*DE3*). The transformant was grown in Luria-Bertani(LB) medium containing 25 μg/ml of kanamycin and 25 μg/ml of ampicillin at 37℃ until the cell concentration reached to 0.6 of $OD_{600nm}$, and

isopropyl-thio-β-D-galactopyranoside (IPTG) and δ-aminolevulinic acid which is heme precursor were added to a final concentration of 0.5 mM, followed by growing the cell at 30℃ for 12 hours. The recombinant cell were harvested and were resuspended in 5ml of sonication buffer composed of 10mM Tris–HCl (pH 7.0), 2mM EDTA, 1mM PMSF, and 0.01% (v/v) 2-mercaptoethanol, and disrupted by sonication. The disrupted soluble fraction was collected by centrifugation. UV absorption spectra of CO-bound recombinant CYP proteins after sodiumdithionite reduction were measured by UV/vis spectrometry (SPECTRONIC, GENESYS, MILTON ROY, USA) by scanning wavelength from 400 to 500 nm. Concentrations of each protein were measured based on CO-difference spectra using an extinction coefficient of 91mM−1 cm−1 at 450nm.

**Reaction condition for END biotransformation with wild type *S. avermitilis* MA-4680, *N. farcinica* IFM10152 and *E. coli* BL21(DE3) co-expressing both P450 and redox proteins**

After grown, the cells were harvested, washed twice with PBS buffer(pH 7.2), and resuspended in 15 ml of 100 mM phosphate buffer(pH 7.5). END dissolved in 10 mM MeOH was added into 20ml of the cell suspension to make a final concentration of 50 μM. The mixture was shaken in 200 rpm for oxygen supply at 30℃ for 20 hours.

**Extraction of products after biotransformation**

After incubation of the cells with END, the reaction was stopped by adding the same volume of ethyl acetate (JUNSEI, Japan) and vortexed vigorously. The

mixtures were centrifuged at 13,000 rpm for 5 minutes, and the upper organic layer was evaporated by vacuum concentrator (BioTron, South Korea). Subsequently, the residual was dissolved in 50 μl of methanol (MERK, Germany) and ethyl acetate for anlaysis by HPLC and GC/MS, respectively.

**GC/MS analysis**

For GC/MS analysis, reaction products were converted to their trimethylsilyl (TMS) derivatives by incubating for 20 min at 70 ℃ with N,O-bis(trimethylsilyl)trifluoroacetamide (BSTFA). Analysis by GC/MS was performed using a TRACE GC ULTRA gas chromatograph, coupled to an ion trap mass detector ITQ1100. The TMS-derivatives were analyzed using a nonpolar capillary column (5% phenyl methyl siloxane capillary 30 m×250 μm i.d., 0.25 μm film thickness, TR-5ms) with a linear temperature gradient (100 °C 1 min, 30 °C/min to 250 °C, hold for 10 min, 1 °C/min to 280 °C, and hold for 1 min). The injector port temperature was 230 °C. The temperature of the connecting parts was 275 °C and the electron energy for the EI mass spectra was 70 eV. Identification was performed by comparison of retention time and mass spectral data (recorded by full scan in the selected ion mode; *m/z* 50–1000) of the sample with that of authentic references.

**Computational methods**

Nfa45180 from *N. facinica* IFM10152 (accession number, 3109062) shows a sequence identity of 64.6% to CYP154A1 of *S. coelicolor*. The corresponding crystallographic structure [protein data bank (PDB) entry 1ODO] was chosen as

structural template. The alignment generated with ClustalW 1.83 (Thompson, Higgins et al. 1994) and SPEM (Zhou and Zhou 2005). A model were generated by Modeller 9.4 (Sali and Blundell 1993) with hetero-atom contain mode. The coordinates of END for docking were generated manually and energetically optimized using the MM + force field using Chem3D Ultra 8.00. AutoDock (version 3.00) was applied for docking of END into the homology model of Nfa45180 (Sali and Blundell 1993). 1000 docking runs were carried out, and the minimum energy value was -1.43kcal/mol.

## AI.4 Results and Discussion

### Whole cell reaction of END by *S. avermitilis* MA-4680 and *N. farcinica* IFM10152

Recently completed genome sequences of a couple of *Actinomycetes sp.* strains revealed that more than a dozen of CYP monooxygenases are present in their genome. The CYP enzymes are known to be involved in various hydroxylation steps of primary and secondary metabolites (Roh, Seo et al. 2009). Based on this observation, *Streptomyces sp.*, *Bacillus sp.*, and *Nocardia sp.* were examined for their ability to convert END into their corresponding hydroxylated products (Table A1). Among the strains examined, two strains showed hydroxylation activities for END. The products of *S. avermitilis* MA-4680 and *N. farcinica* were separated by GC and their structures were identified by mass spectrometry. Various hydroxylation products were observed and they were divided into two major groups, hydroxylated ENDs at aliphatic moiety and aromatic moiety. From the

previous studies on the microsomal metabolism of END and ENL (Jacobs and Metzler, 1999) and on the urinary metabolites of lignans in humans (Jacobs et al., 1999), the mass values of the monohydroxylated ENDs at the aromatic or aliphatic moiety were reported. Table A2 shows the major ions in the mass spectra of the TMS derivative of END and its monohydroxylated products. The GC separation showed different patterns of hydroxylated ENDs (Figure A1). Among the seven products from the reaction with *S. avermitilis*, four Al-OH-ENDs and three Ar-OH-ENDs were observed (Figure A1a and Figure A2). The *m/z* values of three highest ions at GC peaks I, II, III and VI in Figure A1a were 395, 408 and 588 corresponding to GC/MS fragment patterns of Al-OH-END. However, any reference compounds of Al-OH-END were not observed here. So the specific hydroxylation position was not identified. The *m/z* value of major ions of fragmented Ar-OH-END were equivalent to the *m/z* value of three highest ions at GC peaks IV, V and VII in Figure A1a as 268, 498 and 588. The position of the additional hydroxyl group was identified using GC chromatography of three synthetic reference compounds of the Ar-OH-END(Jacobs and Metzler, 1999). As a result, GC peak IV was 6-hydroxy-END (6-OH-END), that is, hydroxylation in para position, GC peak V was 2-OH-END, that is, hydroxylation in ortho position and GC peak VII was 4-OH-END, that is, hydroxylation in another ortho position (Figure A3). The mass fragmentation pattern was proposed in Figure A4. From the whole cell reaction by *N. farcinica* IFM10152, two hydroxylated products were analyzed, and those corresponded with ortho-hydroxylation END showing the identical retention time in Figure A1b and mass spectra compared to the results from *S. avermitilis* MA-4680. (data are not shown) From 15mg/L of END, 900ug/L

of Al-OH-END and 210ug/L of 4-OH-END were produced by *S. avermitilis* and 300 ug/L of 2-OH-END and 480ug/L of 4-OH-END were biotransformated by *N. facinica* IFM10152. (Table A3)

**Table A1. List of strains used in screening for hydroxylation activity toward enterodiol**

| Strains |
|---|
| ***Streptomyces avermitilis*** **MA4680** |
| ***Streptomyces coelicolor*** **A3(2)** |
| ***Streptomyces carbophilus*** |
| ***Streptomyces venezuelae*** |
| ***Streptomyces peucetius*** **ATCC 27952** |
| ***Streptomyces lividans*** |
| ***Streptomyces griseolus*** |
| ***Nocardia farcinica*** **IFM10152** |
| ***Bacillus subtilis subsp. subtilis*** |
| ***Bacillus licheniformis*** **ATCC14580** |
| ***Bacillus megaterium*** **DSM319** |
| ***Bacillus cereus*** **KCCM12145** |
| ***Bacillus amyloliquefaciens*** **ATCC10987** |

**Table A2. Three major ions in the mass spectra of the TMS derivatives of END and its monohydroxylated products.**

| | m/z |
|---|---|
| **enterodiol (END)** | **500, 410, 180** |
| **hydroxylated in aromatic ring** | **588, 498, 268** |
| **hydroxylated in aliphatic position** | **588, 408, 395** |

**Table A3. The yield of major three hydroxylated products by *S. avermitilis* MA-4680 and *N. facinica* IFM10152**

| Strains | Yield (ug/L) | | |
|---|---|---|---|
| | **Al-OH-END** | **2-OH-END** | **4-OH-END** |
| ***S.avermitilis* MA-4680** | **900** | **90** | **210** |
| ***Nocardia facinica* IFM10152** | **n.d.**[a)] | **300** | **480** |

[a)] not detected

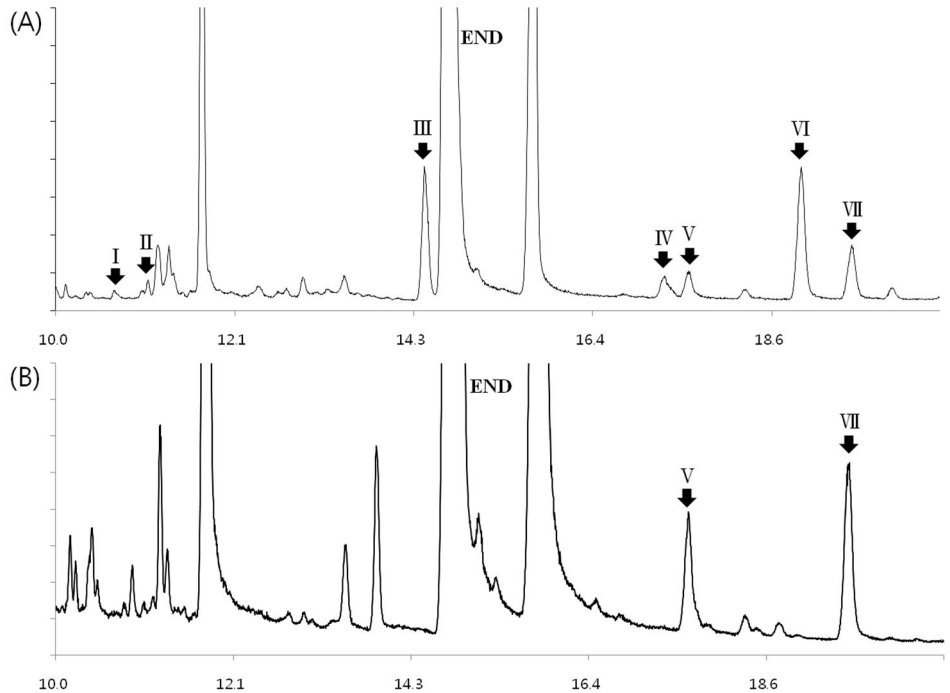


**Figure A1 GC/MS total ion current (TIC) of extract from whole cell reaction with END**

(A) Seven hydroxylation products from *S. avermitlis* MA-4680 were separated. (B) Two hydroxylation products from *N. facinica* IFM10152 were shown.

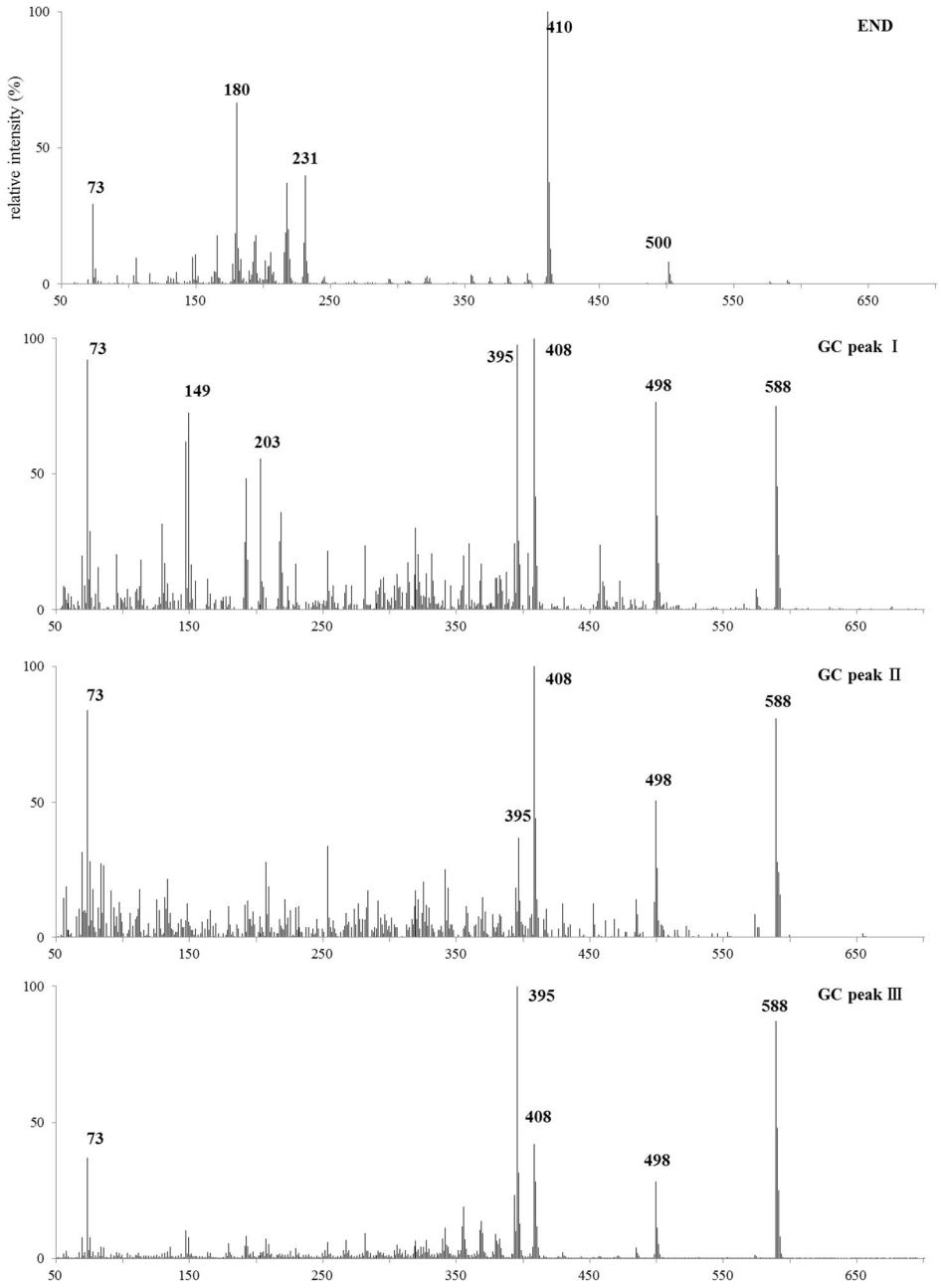
relative intensity (%)
END
410
180
231
73
500
GC peak Ⅰ
73
149
203
395
408
498
588
GC peak Ⅱ
73
408
588
498
395
GC peak Ⅲ
395
588
408
73
498

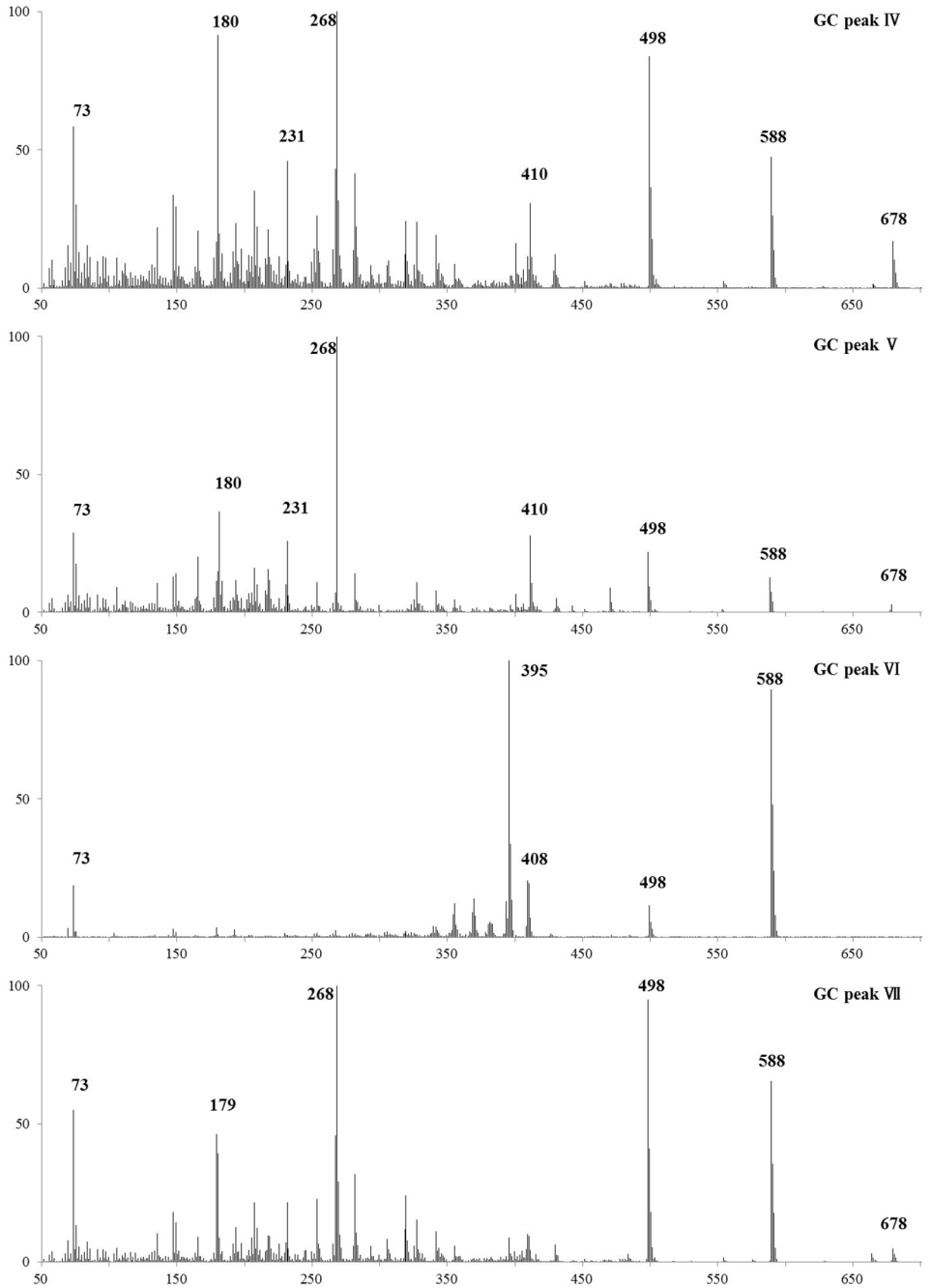
GC peak IV
73
180
231
268
410
498
588
678
GC peak V
73
180
231
268
410
498
588
678
GC peak VI
73
408
395
498
588
GC peak VII
73
179
268
498
588
678
100
50
0
50
150
250
350
450
550
650

**Figure A2 Mass spectra of hydroxylated END (TMS derivatives)**

The GC peak numbers refer to Figure A1. There were four Al-OH-ENDs and three Ar-OH-ENDs. The m/z value of three highest ions at GC peaks I, II, III and VI in Figure A1a were 395, 408 and 588 corresponding to GC/MS fragment pattern of Al-OH-ENDs. And, the m/z value of major ions of fragmented Ar-OH-ENDs were equal to the m/z value of three highest ions at GC peaks IV, V and VII in Figure A1a as 268, 498 and 588.

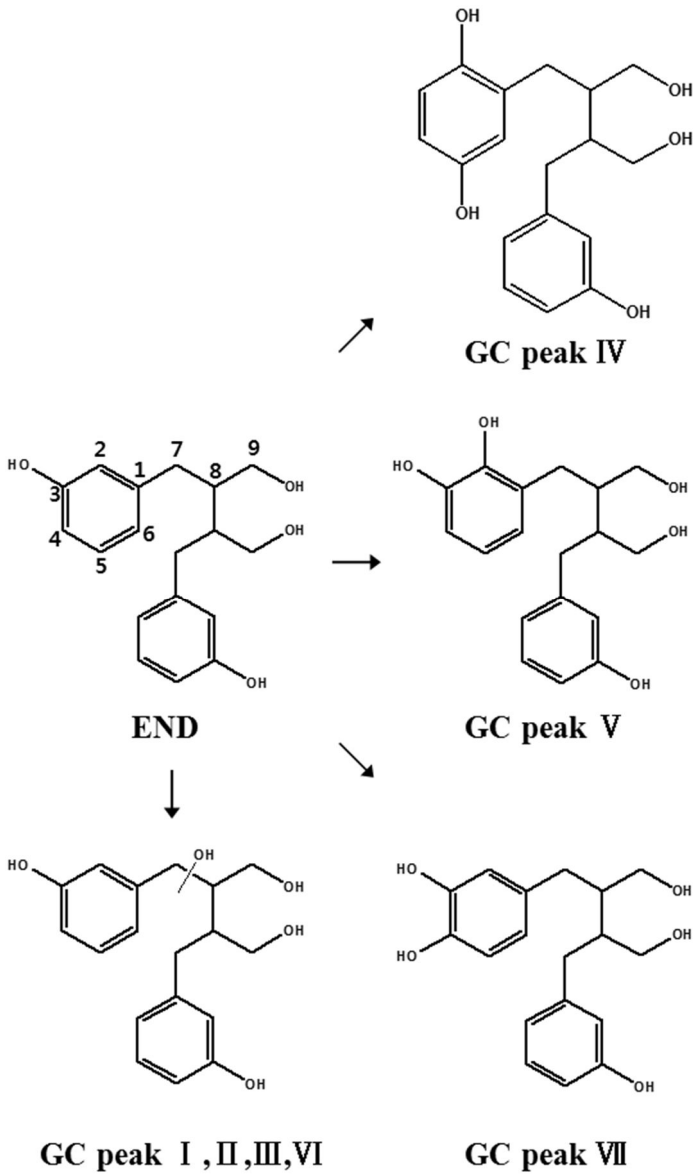


**Figure A3 Structures of END and hydroxylation products**

The GC peak numbers refer to Figure A1 and Figure A2.

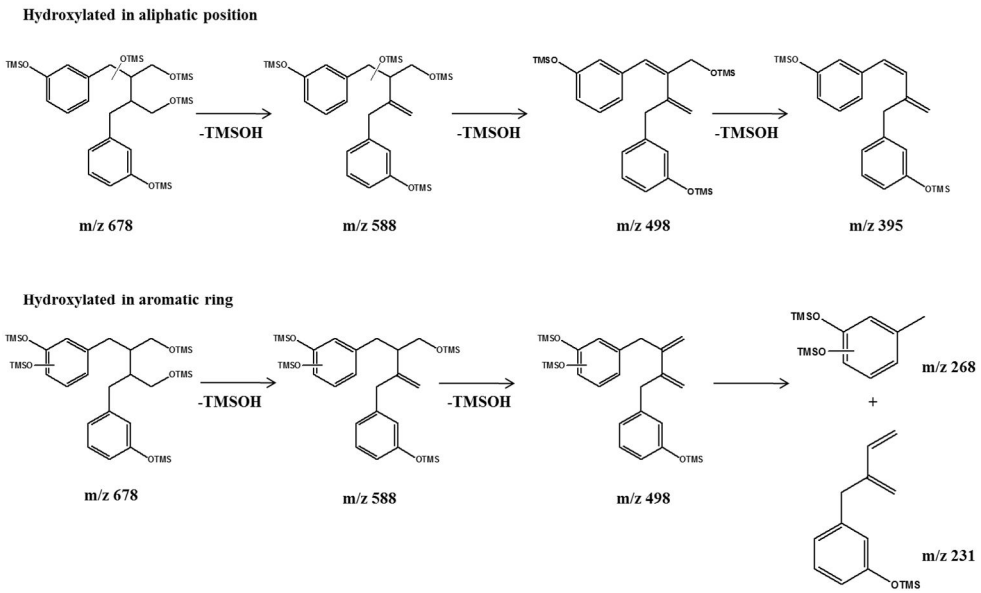


**Figure A4 Proposed mass fragmentation scheme for Al-OH-ENDs and Ar-OH-ENDs**

**Identification of P450 genes responsible for the END monohydroxylation reaction**

To identify P450s which are responsible for the END hydroxylation activity, the P450 library in *E.coli* was constructed. First, 33 P450s from *S. avermitilis* and 26 P450s from *N. facinica* were cloned and expressed in *E. coli*. 59 P450s belong to 29 CYP families, which have sequence identity above 40% compared to P450s in same families (Table A4). Using cell extract, CO binding spectra were measured to confirm the protein soluble expression. As a result, 14 P450s from *S. avermitilis* MA-4680 and 26 P450s from *N. facinica* IFM10152 showed UV absorption CO binding spectra, suggesting that those were expressed with functionality. For their electron transfer proteins, putidaredoxin reductase (CamA) and putidaredoxin (CamB) from *P.putida* were chosen and coexpressed. Finally, 40 recombinants were constructed and screened for END hydroxylation activity. As a results, three CYPs from *S. avermitilis* MA-4680 and four CYPs from *N. facinica* IFM10152 showed the activity for hydroxylation of END (Table A5). Especially, one CYP encoded by *nfa45180* showed the highest activity. This CYP enzyme belongs to CYP154 family which is well known for its activity toward aromatic compounds. (Choi, Park et al. 2010) By GC/MS analysis, the structure of product was revealed as 4-hydroxylation END due to the identical retention time and mass spectra compared to the results from *N. facinica* (Figure A5).

**Table A4 List of CYPs cloned from *Streptomyces avermitilis* and *Nocardia facinica***

| strain | P450 | family | P450 | family | P450 | family |
|---|---|---|---|---|---|---|
| *S.avermitilis* | Sav109 | CYP154A | Sav412 | CYP105D | Sav413 | CYP105P |
| | Sav575 | CYP102D | Sav584 | CYP147B | Sav838 | CYP178A |
| | Sav941 | CYP171A | Sav1171 | CYP107F | Sav1308 | CYP154D |
| | Sav1611 | CYP105Q | Sav1987 | CYP107L | Sav2061 | CYP179A |
| | Sav2165 | CYP180A | Sav2377 | CYP107Y | Sav2385 | CYP181A |
| | Sav2806 | CYP182A | Sav2894 | CYP107W | Sav2999 | CYP183A |
| | Sav3031 | CYP170A | Sav3519 | CYP107V | Sav3536 | CYP107U |
| | Sav3704 | CYP154B | Sav3881 | CYP157A | Sav3882 | CYP154C |
| | Sav4539 | CYP107P | Sav5111 | CYP184A | Sav5841 | CYP125A |
| | Sav6249 | CYP107X | Sav6706 | CYP157C | Sav7130 | CYP158A |
| | Sav7186 | CYP105R | Sav7426 | CYP102B | Sav7469 | CYP105D |
| *N. farcinica* | Nfa4950 | CYP157A | Nfa5180 | CYP191A | Nfa11380 | CYP136B |
| | Nfa11960 | CYP157A | Nfa12130 | CYP193A | Nfa12160 | CYP193A |
| | Nfa21340 | CYP157A | Nfa21760 | CYP210A | Nfa22290 | CYP140A |
| | Nfa22920 | CYP157A | Nfa22930 | CYP154B | Nfa24320 | CYP125A |
| | Nfa25810 | CYP109A | Nfa25870 | CYP125A | Nfa25890 | CYP51A |
| | Nfa30590 | CYP104A | Nfa33510 | CYP151A | Nfa33880 | CYP107E |
| | Nfa34990 | CYP159A | Nfa43600 | CYP120A | Nfa45170 | CYP157A |
| | Nfa45180 | CYP154A | Nfa46410 | CYP107A | Nfa53100 | CYP157A |
| | Nfa53110 | CYP154H | Nfa56380 | CYP110D | | |

**Table A5 List of CYPs used in screening for hydroxylation activity toward enterodiol**

| Strain | P450 | activity | Strain | P450 | activity |
|---|---|---|---|---|---|
| *S.avermitilis* | Sav412 | −[a)] | *N. farcinica* | Nfa21340 | − |
| | Sav413 | +[b)] | | Nfa21760 | − |
| | Sav838 | − | | Nfa22290 | − |
| | Sav1171 | − | | Nfa22920 | − |
| | Sav1987 | − | | Nfa22930 | − |
| | Sav2377 | + | | Nfa24320 | − |
| | Sav2894 | + | | Nfa25810 | − |
| | Sav3519 | + | | Nfa25870 | − |
| | Sav3882 | − | | Nfa25890 | − |
| | Sav4539 | − | | Nfa30590 | − |
| | Sav5111 | − | | Nfa33510 | − |
| | Sav6249 | − | | Nfa33880 | − |
| | Sav7186 | − | | Nfa34990 | − |
| | Sav7469 | - | | Nfa43600 | − |
| *N. farcinica* | Nfa4950 | − | | Nfa45170 | − |
| | Nfa5180 | ++[c)] | | Nfa45180 | +++[d)] |
| | Nfa11380 | − | | Nfa46410 | − |
| | Nfa11960 | − | | Nfa53100 | − |
| | Nfa12130 | − | | Nfa53110 | − |
| | Nfa12160 | + | | Nfa56380 | − |

a) No activity

b) Relative hydroxylation activity is within 30%

c) Relative hydroxylation activity is from 30 to 70%

d) Relative hydroxylation activity is up to 70%

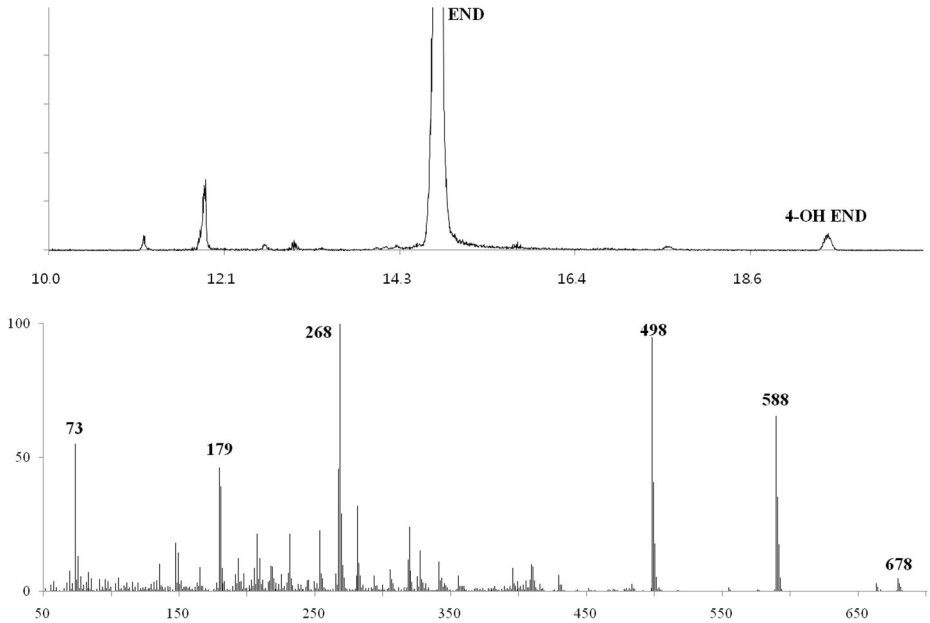


Figure A5 GC/MS chromatography of END conversion using Nfa45180

(A) GC/MS total ion current (TIC) of END conversion in the presence of Nfa45180 in *E.coli.* The product peak (tR=19.52) was identified as 4-OH-END. (B) mass spectra of 4-OH-END.

**Docking simulation of Nfa45180 with substrates and identification of key residues**

Computer modeling of Nfa45180 and its complexes with END was performed to obtain more insight about the structural basis for the regio-specific hydroxylation of END. Nfa45180 from *N. facinica* has the highest amino acid identity (64.6%) with CYP154A1 from *Streptomyces coelicolor* among the known crystal structures of bacterial cytochrome P450s deposited in the PDB. The corresponding crystallographic structure (PDB entry 1ODO) was chosen as structural template. Docking simulation of Nfa45180 with enterodiol as a substrate was performed to identify the key residues involved in interaction between the enzyme and the substrate. Figure A6 shows the heme active site with enterodiol and there are four residues (Asn90, Phe92, Leu240, and Ala244) which interacts with enterodiol. The distances toward the iron atom are 3.92 Å for END. As Asn90/Phe92 and aromatic moiety of END forms hydrophobic interaction, another aromatic moiety of END is located near heme geometrically. Also, Ala244 which is the nearest residue from heme provides a room for the aromatic moiety of END. This indicates the reason for the regioselective hydroxylation of END in structural aspect.

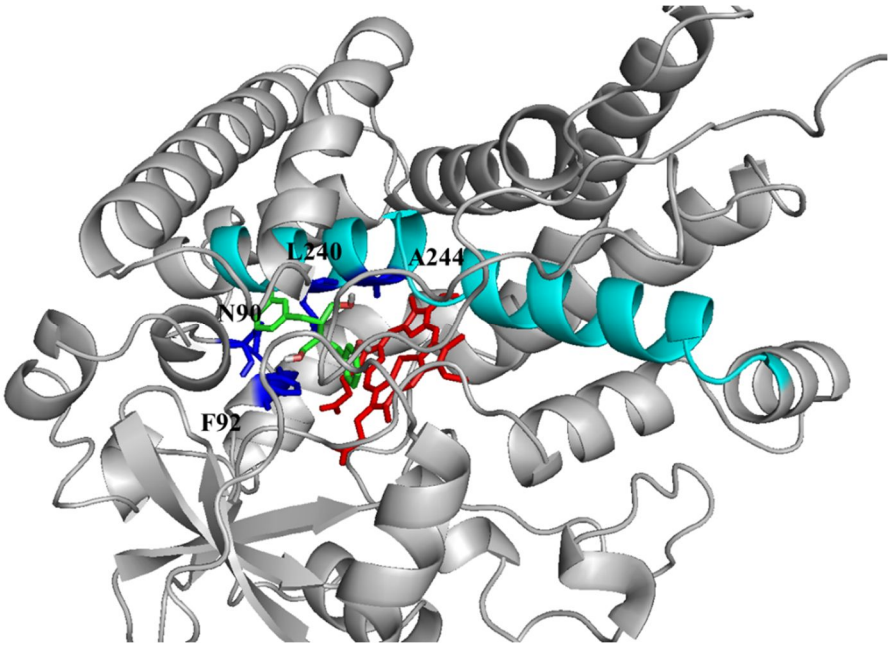


**Figure A6 Docking simulation in the homology model of Nfa45180**

I-helix which is the most important secondary structure around heme is shown in cyan and key residues surrounding substrate are shown in blue.

## AI.5 Conclusion

In the present study, we have investigated the hydroxylation of mammalian lignin END using whole cell reaction of *S. avermitilis* and *N. farcinica*. Seven and two hydroxylated products were separated from *S. avermitlis* and *N. facinica,* respectively, and their structures were identified by mass fragmentation (GC/MS/MS) study. In the GC spectra, seven hydroxylated products from *S. avermitilis* were identified as four ENDs with aliphatic hydroxylation and three ENDs with aromatic hydroxylation, whereas the two hydroxylated END products from *N. facinica* IFM10152 were all hydroxylated at ortho-position of an aromatic ring. All the P450s of *S. avermitilis* and *N. farcinica* were examined to determine the P450s responsible for hydroxylation reaction. Among them, Nfa45180 was screened to have hydroxylation activity at C4 position of END. To elucidate the structural understanding of regio-selectivity of the Nfa45180 for END, docking studies were performed using a homology model of Nfa45180. As a results, the model with the shortest distance between heme and C4 position in enterodiol had the lowest energy. This model thoroughly explains the high regio-specificity of CYP154 toward enterodiol.

# 국문 초록

본 연구는 유사세라마이드의 전구체로 사용되는 탄소수 16 이상의 오메가 수산화 지방산 생산을 위한 시토크롬 P450 수산화 효소의 전자전자 시스템의 이해, 공학적 변이, 링커 디자인, 단백질 발현 최적화의 연구를 다루고 있다.

첫 번째로, 지방산 오메가 수산화 효소로 잘 알려진 CYP153 패밀리에 속하는 유전자 중, *Marinobacter aquaeolei* VT8 유래의 CYP153A33, *Alcanivorax borkumensis* SK2 유래의 CYP153A13, *Gordonia alkanivorans* 유래의 CYP153A35를 대장균에 클로닝하여 효소 활성과 오메가 수산화 팔미트산 생산을 비교하였다. 수산화 효소의 반응에 사용되는 전자를 전달하기 위하여 *Pseudomonas putida*유래의 CamAB를 전자 전달 단백질로 사용하였을 때, 정제된 단백질 활성은 CYP153A13이, 전세포 반응에서의 생산성은 CYP153A35가 각각 제일 높았다.

두 번째로, CYP153A35에 대한 전자 전달 시스템의 연구를 위하여, CYP153A35와 *Bacillus megaterium* 유래의 CYP102A1의 FMN/FAD 결합부위를 접합한 신규 자립형 P450 효소를 제작하였다. 정제된 CYP153A35 자립형 P450 효소는 CYP153A35 효소 단백질과 CamAB 단백질을 이용한 시스템과 비교하였을 때, CYP153A35 자립형 P450 효소의 전자 전달 효율이 CamAB

시스템보다 4배 높았다. 그러나 두 시스템을 전세포 반응에서 비교하였을 경우, CamAB 시스템의 생산성이 1.5배 더 높았다.

추가적으로, CYP153A35의 활성은 전자전달 단백질인 CamAB의 농도 비율에 영향을 받는데, 특히 CamB 단백질의 농도가 율속인자이다. 대장균내의 세 개의 단백질을 발현할 때, 프로모터 세기, 유전자 배열 순서를 고려하여 5개의 다양한 발현 시스템을 구축하였고, 오메가 수산화 팔리트산 생산을 비교하였다. 5 mM의 팔미트산을 기질로 사용하였을 때, T7 프로모터 아래 camB, cyp153A35, camA 순서의 오페론 제작 균주인 A35-AB2가 9시간 반응 이내, 회분식 반응 시스템에서 가장 높은 생산성을 보였다. 그러나 유가식 반응 시스템에서는, 세 개의 단백질을 각각 T7 프로모터를 사용하여 발현을 한 A35-AB1 균주가 20 mM (5.1 g/L)의 팔미트산을 기질로 사용하였을 때, 30시간동안 17.0 mM (4.6 g/L)의 오메가 수산화 팔미트산을 생산을 함으로서 가장 높은 수치를 보였다.

세 번째로, CYP153A35의 수산화 활성을 증가시키기 위하여, 호몰로지 모델링을 이용하여 CYP153A35의 구조를 예측하였다. 그 다음으로, CAVER 3.0 프로그램을 사용하여 CYP153A35 내부에 존재하는 주요 구멍을 예측하여 기질인 지방산과 상호작용 할 것으로 예상되는 아미노산을 탐색하였다. 고활성 P450 효소를 선별하기 위하여, 우선 P450의 탈메틸 반응에 의해 부산물로 생성되는 포름알데하이드를 Purpald 시약을 이용하여 검출하는 고속스크리닝

방법을 개발하였다. 19개의 아미노산에 대하여 위치 특이적 포화변이를 수행한 결과 D131S와 D131F 단일 아미노산 변이체가 탐색되었다. 그 중 D131S 변이체는 야생형 대비 17배의 효소 활성 증가를 보였다.

마지막으로, CYP153A33와 CYP102A1의 조효소 결합 부위의 융합 단백질을 개발함에 있어서 두 도메인 간의 링커 서열을 최적화하였다. 이를 위하여 유연성의 또는 견고한 펩타이드 서열의 반복성을 임의적으로 디자인하여 라이브러리를 구축하였다. 그 결과, EAAAK-$(GGGGS)_3$-EAAAK의 링커 서열을 갖는 변이체가 탐색되었으나 융합 단백질의 대장균 내에서의 불용성에 의하여 생산 균주 개발의 한계를 남겼다.

주요어: 오메가 수산화 지방산, 시토크롬 P450 모노옥시다아제, CYP153, 전자 전달 시스템, 효소 단백질 공학적 변이, 링커 디자인, 단백질 발현 최적화

학번: 2009-21025